National Library
of Canada

Canadian Theses Service

Ottawa, Canada
K1A 0N4

Bibliothèque nationale
du Canada

Services des thèses canadiennes

CANADIAN THESES

THÈSES CANADIENNES

NOTICE

The quality of this microfiche is heavily dependent upon the quality of the original thesis submitted for microfilming. Every effort has been made to ensure the highest quality of reproduction possible.

If pages are missing, contact the university which granted the degree.

Some pages may have indistinct print especially if the original pages were typed with a poor typewriter ribbon or if the university sent us an inferior photocopy.

Previously copyrighted materials (journal articles, published tests, etc.) are not filmed.

Reproduction in full or in part of this film is governed by the Canadian Copyright Act, R.S.C. 1970, c. C-30. Please read the authorization forms which accompany this thesis.

AVIS

La qualité de cette microfiche dépend grandement de la qualité de la thèse soumise au microfilmage. Nous avons tout fait pour assurer une qualité supérieure de reproduction.

S'il manque des pages, veuillez communiquer avec l'université qui a conféré le grade.

La qualité d'impression de certaines pages peut laisser à désirer, surtout si les pages originales ont été dactylographiées à l'aide d'un ruban usé ou si l'université nous a fait parvenir une photocopie de qualité inférieure.

Les documents qui font déjà l'objet d'un droit d'auteur (articles de revue, examens publiés, etc.) ne sont pas microfilmés.

La reproduction, même partielle, de ce microfilm est soumise à la Loi canadienne sur le droit d'auteur, SRC 1970, c. C-30. Veuillez prendre connaissance des formules d'autorisation qui accompagnent cette thèse.

THIS DISSERTATION
HAS BEEN MICROFILMED
EXACTLY AS RECEIVED

LA THÈSE A ÉTÉ
MICROFILMÉE TELLE QUE
NOUS L'AVONS REÇUE

NL 339 (r. 86/01)

Canada

163

National Library
of Canada

Canadian Theses Division

Ottawa, Canada
K1A 0N4

Bibliothèque nationale
du Canada

Division des thèses canadiennes

0-315-24899-8

PERMISSION TO MICROFILM — AUTORISATION DE MICROFILMER

- Please print or type — Écrire en lettres moulées ou dactylographier

Full Name of Author — Nom complet de l'auteur
ZBIGNIEW WOLANSKI

Date of Birth — Date de naissance
24 AUGUST 1945

Country of Birth — Lieu de naissance
POLAND

Permanent Address — Résidence fixe
201-Vanier House, Michener Park
EDMONTON, ALBERTA - T6H 4N1

Title of Thesis — Titre de la thèse
TRANSIENT RESPONSE OF LOW-TUNED STRUCTURES SUPPORTING ROTATING MACHINERY

University — Université
THE UNIVERSITY OF ALBERTA

Degree for which thesis was presented — Grade pour lequel cette thèse fut présentée
M.Sc.

Year this degree conferred — Année d'obtention de ce grade
1984

Name of Supervisor — Nom du directeur de thèse
F. ELLYIN

Permission is hereby granted to the NATIONAL LIBRARY OF CANADA to microfilm this thesis and to lend or sell copies of the film.

The author reserves other publication rights, and neither the thesis nor extensive extracts from it may be printed or otherwise reproduced without the author's written permission.

L'autorisation est, par la présente, accordée à la BIBLIOTHÈQUE NATIONALE DU CANADA de microfilmer cette thèse et de prêter ou de vendre des exemplaires du film.

L'auteur se réserve les autres droits de publication; ni la thèse ni de longs extraits de celle-ci ne doivent être imprimés ou autrement reproduits sans l'autorisation écrite de l'auteur.

Date
5 OCT. 1984

Signature

NL-91 (4/77)

THE UNIVERSITY OF ALBERTA

Transient Response of Low-Tuned Structures Supporting Rotating Machinery

by

Ⓒ Zbigniew Wolanski

A THESIS
SUBMITTED TO THE FACULTY OF GRADUATE STUDIES AND RESEARCH
IN PARTIAL FULFILMENT OF THE REQUIREMENTS FOR THE DEGREE
OF Master of Science

Department of Mechanical Engineering

EDMONTON, ALBERTA
Fall 1984

THE UNIVERSITY OF ALBERTA

RELEASE FORM

NAME OF AUTHOR Zbigniew Wolanski

TITLE OF THESIS Transient Response of Low-Tuned Structures Supporting Rotating Machinery

DEGREE FOR WHICH THESIS WAS PRESENTED Master of Science

YEAR THIS DEGREE GRANTED Fall 1984

Permission is hereby granted to THE UNIVERSITY OF ALBERTA LIBRARY to reproduce single copies of this thesis and to lend or sell such copies for private, scholarly or scientific research purposes only.

The author reserves other publication rights, and neither the thesis nor extensive extracts from it may be printed or otherwise reproduced without the author's written permission.

(SIGNED) ....

PERMANENT ADDRESS:

#201 Vanier House, Michener Park
EDMONTON, Alberta
T6H 4N1

DATED 28th September 1984

THE UNIVERSITY OF ALBERTA

FACULTY OF GRADUATE STUDIES AND RESEARCH

The undersigned certify that they have read, and recommend to the Faculty of Graduate Studies and Research, for acceptance, a thesis entitled Transient Response of Low-Tuned Structures Supporting Rotating Machinery submitted by Zbigniew Wolanski in partial fulfilment of the requirements for the degree of Master of Science.

....

Supervisor

A. Craggs

....

T. Hrudey

....

Date: 28th September 1984

Moim Rodzicom

To My Parents

Acknowledgement

The author wishes to express his appreciation and sincere gratitude to:

Professor F. Ellyin, thesis supervisor, for his excellent guidance, assistance and financial support in the form of a research assistantship under The Natural Science and Engineering Research Council (NSERC) of Canada Grant No. A-3808.

The Department of Mechanical Engineering for generous computer funds for this study, excellent facilities and a great academic atmosphere.

Fellow graduate students for their useful discussions on various aspects of this study and especially to D. Spratt for his help in making this thesis readable.

Abstract

The dynamic response of (i) a simple beam, and (ii) a single bay portal frame supporting an unbalanced rotor is investigated in detail using a computer simulation. The method of solution for transient response is based on direct (step-by-step) integration of the system equations of motion through application of a finite time element reccurence scheme. Finite, Timoshenko beam elements are used in modelling both mass and elasticity as distributed parameters of the supporting structures.

Two models of the forcing function due to rotor unbalance are considered, assuming a rigid rotor shaft supported on: (i) rigid bearings, and (ii) oil-film journal bearings. The frequency of the forcing function is time dependent to simulate transients at start-up or shut-down operations. The discussed supporting structures are low-tuned relative to the rotor operating speed. Consequently, the time-dependent frequency of the excitation force passes through at least one critical frequency of the foundation system.

The results of the transient analysis are presented in the graphical form and discussed. The analysis is based on non-dimensional parametric studies of the system. The study shows that the maximum amplitude of vibration of low-tuned supporting structures is highly dependent on rotor acceleration rate through the critical (i.e. natural)

frequency of the foundation system. When compared to the results of classical steady-state analysis, the maximum amplitude obtained through the transient analysis is greater in magnitude and its position is shifted. These results indicate, that in the case of low-tuned structures, the transient analysis should be considered as a standard procedure in the present-day design practices.

The study suggests that the numerical procedure, and the computer program developed for this purpose, are useful for the transient analysis of the models of foundation-structure interacting with rotating machinery. The method of solution is general for any model of forcing function, and the computer program can easily be extended to handle more complex, two or three dimensional structures.

Table of Contents

Chapter Page

1. INTRODUCTION 1

1.1 Background Information 1

1.2 Scope of Study 4

2. FINITE TIME FORMULATION TO INITIAL-VALUE TRANSIENT PROBLEM 10

2.1 Preliminaries 10

2.2 Derivation of Reccurence Formulae 12

3. PHYSICAL MODELS DESCRIPTION 21

3.1 Preliminaries 21

3.2 Model 1 - Beam Supporting an Unbalanced Rotor Mounted on Rigid Bearings 25

3.2.1 Forcing function 25

3.2.2 Finite element model of supporting beam ...27

3.3 Model 2 - Portal Frame Supporting an Unbalanced Rotor Mounted on Rigid Bearings 29

3.3.1 Forcing function 29

3.3.2 Finite element model of supporting frame ..30

3.4 Model 3 - Beam Supporting an Unbalanced Rotor Mounted on Oil-Film Journal Bearings 32

3.4.1 Introduction 32

3.4.2 Dynamic analysis of journal bearing 34

3.4.3 Forcing function 39

4. COMPUTER PROGRAM DESCRIPTION 41

4.1 Main Features of the Computer Program 43

4.2 The Computer Program Organization 45

5. SIMULATION RESULTS AND DISCUSSION 47

5.1 Parametric Studies - Model 1 47

5.1.1 Preliminaries 47
5.1.2 Dynamic analysis 49
5.1.3 Concluding remarks 54
5.2 Parametric Studies - Model 2 68
5.2.1 Preliminaries 68
5.2.2 Dynamic analysis 70
5.2.3 Concluding remarks 73
5.3 Parametric Studies - Model 3 86
5.3.1 Preliminaries 86
5.3.2 Dynamic analysis 88
5.3.3 Concluding remarks 94
6. CONCLUSIONS AND RECOMMENDATIONS 111
REFERENCES 114
APPENDIX A-1: Nomenclature 117
APPENDIX A-2: Timoshenko beam elements' matrices 121
APPENDIX A-3: Computer program listing 126

List of Figures

Figure Page

1.1 Model of rotor and foundation system 8

1.2 Sketch of turbo-generator foundation block 8

1.3 Single-degree of freedom rotor-foundation model and its resonance diagram 9

3.1 Timoshenko beam elements 23

3.2 Beam supporting an unbalanced rotor 25

3.3 A typical transversal beam of the foundation block 27

3.4 Frame supporting an unbalanced rotor 29

3.5 A typical frame of the foundation block 31

3.6 Journal-bearing system 34

4.1 Schematic diagram of the computer program (MAIN) ...45

4.2 Schematic diagram of the computer program (subroutine BEAM) 46

5.1 Effect of rotor mass on the determination of system natural frequencies. 57

5.2 Build-up of beam vibration in response to excitation of an unbalance accelerating rotor. 58

5.3 Dynamic response of a beam, and an envelope of response maximum amplitudes. 59

5.4 Displacement envelopes versus time, for different values of beam slenderness parameter κ. 60

5.5 Displacement envelopes versus time, for different values of rotor acceleration time parameter β. 61

5.6 Relationship between displacement envelope and time, for various values of rotor speed parameter α. 62

5.7 Relationship between response maximum amplitude and rotor acceleration rate through the critical frequency, for different values of parameter α. 63

Figure Page

5.8 Effect of rotor acceleration rate through the critical frequency on shift of maximum amplitude from the critical frequency, for different values of parameter α. 64

5.9 Relationships between: (1) maximum amplitude of vibration, and (2) shift in its position from the critical frequency and constant rotor acceleration rate. 65

5.10 Displacement envelopes versus time, for different values of rotor speed parameter α; damping effect included. 66

5.11 Effect of damping on maximum amplitude of vibration, for different values of rotor speed parameter α. 67

5.12 Effect of frame parameter on natural frequencies of a portal frame; axial deformation in beams considered. 75

5.13 Effect of frame parameter on natural frequencies of a portal frame; axial deformation in beams neglected. 76

5.14 Comparison of lowest three natural frequencies of a portal frame. 77

5.15 Effect of rotor mass and frame geometry on system's lowest two natural frequencies. 78

5.16 Effect of rotor mass on lowest four natural frequencies of a portal frame. 79

5.17 Displacements in horizontal ("X") and vertical ("Y") directions at frame's driving point versus time. 80

5.18 Envelopes of response amplitudes at frame's driving point versus time. 81

5.19 Displacement envelopes versus time, for different values of rotor acceleration time parameter β. 82

5.20 Relationships between displacement envelopes and time, for various values of rotor speed parameter α. 83

Figure Page

5.21 Displacement envelopes versus time, for system with and without damping and for fixed values of parameters α and β. 84

5.22 Displacements at frame's driving point versus time, with rotor operating speed set to pass the third natural frequency. 85

5.23 Effect of rotor unbalance on steady-state whirl orbit of journal centre. 96

5.24 Displacement envelopes versus time for model with (1) journal bearing (JB), and (2) rigid bearing (RB). 97

5.25 Transient whirl orbit of journal centre due to rotor acceleration, for rotor unbalance parameter e/C=0.2. 98

5.26 Comparison of dynamic bearing forces for (1) journal bearing, and (2) rigid bearing. 99

5.27 Oil-film force magnification factor in journal bearing versus time. 100

5.28 Comparison of damping effect on system response for model with (1) journal bearing (JB) and (2) rigid bearing. 101

5.29 Transient whirl orbit of journal centre due to rotor acceleration, for rotor unbalance parameter e/C=0.1. 102

5.30 Effect of rotor unbalance on oil-film force magnification factor. 103

5.31 Displacement envelope versus time, for two different values of rotor unbalance parameter (e/C=0.1, 0.2). 104

5.32 Displacement envelope versus time for different values of rotor acceleration time parameter β. 105

5.33 Family of journal centre whirl loci for different values of rotor unbalance parameter e/C. 106

5.34 Transient whirl orbit of joutnal centre due to unsteady rotor angular velocity. 107

Figure Page

5.35 Displacement envelope versus time for model: with (1) journal bearing (JB), (2) and rigid bearing (RB). 108

5.36 Effect of rotor unbalance on system dynamic response for rotor speed parameter α=0.8, for model with (1) journal bearing, and (2) rigid bearing. 109

5.37 Oil-film force magnification factor versus time, for two different values of rotor unbalance parameter (e/C=0.1, 0.4). 110

1. INTRODUCTION

1.1 Background Information

It is well known that the life, efficiency and overall performance of all kinds of rotating machinery depend largely on the vibration of the machine and its supporting structure. An extensive investigation in the field of machinery vibration has been carried out for many years with numerous results of experimental and analytical works being published. Remarkable progress has been achieved in this field, especially during the past twenty-five years with the development of powerful, fast computers and new numerical techniques.

The demanding design requirements placed on modern rotating machinery have introduced a trend towards building units of larger size, higher speed, increased power and efficiency. As a result the task of minimizing and controlling the system vibration levels has become even more important. The trend to build larger rotary machines which rest on massive reinforced concrete or steel pedestals has brought changes into traditional design of machine foundation system and also created many problems in structural dynamics. Some of those problems are closely associated with the phenomenon of dynamic interaction between an elastic structure and a deformable machinery. While extensive research has been carried out on the rotor-dynamics, relatively little work is done on the machine-foundation interaction. It should be mentioned, however, that this problem has been recently attracting considerable attention from both the industrial and research communities. The dynamic response of the machine- foundation interacting system, in general, depends on design criteria and characteristics of the specific class of machinery and its supporting structure.

Figure 1.1[1] shows a schematic diagram of a large turbo-generator set, and Fig. 1.2, its foundation block. (This foundation block was resently built. Its design and innovative features are outlined by Ellyin [1][2]). There are four distinct elements, namely: (a) rotor, (b) bearings, (c) bearing pedestals, and (d) foundation block. They act as one system, together responding to rotor acceleration, critical speed, external excitation forces, et cetera. It is obvious that any change in the subsystem will affect the vibration levels of the other parts and, consequently, the dynamic response of the system as a whole. Therefore, a basic model for the dynamic analysis of the machine-foundation interacting system should include all those distinct elements.

The rotor, bearings and bearing pedestals are designed by a turbine manufacturer. The foundation block is usually designed by another organization using data and requirements provided by a machine manufacturer. The foundation block is a very important part of the system. It provides not only mass, flexibility and damping but also the essential coupling between other parts. There is a trend to build flexible foundations which are "low-tuned" (or "under-tuned") relative to the machine speed. In such cases, the machine service speed is at least higher than the first natural frequency of the supporting structure. Consequently, as the rotor is brought up in speed during start-up operation, the frequency of the forcing function[3] (i.e., exciting force) passes through one or more critical (i.e., resonant) frequencies of the foundation system. This can be best illustrated by a resonance diagram for an idealized single-degree of freedom model, as shown in Fig. 1.3.

---

[1] First number denotes Chapter. Figures are grouped at the end of each chapter in the order they are referenced to.
[2] numbers in square brackets designate Reference at the end of the thesis

Due to machine-foundation interaction, a turbomachinery designer must analyze the dynamic performance of the integrated system. The problem is extremely complex, and even with analytical and numerical tools available today, it constitutes a formidable task requiring a certain degree of model simplification.

In the present study the problem is approached from the foundation system designer's point of view. Accordingly, the analysis focuses on **the dynamic response of a supporting** structure excited by a force transmitted from the rotating machinery. Consequently, the difficulty now lies in defining a model of the forcing function which approximates the exciting force with reasonable accuracy.

---

[3] The sources of the exciting force are numerous. Here only the most common one (that due to rotor unbalance) is considered

Massive foundation blocks supporting modern turbmachinery are generally constructed from simple beam and frame elements (Fig. 1.2), constituting the main load transfer members of the supporting structure. To appreciate the dynamic behavior of the whole system, it is of great importance to (fully) understand the dynamic response of these simple elements. While there is an abundance of literature on steady-state modal analysis of beam and frame models, in contrast very few works are published on transient analysis of these elements.

1.2 Scope of Study

The dynamic response of a simply supported beam subjected to a force of time-dependent frequency has been investigated by Suzuki [2-4] and Victor & Ellyin [5]. An analytical approach to solving model equations of motion enabled the authors to carry out thorough parametric studies and to draw important conclusions. However, the proposed methods of solution limit their practical application to only: (a) simple structures, and (b) certain models of exciting force, which could be expressed by relatively simple analytical functions.

The present study attempts to fill a gap by basing method of solution on a finite element technique, thus making it suitable for more general models.
The main objectives of the present work are formulated as follows:

1. To develop a method of solution and a computer program, based on the principles of finite element technique, suitable for transient vibration analysis of different supporting structures subjected to any type of forcing function.

2. To verify the method of solution and test the computer program, by applying it to transient analysis of a model, already investigated by others.

3. To perform a transient analysis of a portal frame, as a model of foundation structure, supporting an unbalanced rotor mounted on rigid bearings.

4. To develop a model of a forcing function, assuming an unbalanced rotor mounted on oil-film journal bearings, and analyze dynamic behavior of a simple beam subjected to this excitation.

To achieve these objectives the study is divided into four stages summarized below:

Phase 1. Firstly, a general n-degree of freedom structure and its system of second order dynamic equations of motion is considered. Next, a finite element technique (applied to the time domain) is used to derive a finite-time formulation. Then, an initial value-transient problem is assumed and resulting reccurence scheme derived (Chapter 2). Finally, a computer program is developed which employs the reccurence formulae to advance the solution step-by-step in time (Chapter 4 and Appendix A-3).

Phase 2. A model (Model 1 -"Beam Supporting an Unbalanced Rotor Mounted on Rigid Bearings") is defined (Section 3.2). The forcing function proposed by Victor & Ellyin [5] is adopted (so that readily available results can be used) to verify the method of solution and computer program. Results of detailed parametric studies of the model are presented and discussed (Section 5.1).

Phase 3. A model (Model 2 -"Single Bay Portal Frame Supporting an Unbalanced Rotor Mounted on Rigid Bearings") is described (Section 3.3). Two components (in horizontal and vertical directions) of the exciting force, due to rotor unbalance, are considered. Results of numerical analysis, discussion and conclusions are presented (Section 5.2).

Phase 4. A model (Model 3 -"Beam Supporting an Unbalanced Rotor Mounted on Oil-Film Bearings") is developed (Section 3.4). Short bearing approximation, as suggested by Ocvirk [6], and non-linear performance of journal bearings, Holmes [7-8], are assumed. Results, discussion and concluding remarks are presented (Section 5.3).

A final chapter (Chapter 6) links the separate findings together and provides an overall conclusions and recommendations resulting from the study.

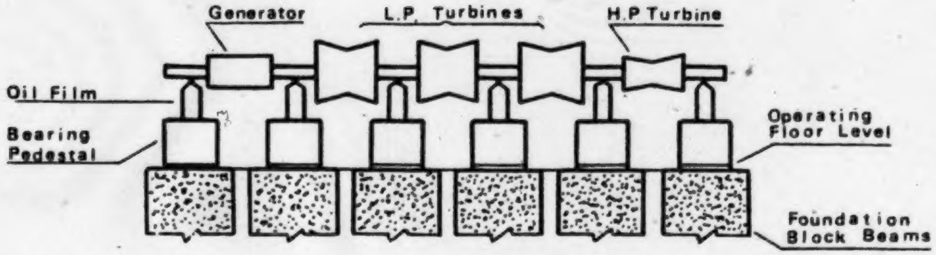
Generator
L.P. Turbines
H.P Turbine
Oil Film
Bearing Pedestal
Operating Floor Level
Foundation Block Beams

Fig. 1.1 Model of rotor and foundation system

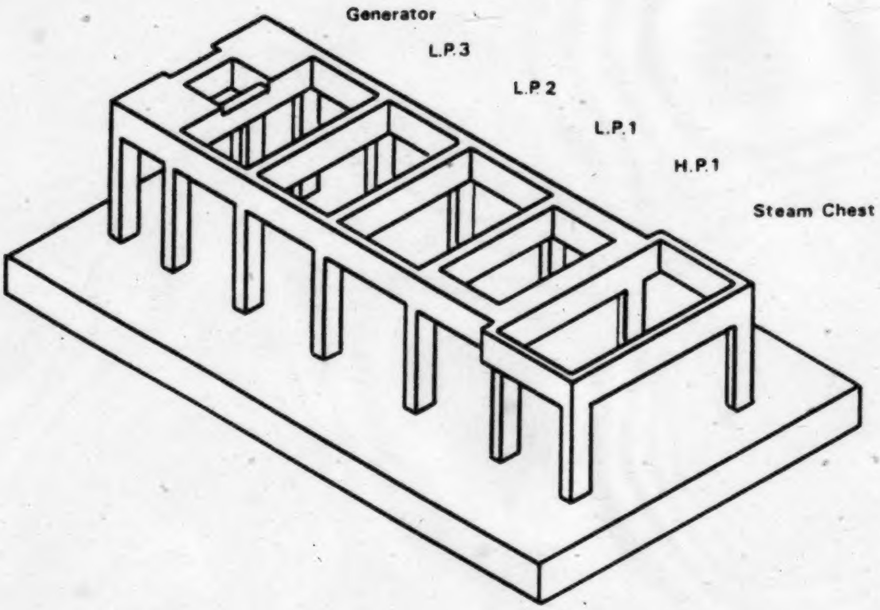
Generator
L.P.3
L.P.2
L.P.1
H.P.1
Steam Chest

Fig. 1.2 Sketch of turbo-generator foundation block

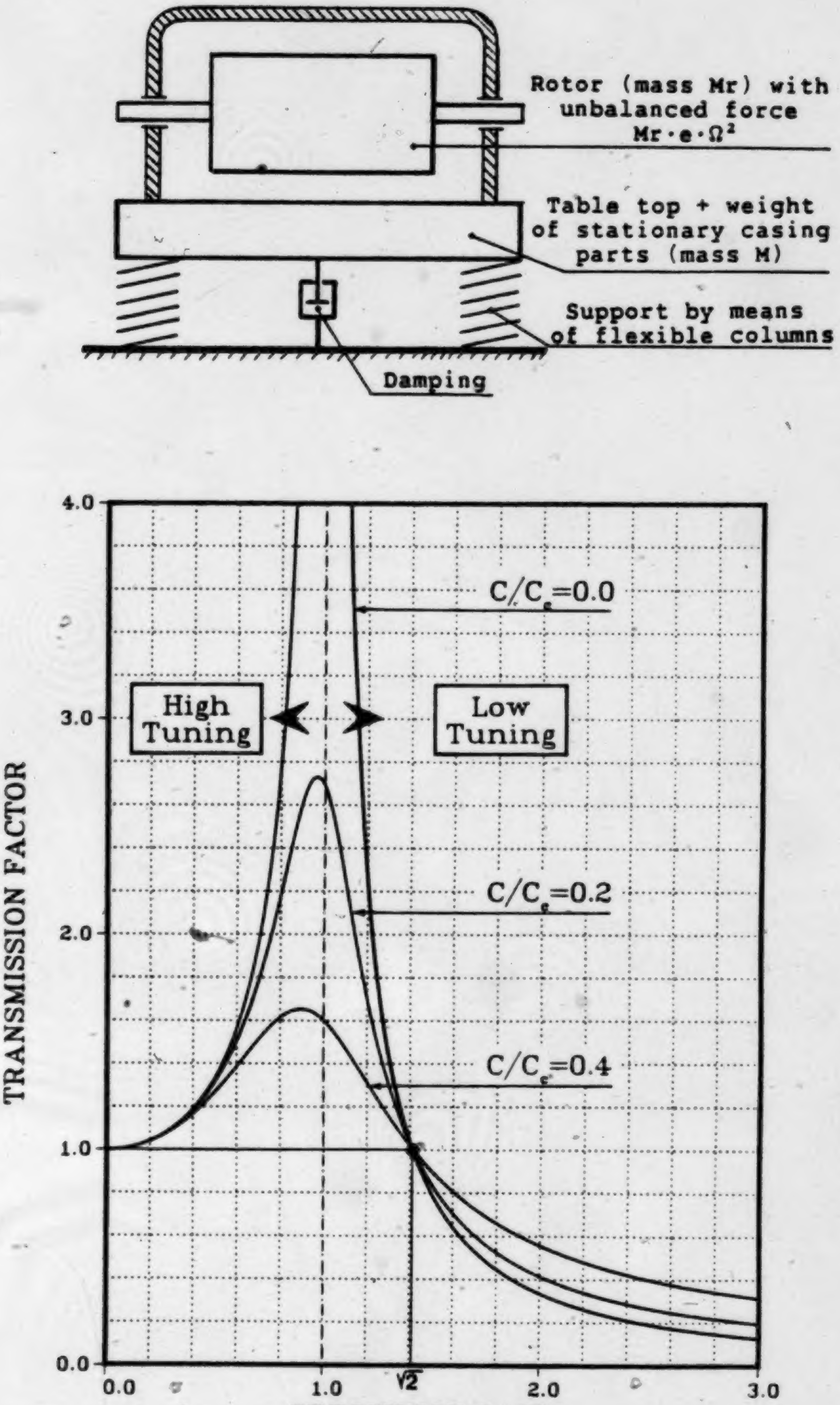
Rotor (mass Mr) with unbalanced force $Mr \cdot e \cdot \Omega^2$
Table top + weight of stationary casing parts (mass M)
Support by means of flexible columns
Damping
4.0
3.0
2.0
1.0
0.0
TRANSMISSION FACTOR
$C/C_c=0.0$
$C/C_c=0.2$
$C/C_c=0.4$
High Tuning
Low Tuning
0.0
1.0
$\sqrt{2}$
2.0
3.0
FREQUENCY RATIO

Fig. 1.3 Single-degree of freedom rotor-foundation model and its resonance diagram

2. FINITE TIME FORMULATION TO INITIAL-VALUE TRANSIENT PROBLEM

2.1 Preliminaries

The transient response analysis of a structural system generally involves discrete modelling of the structure, whereafter the continous physical structure is approximated by a discrete n-degree of freedom model. Regardless of the spatial discretization scheme employed, the resulting set of system dynamic equations of motion (in matrix form) becomes:

$$[M]\{\ddot{q}\}+[C]\{\dot{q}\}+[K]\{q\}=\{F\} \qquad (2.1)$$

where[4]: $[M]$[5], $[C]$ and $[K]$ are the (nxn) mass, damping and stiffness matrices; $\{F\}$ is the $(nx1)$ external load vector, and $\{\ddot{q}\}$, $\{\dot{q}\}$ and $\{q\}$ are the $(nx1)$ nodal acceleration, velocity and displacement vectors, respectively.

The set of ordinary differential equations (2.1) can be integrated forward in time to generate a transient solution. There are a great variety of direct time integration schemes, which fall into one of two major categories (or their combination), namely: explicit procedures and implicit procedures. Both methods have substantial advantages for certain classes of problems and disadvantages for others. Each specific scheme has different accuracy, stability characteristics and numerical efficiency. (An excellent review of the most widely used schemes and their suitability for various engineering problems is given by Donea, et al. [9]).

---

[4] A complete list of notation used is given in Appendix A-1.

[5] In some expressions it is appropriate to simplify matrix and vector notation. Throughout the text two notations are used interchangeably, e.g. $[M]\equiv\mathbf{M}$, $\{\dot{q}\}\equiv\dot{\mathbf{q}}$.

The time integration scheme developed for the purpose of the present analysis is based on a finite element (in time) approximation technique. A finite time element consists simply of a fixed time interval, Δt, which can be treated as a standard, one-dimensional finite element with two nodes at $t=t_1$ and $t=t_2$ ($\Delta t=\tau=t_2-t_1$).

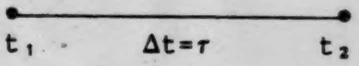

The general finite-element discretization process can, therefore, be applied to the time domain. First, the interval Δt is treated as a finite domain of time, and a **finite time formulation** is derived for the full original matrix equations (2.1). This formulation relates the values of vectors $\{\ddot{q}\}$, $\{\dot{q}\}$ and $\{q\}$ at time t_1 and t_2. As the time dimension is of an infinite extent, the solution for the initial value-transient problem is obtained by repeating the calculations for subsequent finite domains of time with new initial conditions.

2.2 Derivation of Reccurence Formulae

Consider a two-node element with three degrees of freedom per node:

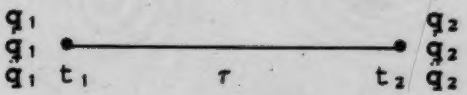

This gives six "time-wise" degrees of freedom per element. The problem now is to find a function **q**(t) which satisfies the equations of motion (2.1) and the following boundary conditions:

$$\begin{aligned} \mathbf{q}(t_1)&=\mathbf{q}_1 \quad \dot{\mathbf{q}}(t_1)=\dot{\mathbf{q}}_1 \quad \ddot{\mathbf{q}}(t_1)=\ddot{\mathbf{q}}_1 \\ \mathbf{q}(t_2)&=\mathbf{q}_2 \quad \dot{\mathbf{q}}(t_2)=\dot{\mathbf{q}}_2 \quad \ddot{\mathbf{q}}(t_2)=\ddot{\mathbf{q}}_2 \end{aligned} \tag{2.2}$$

In order to approximate the function **q**(t), satisfying the conditions (2.2), at least a fifth-order polynomial in time is required, as follows[4]:

$$\begin{aligned} q(t) &= a_1+a_2t+a_3t^2+a_4t^3+a_5t^4+a_6t^5 \\ &= [\ 1 \quad t \quad t^2 \quad t^3 \quad t^4 \quad t^5]\{a\} \end{aligned} \tag{2.3}$$

or rather, remembering that **q**(t) represents a vector (*nx1*) of nodal displacements with each component approximated by the same polynomial, a set of such polynomials is required, as follows:

$$\begin{aligned} \mathbf{q}(t) &= [\ I \quad tI \quad t^2I \quad t^3I \quad t^4I \quad t^5I\ ]\{a\} \\ &= [\Phi]^T\{a\} \end{aligned} \tag{2.4}$$

---

[4] The following formulation was provided to the author by the thesis supervisor, Dr F. Ellyin.

where:

- I - unit matrix of order $(n \times n)$
- $[\Phi]$ - matrix of time terms $(6n \times 6)$
- $\{a\}$ - vector of undetermined coefficients $(6n \times 1)$

The first and second derivatives of $\mathbf{q}(t)$ are obtained from eq. (2.4) as:

$$\begin{aligned} \dot{q}(t) &= [0 \quad I \quad 2tI \quad 3t^2I \quad 4t^3I \quad 5t^4I]\{a\} = [\dot{\Phi}]^T\{a\} \\ \ddot{q}(t) &= [0 \quad 0 \quad 2I \quad 6tI \quad 12t^2I \quad 20t^3I]\{a\} = [\ddot{\Phi}]^T\{a\} \end{aligned} \qquad (2.5)$$

The $(6n \times 1)$ coefficients $\{a\}$ can be evaluated in terms of nodal variables by matching the displacements, velocities and accelerations at the nodal points $t_1=0$ and $t_2=\tau$, which leads to:

$$\{q_n\} = \underset{(6n \times 1)}{\begin{bmatrix} \{q_1\} \\ \{\dot{q}_1\} \\ \{\ddot{q}_1\} \\ \{q_2\} \\ \{\dot{q}_2\} \\ \{\ddot{q}_2\} \end{bmatrix}} = \underset{(6n \times 6n)}{\begin{bmatrix} I & 0 & 0 & 0 & 0 & 0 \\ 0 & I & 0 & 0 & 0 & 0 \\ 0 & 0 & 2I & 0 & 0 & 0 \\ I & \tau I & \tau^2 I & \tau^3 I & \tau^4 I & \tau^5 I \\ 0 & I & 2\tau I & 3\tau^2 I & 4\tau^3 I & 5\tau^4 I \\ 0 & 0 & 2I & 6\tau I & 12\tau^2 I & 20\tau^3 I \end{bmatrix}} \underset{(6n \times 1)}{\begin{bmatrix} \{a_1\} \\ \{a_2\} \\ \{a_3\} \\ \{a_4\} \\ \{a_5\} \\ \{a_6\} \end{bmatrix}} \qquad (2.6)$$

or,

$$\{q_n\}=[T]\{a\} \qquad (2.7)$$

Therefore,

$$\{a\}=[T]^{-1}\{q_n\} \qquad (2.8)$$

where:

$$[T]^{-1}=1/2\tau^{9}\begin{bmatrix} 2\tau^{9}I & 0 & 0 & 0 & 0 & 0 \\ 0 & 2\tau^{9}I & 0 & 0 & 0 & 0 \\ 0 & 0 & \tau^{9}I & 0 & 0 & 0 \\ -20\tau^{6}I & -12\tau^{7}I & -3\tau^{8}I & 20\tau^{6}I & -8\tau^{7}I & \tau^{8}I \\ 30\tau^{5}I & 16\tau^{6}I & 3\tau^{7}I & -30\tau^{5}I & 14\tau^{6}I & -2\tau^{7}I \\ -12\tau^{4}I & -6\tau^{5}I & -\tau^{6}I & 12\tau^{4}I & -6\tau^{5}I & \tau^{6}I \end{bmatrix}$$

Hence, substituting eq. (2.8) into eqs. (2.4) and (2.5) gives an approximation for displacements, velocities and accelerations in terms of nodal variables $\{q_n\}$, as follows:

$$\begin{aligned} q(t) &\simeq [\Phi]^{T}[T]^{-1}\{q_n\} = [N]\{q_n\} \\ \dot{q}(t) &\simeq [\dot{\Phi}]^{T}[T]^{-1}\{q_n\} = [\dot{N}]\{q_n\} \\ \ddot{q}(t) &\simeq [\ddot{\Phi}]^{T}[T]^{-1}\{q_n\} = [\ddot{N}]\{q_n\} \end{aligned} \qquad (2.9)$$

where:

$$[N]=[\Phi]^{T}[T]^{-1}=[N_1\ N_2\ N_3\ N_4\ N_5\ N_6]$$

is the matrix of interpolation or shape functions, which in this case are fifth-order Hermitian polynomials [10].

Substituting eq. (2.9) into the equations of motion (2.1) gives

$$[M][\ddot{N}]\{q_n\}+[C][\dot{N}]\{q_n\}+[K][N]\{q_n\}-\{F\}\neq 0=\{R\} \qquad (2.10)$$

Note that upon substitution of the approximated functions (2.9), the equations of motion will generally not be satisfied. In fact, there is some residual $\{R\}$ left.

Now, the Galerkin (weighted residual) method can be employed to find l unknowns of the vector $\{q_n\}$ in such a way that the residual, $\{R\}$, over the entire domain, τ, is minimized with respect to the shape functions, N_i. This process can be expressed in the form of an integral equation as

$$\int_0^\tau N_i\{R\}dt = 0$$

or,

$$\int_0^\tau N_i([M][\ddot{N}]\{q_n\}+[C][\dot{N}]\{q_n\}+[K][N]\{q_n\}-\{F\})dt=0 \qquad (2.11)$$

Equation (2.11) represents l simultaneous equations in the l unknowns. In the case of an initial value problem, q_1, $\dot{q}_1$ and $\ddot{q}_1$ are assumed known and the above equation serves to approximately determine q_2, $\dot{q}_2$ and $\ddot{q}_2$. Quite generally, however, equation (2.11) can be rewriten in the form

$$\int_0^\tau [N]^T([M][\ddot{N}]\{q_n\}+[C][\dot{N}]\{q_n\}+[K][N]\{q_n\}-\{F\})dt=0 \qquad (2.12)$$

Substituting relationships (2.9) and $[N]^T=[T^{-1}]^T[\Phi]$ into (2.12) gives

$$[T^{-1}]^T\int_0^\tau(\{[\Phi][M][\ddot{\Phi}]^T+[\Phi][C][\dot{\Phi}]^T+[\Phi][K][\Phi]^T\}[T]^{-1}\{q_n\}$$
$$-[\Phi]\{F\})dt = 0 \qquad (2.13)$$

Carrying out simple integration and matrix multiplication leads to

$$([Z]_M+[Z]_C+[Z]_K)\{q_n\} = \{P\} \qquad (2.14)$$

where:

$$\{P\} = \int_0^{\tau} \begin{bmatrix} I \\ tI \\ t^2I \\ t^3I \\ t^4I \\ t^5I \end{bmatrix} \{F\}dt = \begin{bmatrix} \{P_1\} \\ \{P_2\} \\ \{P_3\} \\ \{P_4\} \\ \{P_5\} \\ \{P_6\} \end{bmatrix} \tag{2.15}$$

or,

$$\{P_i\} = \int_0^{\tau} t^{(i-1)}[I]\{F\}dt \qquad i=1,2,\ldots 6 \tag{2.16}$$

$$[Z]_M = \begin{bmatrix} 0 & -M & 0 & 0 & M & 0 \\ M & 0 & 0 & -M & \tau M & 0 \\ \tau M & \frac{1}{5}\tau^2M & \frac{1}{60}\tau^3M & -\tau M & \frac{4}{5}\tau^2M & \frac{1}{60}\tau^3M \\ \frac{6}{7}\tau^2M & \frac{6}{35}\tau^3M & \frac{3}{140}\tau^4M & \frac{-6}{7}\tau^2M & \frac{22}{35}\tau^3M & \frac{1}{35}\tau^4M \\ \frac{5}{7}\tau^3M & \frac{3}{14}\tau^4M & \frac{3}{140}\tau^3M & \frac{-5}{7}\tau^3M & \frac{1}{2}\tau^4M & \frac{1}{28}\tau^5M \\ \frac{25}{42}\tau^4M & \frac{4}{21}\tau^5M & \frac{5}{252}\tau^6M & \frac{-25}{42}\tau^4M & \frac{17}{42}\tau^5M & \frac{5}{126}\tau^6M \end{bmatrix} \tag{2.17}$$

$$[Z]_C = \begin{bmatrix} -C & 0 & 0 & C & 0 & 0 \\ \frac{-1}{2}C & \frac{-1}{10}\tau^2C & \frac{-1}{120}\tau^3C & \frac{1}{2}\tau C & \frac{1}{10}\tau^2C & \frac{-1}{120}\tau^3C \\ \frac{-2}{7}\tau^2C & \frac{-8}{105}\tau^3C & \frac{-1}{140}\tau^4C & \frac{2}{7}\tau^2C & \frac{13}{105}\tau^3C & \frac{-1}{105}\tau^4C \\ \frac{-5}{28}\tau^3C & \frac{-3}{56}\tau^4C & \frac{-3}{560}\tau^5C & \frac{5}{28}\tau^3C & \frac{1}{8}\tau^4C & \frac{-1}{112}\tau^5C \\ \frac{-5}{42}\tau^4C & \frac{-4}{105}\tau^5C & \frac{-1}{252}\tau^6C & \frac{5}{42}\tau^4C & \frac{5}{42}\tau^5C & \frac{-1}{126}\tau^6C \\ \frac{-1}{12}\tau^5C & \frac{-1}{36}\tau^6C & \frac{-1}{336}\tau^7C & \frac{1}{12}\tau^5C & \frac{1}{8}\tau^6C & \frac{-1}{144}\tau^7C \end{bmatrix} \quad (2.18)$$

$$[Z]_K = \begin{bmatrix} \frac{1}{2}\tau K & \frac{1}{10}\tau^2K & \frac{1}{120}\tau^3K & \frac{1}{2}\tau K & \frac{-1}{10}\tau^2K & \frac{1}{120}\tau^3K \\ \frac{1}{7}\tau^2K & \frac{4}{105}\tau^3K & \frac{1}{280}\tau^4K & \frac{5}{14}\tau^2K & \frac{-13}{210}\tau^3K & \frac{1}{210}\tau^4K \\ \frac{5}{84}\tau^3K & \frac{1}{56}\tau^4K & \frac{1}{560}\tau^5K & \frac{23}{84}\tau^3K & \frac{-1}{24}\tau^4K & \frac{1}{336}\tau^5K \\ \frac{5}{168}\tau^4K & \frac{1}{105}\tau^5K & \frac{1}{1008}\tau^6K & \frac{37}{168}\tau^4K & \frac{-5}{168}\tau^5K & \frac{1}{504}\tau^6K \\ \frac{1}{60}\tau^5K & \frac{1}{180}\tau^6K & \frac{1}{1680}\tau^7K & \frac{11}{60}\tau^5K & \frac{-1}{45}\tau^6K & \frac{1}{720}\tau^7K \\ \frac{1}{99}\tau^6K & \frac{4}{1155}\tau^7K & \frac{1}{2640}\tau^8K & \frac{31}{198}\tau^6K & \frac{-17}{990}\tau^7K & \frac{1}{990}\tau^8K \end{bmatrix} \quad (2.19)$$

Introducing

$$[Z] = [Z]_M + [Z]_C + [Z]_K$$

into equation (2.14), the general relationship can be written as

$$[Z]\{q_n\} = \{P\} \quad (2.20)$$

or,

$$\underset{(6n\mathrm{x}6n)}{\left[\begin{array}{c:c} [Z_{11}] & [Z_{12}] \\ \hdashline [Z_{21}] & [Z_{22}] \end{array}\right]} \underset{(6n\mathrm{x}1)}{\begin{bmatrix} \{q_1\} \\ \{\dot{q}_1\} \\ \{\ddot{q}_1\} \\ \cdots \\ \{q_2\} \\ \{\dot{q}_2\} \\ \{\ddot{q}_2\} \end{bmatrix}} = \underset{(6n\mathrm{x}1)}{\begin{bmatrix} \{P_1\} \\ \{P_2\} \\ \{P_3\} \\ \cdots \\ \{P_4\} \\ \{P_5\} \\ \{P_6\} \end{bmatrix}} \qquad (2.21)$$

For an initial value problem, only part of the general time formulation (2.21) is required to determine q_2, $\dot{q}_2$ and $\ddot{q}_2$. Thus,

$$\begin{bmatrix} Z_{11} \end{bmatrix} \begin{bmatrix} \{q_1\} \\ \{\dot{q}_1\} \\ \{\ddot{q}_1\} \end{bmatrix} + \begin{bmatrix} Z_{12} \end{bmatrix} \begin{bmatrix} \{q_2\} \\ \{\dot{q}_2\} \\ \{\ddot{q}_2\} \end{bmatrix} = \begin{bmatrix} \{P_1\} \\ \{P_2\} \\ \{P_3\} \end{bmatrix} \qquad (2.22)$$

Applying simple matrix algebra and rearranging terms in eq. (2.22) leads to the formulae:

$$\begin{bmatrix} \{q_2\} \\ \{\dot{q}_2\} \\ \{\ddot{q}_2\} \end{bmatrix} = \begin{bmatrix} Z_{12} \end{bmatrix}^{-1} \left\{ \begin{bmatrix} \{P_1\} \\ \{P_2\} \\ \{P_3\} \end{bmatrix} - \begin{bmatrix} Z_{11} \end{bmatrix} \begin{bmatrix} \{q_1\} \\ \{\dot{q}_1\} \\ \{\ddot{q}_1\} \end{bmatrix} \right\} \qquad (2.23)$$

In the foregoing it has been assumed that the domain of the approximation corresponds to interval Δt. Equation

(2.23) represents a reccurence relation between two sucessive values of vectors $\mathbf{q}(t+\Delta t)$, $\dot{\mathbf{q}}(t+\Delta t)$,$\ddot{\mathbf{q}}(t+\Delta t)$ and $\mathbf{q}(t)$, $\dot{\mathbf{q}}(t)$, $\ddot{\mathbf{q}}(t)$. This relation will be used in a computer program for a sequence of such domains in a step-by-step manner to advance a solution in time.

The step-by-step reccurance scheme just derived is conditionally stable. This means that for numerical stability (convergence of solution), the time step Δt cannot exceed some critical value. This critical value, in general, is "controlled" by the system's highest natural frequency (ω_m) and the requirement for stability is $\Delta t<a/\omega_m$. A value of constant "a" depends on stability characteristics of a specific scheme used. Stability analysis for several widely used schemes and resulting analytical expressions for a's are given in reference [11]. Such analysis for the present scheme (due to the high order interpolation used) proved to be difficult. It should suffice to say that from the practical experience of this work $a\simeq1.4$.

In general, the dynamic equations of motion (2.1) can be non-linear if, for instance, the damping matrix is frequency dependent or, as in the case of large deformation, the stiffness matrix depends on displacements. However, in the present analysis, only linear systems are considered. It is, therefore, assumed that the system [M], [C] and [K] matrices **are not time dependent** and consequently neither are $[Z_{11}]$ and $[Z_{12}]$. As a result, in comparison with the non-linear system, a small amount of computing time and simple program organization is required. Matrix $[Z_{12}]$ has to be inverted only once and then, for each time step, only integration (to evaluate components P_i, eq. 2.16) and simple matrix multiplication is involved.

3. PHYSICAL MODELS DESCRIPTION

3.1 Preliminaries

In the present analysis the dynamic response of two simple models of support structure subjected to the action of an unbalanced rotor are examined, namely:

1. a beam simply supported at its ends
2. a single bay portal frame with both legs clamped

Distributed inertial and elastic properties of these structures are modelled, using the consistent mass and stiffness matrices of the finite element approximation [11]. A number of finite beam elements have been proposed in the literature [12-21]. They are based on either: (i) Bernoulli-Euler or (ii) Timoshenko beam bending theories.

The classical Bernoulli-Euler theory of flexural vibration of beams considers only the lateral inertial and elastic forces due to bending deflections. This theory is satisfactory for dynamic analysis of long, thin beam models with a small slenderness ratio, k/L (i.e. $\sqrt{I/A}/L$). However, large rotating machinery support systems are usually composed of short stubby beams. In such cases, the secondary effects of the shear deformation and rotary inertia of the cross-section of the beam cannot be neglected. These secondary effects are included in the Timoshenko beam theory. Therefore, the finite elements based on this theory, known as the Timoshenko beam finite elements, are used in this study.

Two different models of the Timoshenko beam finite element are used in the present work, namely those: (a) proposed by Davis, et al [13], and (b) by Akella & Craggs [21]. The nodal variable *u* (axial displacements) is added to the original beam elements to enable axial-flexural coupling in the framework models (see Fig. 3.1). For easy reference, mass and stiffness matrices for both these elements are given in explicit form in Appendix A-2. The generalized coordinates at each node of element (a) represent: w- transverse displacement, θ- cross-section rotation, u- axial displacement, and for element (b): w- transverse displacement, ϕ- bending slope, $A\psi$- shear slope, hence shear force, $I\phi'$- bending moment and u- axial displacement.

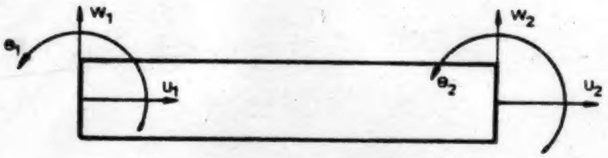

a) Simple

$\theta = dw/dx + \psi$

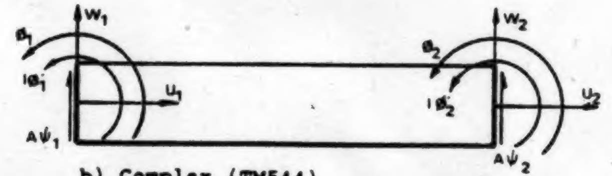

b) Complex (TM544)

$\phi = dw/dx + \psi$
$V = GKA\psi$
$M = EI\phi'$

Fig. 3.1 Timoshenko beam elements

The aforementioned element matrices are used in the structure discretization process as follows:

1. A model of the concerned structure is divided into a number of elements, for which each of the element mass [EM] and stiffness [EK] matrices are evaluated.
2. A standard finite element assemblage process is employed to form global mass [GM] and stiffness [GK] matrices.
3. Global matrices are modified to incorporate system constraints and boundary conditions.

Upon completion of this proces, a continous structure is approximated by using the spatially discrete n-degree of freedom model with $(n\mathrm{x}n)$ system mass [M] and stiffness [K] matrices.

For most practical structures, the exact form of damping is unknown, and damping properties are frequency dependent. However, in order to take advantage of the explicit time stepping scheme, it is necessary to evaluate the damping matrix explicitly. One procedure for defining a system damping matrix is to employ a particular form of proportional damping, given as

$$[C] = a[M] + b[K] \tag{3.1}$$

where, a and b are proportionality constants. Such damping, known as "Rayleigh damping" [22], is used in the present analysis.

As mentioned in the Introduction, a self-excited vibration of rotating machinery could be generated by many different sources of excitation (e.g. rotor imbalance, internal friction, misalignment, gyroscopic moments, hydrodynamic fluid-film forces, et cetera [23]). In the present study, only the most common source of excitation, i.e., the rotor unbalance, is considered.

A force transmitted from an unbalanced rotor to its foundation is an extremely complex function of many parameters. In general, it depends on rotor geometry and flexibility, and on mounting details, that is characteristics of bearings, bearing seals, bearing pedestals, and so on.

In the present work the following simplifying assumptions (general for all models) are made:

1. Symmetric rotors are represented by a lumped mass (2Mr) located centrally between two identical bearings.
2. Rotor shafts are massless and absolutely rigid.
3. Bearing pedestals are neglected.
4. Loads are only in one plane.

3.2 Model 1 - Beam Supporting an Unbalanced Rotor Mounted on Rigid Bearings

3.2.1 Forcing function

To further simplify the study, rigid bearings are assumed for the model shown in Fig. 3.2.

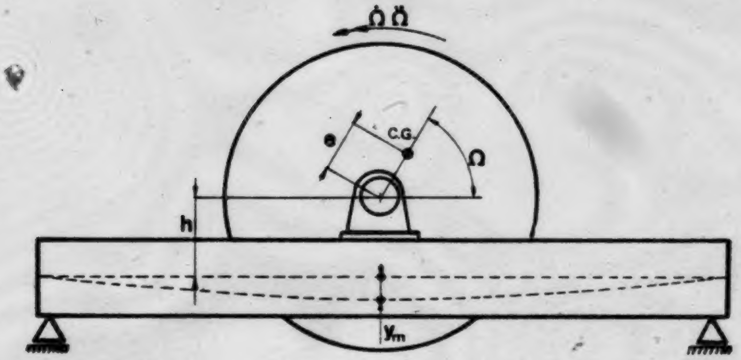

Fig. 3.2 Beam supporting an unbalanced rotor

Taking all the assumptions from the previous section into consideration, the forcing function for this model can be expressed by the following equation:

$$F_y(t)=-Mr\cdot d^2[e\cdot \sin\Omega(t)+h+y_m(t)]/dt^2 \qquad (3.2)$$

Carrying out the deriviation leads to

$$F_y(t)= Mr\cdot e(\dot{\Omega}^2\sin\Omega-\ddot{\Omega}\cos\Omega) - Mr\cdot \ddot{y}_m \qquad (3.3)$$

or

$$F_y(t)=\bar{F}_y(t)-Mr\cdot \ddot{y}_m(t) \qquad (3.4)$$

where:

$\bar{F}_y$ - a vertical component of an inertia force due to rotational motion of an unbalanced rotor

$Mr\cdot \ddot{y}_m$ - an inertia force due to rotor acceleration in its linear motion

As in reference [5], it is assumed that the torque applied to the rotor by the power source is constant during the acceleration time (T_1). This means that in an ideal situation (with no vibration) the rotor angular acceleration would also be constant. In reality, however, part of the torque is absorbed by the vibration. Because of the build up of vibration, the torque associated with the unbalance reduces the rotor angular acceleration. Thus, the angular acceleration $\ddot{\Omega}$, velocity $\dot{\Omega}$, and travel Ω, are assumed to vary with time according to the formula:

$$\begin{array}{ll}
\text{for} \quad 0<t\le T_1 & \text{for} \quad t>T_1 \\
 & \\
\ddot{\Omega}=\omega_s(1-t/T_1)2/T_1 & \ddot{\Omega}=0 \\
\dot{\Omega}=\omega_s(2t/T_1-t^2/T_1^2) & \dot{\Omega}=\omega_s \\
\Omega=\omega_s T_1(3t^2/T_1^2-t^3/T_1^3)/3 & \Omega=\omega_s(t-T_1/3)
\end{array} \qquad (3.5)$$

3.2.2 Finite element model of supporting beam

A typical transversal beam of the reinforced-concrete foundation block (shown in Fig. 1.2) is chosen for the dynamic analysis. Its geometric parameters and material constants are given below

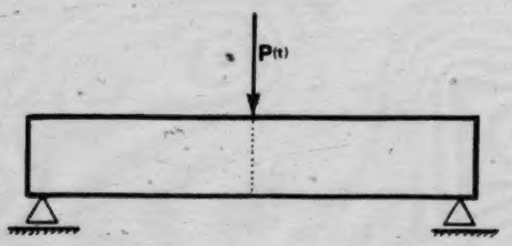

$L = 300.0$ in $\nu = 0.15$ $K = 0.85$

$A = 7150.0$ in^2 $\rho = 146.9$ lb/ft^3

$I = 9266400.0$ in^4 $E = 5500000.0$ lb/in^2

Fig. 3.3 A typical transversal beam of the foundation block

The high order finite element (TM544) is used to approximate inertial and elastic properties of the continous beam. This finite element is chosen for the numerical analysis because, in comparison with other available Timoshenko beam elements, it is more accurate and converges faster per degree of freedom for beams with $k/L>0.05$. The beam selected for the analysis (Fig. 3.3) has a k/L ratio equal to 0.12.

The accuracy of a finite element approximation depends on the number of elements used in the discretization process. In general, the greater this number, the more degrees of freedom considered and the better accuracy. However, at the same time, the size of the problem and consequently the cost of numerical analysis is greater.

In order to assess a minimal number of finite elements required for beam approximation (sufficient for the purpose of this project), a preliminary study was carried out. Natural frequencies and dynamic response of the beam idealized by 2 elements and by 4 elements (which gives 9 and 19 D.O.F of the constrained systems respectively) were calculated and compared. No appreciable difference in dynamic response but dramatic increase in the cost of solution was observed in the second case. This can be explained by the fact that the response is dominated by the frequencies of lower modes which are predicted with sufficient accuracy by the 2-element model. On the other hand, the dimensions of the finite element matrices, which determine the size of the problem, increased from (27x27) in the first case to (57x57) in the second. Moreover, since the time step required for numerical stability is controlled by the highest mode frequency, for the 4-element model this time step has to be reduced considerably. Taking the above into consideration, the 2-element model approximation is used for further analysis of the beam.

3.3 Model 2 - Portal Frame Supporting an Unbalanced Rotor Mounted on Rigid Bearings

3.3.1 Forcing function

All the simplifying assumptions discussed in the previous section are also applied to Model 2, of which a schematic diagram is shown in Fig. 3.4.

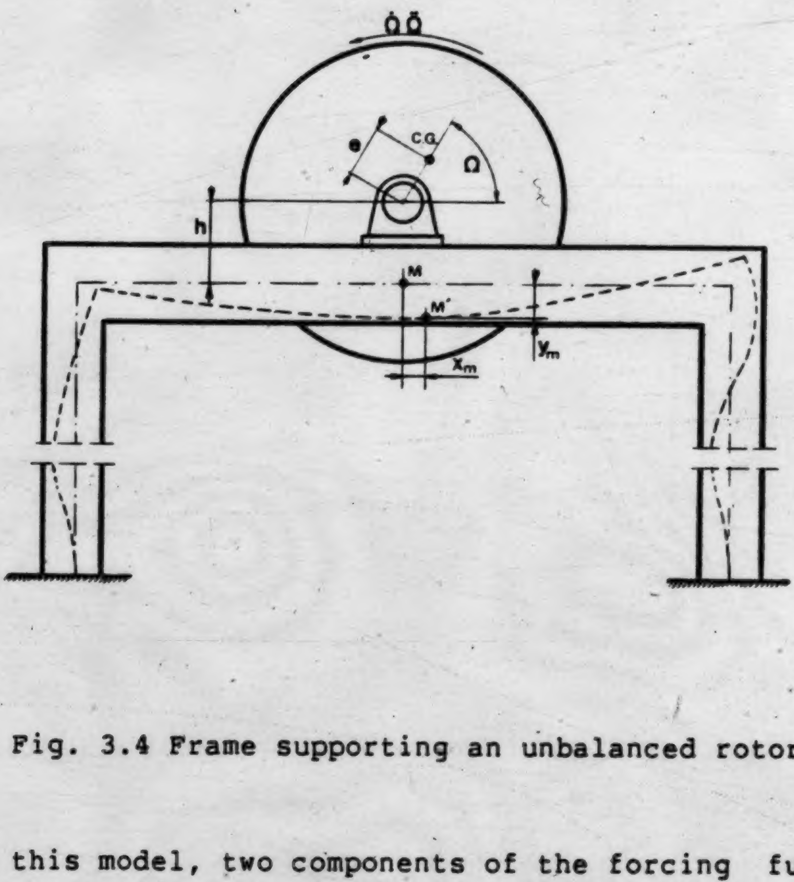

Fig. 3.4 Frame supporting an unbalanced rotor

In this model, two components of the forcing function, are considered, in horizontal and vertical directions. Applying the same reasoning as in Model 1 leads to the expressions

$$\begin{aligned} F_x(t) &= Mr\cdot e(\dot{\Omega}^2\cos\Omega+\ddot{\Omega}\sin\Omega) - Mr\cdot\ddot{x}_m \\ F_y(t) &= Mr\cdot e(\dot{\Omega}^2\sin\Omega-\ddot{\Omega}\cos\Omega) - Mr\cdot\ddot{y}_m \end{aligned} \qquad (3.6)$$

where Ω, $\dot{\Omega}$ and $\ddot{\Omega}$ are assumed to vary with time according to eqs. (3.5).

3.3.2 Finite element model of supporting frame

A typical frame of the turbo-generator foundation block (shown in Fig. 1.2) is chosen for numerical analysis as a supporting structure in Model 2. Geometric parameters of the frame columns are given in Fig. 3.5. Material constants and beam geometry are identical to those in Model 1 (Fig. 3.3).

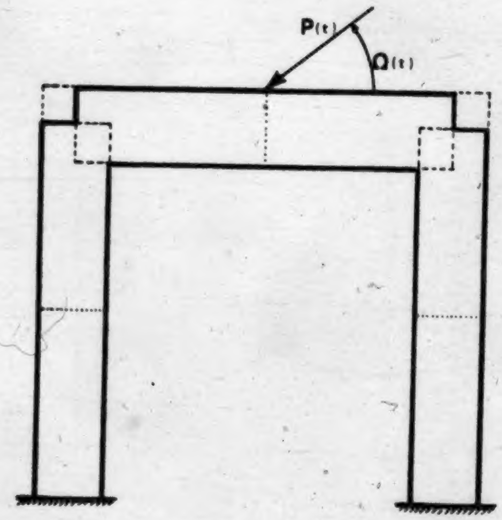

Column geometric parameters:

L= 600.0 in   A= 3980.0 in²   I= 895500.0 in⁴

Fig 3.5 A typical frame of the foundation block

A preliminary study done on this model showed no advantage in using complex Timoshenko beam elements for idealizing the frame. In fact, the use of simple elements manifests faster convergence per degree of freedom. This is so because the columns of the frame selected for numerical analysis are fairly slender (k/L=0.025), while the high order elements prove to be superior for shorter stubby beams in which shear and rotary inertia are particularly important. The simplest Timoshenko beam element (with centroidal displacement and cross-section rotation as nodal variables) is the most suitable for the analysis of complex structure and the most commonly used in general purpose computer packages [20-21]. As a result of the preliminary study, the 6-element model approximation was chosen for the dynamic analysis of the frame, giving 15 D.O.F. for the constrained structure.

In the present finite element model of the frame, there is geometric misrepresentation of the structure at the corners where two beams are joined at right angles (see Fig. 3.5). However, this misrepresentation can be avoided in general analyses of frameworks by developing beam finite elements with special ends [13].

3.4 Model 3 - Beam Supporting an Unbalanced Rotor Mounted on Oil-Film Journal Bearings

3.4.1 Introduction

Hydrodynamic bearings play a very important part in rotating machinery vibration problems. Their three major functions are: (a) to support loads (static and dynamic), (b) to control rotor position, and (c) to provide stiffness and damping. Bearing film damping has a dominant effect on rotor vibration. The importance of correct selection of the bearing and lubricant parameters, depending on design load and speed, cannot be exaggerated.

The dynamics of rotor-bearing systems has become of great importance due to the technological advancement in modern rotating equipment, and has been studied extensively [6-8],[24-34]. The field is very broad and complex. Researchers usually devise simplified models and focus their studies on particular problem such as, system instability, response to shock or unbalance excitation, effect of rotor and support flexibility and/or damping on system response, et cetera. The vast majority of papers reviewed by the author, in relation to this project, consider the system behavior about its equilibrium position, that is assuming constant rotor speed. In fact, the complete transient analysis of rotor-bearing system during the whole period of start-up until the steady state operation does not seem to have been reported in the literature.

In the following section, a simplified analysis is presented, which leads to determination of the dynamic oil-film forces induced in the journal bearing by an unbalanced accelerating rotor. The resultant of these forces (in vertical direction) is then considered in the original problem as a component of forcing function exciting rotor supporting beam.

The analysis is based on the following simplifying assumptions:

1. An ideal, symmetric rotor allows to consider the motion of one journal only.
2. The Reynolds' equation (lubrication equation) for an incompressible lubricant is applicable.
3. Viscosity is constant throughout the oil-film, and does not change with time.
4. Oil-film pressure at the ends of the bearing is atmospheric.
5. Flow of lubricant in the bearing axial direction can be neglected.
6. Only positive pressure contributes to the bearing dynamic film forces.

3.4.2 Dynamic analysis of journal bearing

Consider a journal-bearing system shown schematically in Fig. 3.6

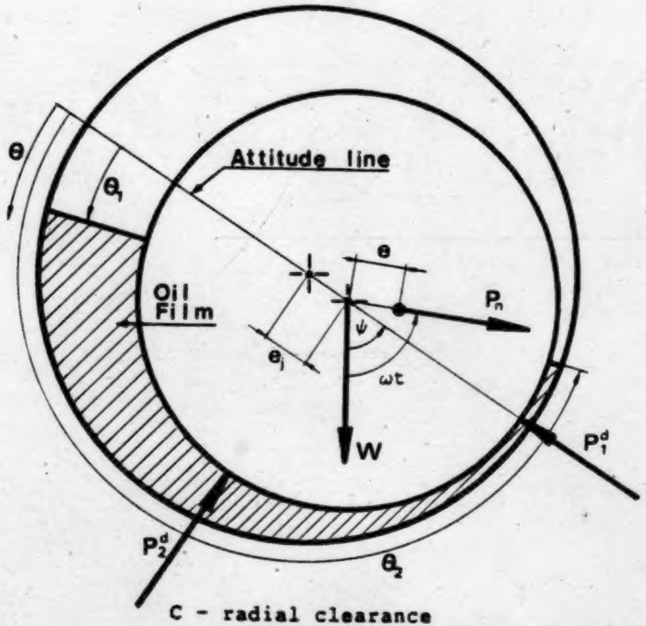

C - radial clearance
$\epsilon = e_j/C$ - journal centre eccentricity
$h = C(1 + \epsilon\cos\theta)$ - oil film thickness

Fig. 3.6 Journal-bearing system

Consider first the case when shaft angular velocity ω is constant. The journal is in motion due to the action of four external forces, namely: static load (weight) W, centrifugal force due to rotor unbalance P_n, and hydrodynamic oil-film forces P_1^d and P_2^d. In analyzing the motion of the journal, it is convenient to employ polar coordinates rather than Cartesian. (The polar coordinates used are, the eccentricity ratio ϵ and the attitude angle ψ). Assuming that the hydrodynamic force P_1^d acts in the positive ϵ-direction (i.e. opposite to that shown in Fig. 3.6), the equations of the journal centre motion may be written

$$\begin{aligned} &P_1^d+W\cos\psi+P_n\cos(\omega t-\psi)=MrC(\ddot{\epsilon}-\dot{\psi}^2\epsilon) \\ &P_2^d-W\sin\psi+P_n\sin(\omega t-\psi)=MrC(\epsilon\ddot{\psi}+2\dot{\epsilon}\dot{\psi}) \end{aligned} \qquad (3.7)$$

The set of equations (3.7) can be easily solved using one of many available numerical schemes. The only problem is, that it requires evaluation of the dynamic film forces (P_1^d, P_2^d) at each time step. These forces are determined by integrating oil-film pressure distribution around the journal circumference. The pressure distribution, in turn, is obtained by integrating Reynolds' lubrication equation which, in general, has to be done numerically. Considering the fact that the time step required for solution of eqs. (3.7) has to be small enough to give 100 increments per cycle of shaft motion [32], the calculation of bearing forces for relatively long transient period can prove to be very expensive in terms of computer time.

The Reynolds' equation for a plain cylindrical bearing, whose journal centre position is time dependent, is usually written in the form [35]:

$$(1/R)\partial[(h^3/R)\partial p/\partial\theta]/\partial\theta+\partial(h^3\partial p/\partial z)/\partial z=6\mu(\omega-2\dot{\psi})\partial h/\partial\theta+12\mu C\dot{\epsilon}\cos\theta \qquad (3.8)$$

Holmes [7], reports that his experimental works support the use of short bearing approximation (due to Ocvirk [6]) in describing the dynamic behavior of modern turbine bearings. Ocvirk showed that for short bearing $(L/D<1)$ $\partial p/\partial\theta \ll \partial p/\partial z$, which allows to neglect the first term in equation (3.8). Thus

$$\partial(h^3\partial p/\partial z)/\partial z=6\mu(\omega-2\dot{\psi})\partial h/\partial\theta+12\mu C\dot{\epsilon}\cos\theta \qquad (3.9)$$

This greately simplifies the problem, since the reduced Reynolds' equation (3.9) can be integrated analytically. Integrating twice with respect to z and applying boundary conditions: $p=0$[7] at $z=0$ and at $z=L$ yields

$$p=3\mu z(z-L)[2\dot{\epsilon}\cos\theta-(\omega-2\dot{\psi})\epsilon\sin\theta][C^2(1+\epsilon\cos\theta)^3]^{-1} \qquad (3.10)$$

The oil-film forces, P_1^d and P_2^d, can now be obtained by integration as follows:

$$\begin{aligned} P_1^d &= R\int_0^L \int_{\theta_1}^{\theta_2} p\cos\theta\, d\theta\, dz \\ P_2^d &= R\int_0^L \int_{\theta_1}^{\theta_2} p\sin\theta\, d\theta\, dz \end{aligned} \qquad (3.11)$$

Integration of eq. (3.11) is straight forward provided that the limits of integration θ_1 and θ_2 are known. In his earlier work, Holmes [7], suggests that these limits lie at the points were the pressure, p, becomes zero (see Fig. 3.6) and can be determined from eq. (3.10) as:

$$\begin{aligned} \theta_1 &= \tan^{-1}[2\dot{\epsilon}/\{\epsilon(\omega-2\dot{\psi})\}] \\ \theta_2 &= \theta_1 + \pi \end{aligned} \qquad (3.12)$$

---

[7] zero pressure corresponds to atmospheric pressure

According to his later paper [8], much better agreement with the experimental results is achieved by putting

$$\theta_1 = 0 \quad \text{and} \quad \theta_2 = \pi \tag{3.13}$$

Carrying out integration of eqs. (3.11), with the limits of integration given by (3.13) yields

$$\begin{aligned} P_1^d &= -(\mu L^3 R/2C^2)[\pi(1+2\epsilon^2)\dot{\epsilon}+2(\omega-2\dot{\psi})\epsilon^2(1-\epsilon^2)^{1/2}](1-\epsilon^2)^{-5/2} \\ P_2^d &= (\mu L^3 R/2C^2)[4\epsilon\dot{\epsilon}+\pi\epsilon(\omega-2\dot{\psi})(1-\epsilon^2)^{1/2}/2](1-\epsilon^2)^{-2} \end{aligned} \tag{3.14}$$

Under static conditions (i.e. in an ideal case of perfectly balanced rotor) the journal centre takes an equilibrium position (ϵ_0, ψ_0), which depends on bearing geometry (L, R and C), lubricant viscosity (μ), static load (W) and angular shaft velocity (ω). This position is given by the well known relationships [35]:

$$S_m=(1-\epsilon_0^2)^2[\epsilon_0\{16\epsilon_0^2+\pi^2(1-\epsilon_0^2)\}^{1/2}]^{-1} \tag{3.15}$$

$$\psi_0=\tan^{-1}[\pi(1-\epsilon_0^2)^{1/2}/4\epsilon_0] \tag{3.16}$$

where S_m, known as modified Sommerfeld Number, is defined as:

$$S_m=\mu L^3 R\omega/4C^2 W \tag{3.17}$$

Relationship (3.17) can be rewritten

$$(\mu L^3 R/2C^2)=2S_m W/\omega \tag{3.18}$$

It is apparent, when comparing eqs. (3.18) and (3.14), that for the given load W, and angular velocity ω, dynamic bearing forces, P_1^d and P_2^d are functions of: $\epsilon_0, \epsilon, \dot{\epsilon}, \psi$ and $\dot{\psi}$.

Now, for the given system parameters, if initial values for ϵ, $\dot{\epsilon}$, ψ and $\dot{\psi}$ are known or assumed, the dynamic bearing forces can be calculated using eqs. (3.14) afterwhich the equations of motion (3.7) can be solved. Repeating the calculations in a time stepping manner, the solution for the shaft centre motion and dynamic oil-film forces is advanced in time. By non-dimensionalizing eqs. (3.7) it can be shown [7] that, for constant angular velocity ω, the shaft center motion is governed by three independent non-dimensional parameters, namely: ϵ_0, e/C and $g/C\omega^2$.

Considering the case when angular shaft velocity is time dependent, the equations of motion for the journal centre may be written

$$\begin{aligned} &P_1^d+W\cos\psi+Mr\cdot e\dot{\Omega}^2\cos(\Omega-\psi)+Mr\cdot e\ddot{\Omega}\sin(\Omega-\psi)=MrC(\ddot{\epsilon}-\dot{\psi}^2\epsilon) \\ &P_2^d-W\sin\psi+Mr\cdot e\dot{\Omega}^2\sin(\Omega-\psi)-Mr\cdot e\ddot{\Omega}\cos(\Omega-\psi)=MrC(\epsilon\ddot{\psi}+2\dot{\epsilon}\dot{\psi}) \end{aligned} \qquad (3.19)$$

These equations differ from eqs. (3.7) only by one additional term,- that is an inertia force due to shaft circumferential acceleration.

The Reynolds' equation of lubrication (3.8) is derived from the general Navier-Stokes equations [35] by considering several simplifying assumptions. One of the assumptions underlying this derivation is that inertia forces of lubricant are negligible. These inertia forces consist of fluid gravity, centrifugal forces acting in curved films and acceleration of the fluid. This means that the lubrication equation ignores the inertia term due to unsteady velocity of the journal surface. During start-up operation, there is always tangential acceleration of shaft. The effect of this acceleration[*] tends to reduce the magnitude of oil-film pressure which, consequently, reduces instantaneous load carrying capacity of journal bearing. This effect can be accounted for by including some of the terms originally dropped from the Navier-Stokes equations. This, however, would considerably increase difficulty of the problem and considerably augment the cost of the numerical solution. Therefore, in the present analysis oil-film forces are calculated assuming that the Reynolds' lubrication equation holds for transient journal angular velocity.

3.4.3 Forcing function

Equations (3.19) are solved using the fourth-order Runge-Kutta step procedure [37]. The dynamic film forces, P_1^d and P_2^d, and their resultant in the vertical direction, are calculated at each time step. A force, F_d, equal in magnitude and opposite in sign to this resultant is taken as the force (due to rotor imbalance) transmitted to foundation through the bearing. As with Model 1 (see Fig. 3.2 and eq. 3.4), the forcing function for this model can be written

$$F_y(t) = F_d - Mr \cdot \ddot{y}_m \qquad (3.20)$$

---

[*] Simplified analysis of this effect is presented in [35]

In order to avoid metal to metal friction at early stage of start-up operation, a rotor is lifted up by pressurized oil supplied into journal bearing. This pressure is dropped when rotor angular velocity is high enough to secure sufficient load carrying capacity of bearing oil film. In view of the above, transient analysis of this model always starts with a rotor having some initial speed, ω_i.

Thus, applying the reasoning discussed in connection with Model 1 (Section 3.2.1), rotor angular acceleration, velocity and acceleration are assumed to vary with time according to the formula:

$$
\begin{array}{ll}
\text{for} \quad 0<t\leq T_1 & \text{for} \quad t>T_1 \\[2ex]
\ddot{\Omega}=(\omega_s-\omega_i)(1-t/T_1)2/T_1 & \ddot{\Omega}=0 \\
\dot{\Omega}=(\omega_s-\omega_i)(2t/T_1-t^2/T_1^2)+\omega_i & \dot{\Omega}=\omega_s \\
\Omega=(\omega_s-\omega_i)T_1(3t^2/T_1^2-t^3/T_1^3)/3+\omega_i t & \Omega=\omega_s t-(\omega_s-\omega_i)T_1/3
\end{array}
\qquad (3.21)
$$

4. COMPUTER PROGRAM DESCRIPTION

In order to implement the reccurence formulae (2.23) in a computer program, components of generalized load vector (P_1, P_2, and P_3) have to be evaluated at each time step, according to eq. (2.16).

Consider first Model 1 with the forcing function given by eq. (3.4). The following integration is required.

$$\begin{aligned} P_1^m &= \int_0^\tau \bar{F}_y(t)dt - Mr\int_0^\tau \ddot{y}_m(t)dt \\ P_2^m &= \int_0^\tau t\bar{F}_y(t)dt - Mr\int_0^\tau t\ddot{y}_m(t)dt \qquad (4.1) \\ P_3^m &= \int_0^\tau t^2\bar{F}_y(t)dt - Mr\int_0^\tau t^2\ddot{y}_m(t)dt \end{aligned}$$

The first integral in each of the above equations can be easily evaluated since $\bar{F}_y(t)$ is a known function of time, as described in eqs. (3.3) and (3.5). The computer program employs a 4-point Gaussian quadrature integration scheme; results are stored in vector **Q**. In the process of deriving the finite time formulation (Chapter 2), shape functions **N** and their derivatives are determined, and vector $\ddot{q}(t)$ is approximated by $\ddot{q}(t)\approx[\ddot{N}]\{q_n\}$ in eq. (2.9). The function $\ddot{y}_m(t)$, as a component of vector $\ddot{q}(t)$, is assumed to vary in the time interval, τ, according to the same approximation. Simple integration yields

$$\begin{aligned} P_1^m &= Q_1^m - Mr(\dot{q}_2^m - \dot{q}_1^m) \\ P_2^m &= Q_2^m - Mr(\tau\dot{q}_2^m - q_2^m + q_1^m) \qquad (4.2) \\ P_3^m &= Q_3^m - Mr(\tfrac{1}{60}\tau^3\ddot{q}_2^m + \tfrac{1}{60}\tau^3\ddot{q}_1^m + \tfrac{4}{5}\tau^2\dot{q}_2^m + \tfrac{1}{5}\tau^2\dot{q}_1^m - \tau q_2^m + \tau q_1^m) \end{aligned}$$

The superscript "m" in eqs. (4.1) and (4.2) indicates that the above quantities represent only one component (corresponding to nodal variable $\ddot{y}_m$) in each of the global $(nx1)$ vectors. Substituting eq. (4.2) into the reccurence scheme (2.32) leads to the formulae:

$$\begin{bmatrix} \{q_2\} \\ \{\dot{q}_2\} \\ \{\ddot{q}_2\} \end{bmatrix} = \begin{bmatrix} Z_{12} \end{bmatrix}_m^{-1} \left\{ \begin{bmatrix} \{Q_1\} \\ \{Q_2\} \\ \{Q_3\} \end{bmatrix} - \begin{bmatrix} Z_{11} \end{bmatrix}_m \begin{bmatrix} \{q_1\} \\ \{\dot{q}_1\} \\ \{\ddot{q}_1\} \end{bmatrix} \right\} \quad (4.3)$$

which is actually employed in the computer program to advance transient solution in time. The subscript "m" indicates that the matrices Z_{11} and Z_{12} are "modified", by adding and subtracting from their appropriate components the terms given by eq. (4.2).

The procedure just described is also used in the analysis of Model 2. In this case, however, two components (F_x, F_y) of the forcing function given by eq. (3.6) have to be considered. Accordingly, two sets of equations' must be integrated to evaluate components of generalized load vector **P**. As a result, vector Q has additional components and matrices Z_{11} and Z_{12} are modified by additional terms.

In the analysis of Model 3, matrices Z_{11} and Z_{12} are modified in exactly the same way as in Model 1. However, the components of vector Q are obtained differently, since the

---

' That is, eqs. (4.1) for the x-components and similar ones for y-components term F_d in the forcing function (eq. 3.20) is not given by an analytical expression. The procedure used in this case can be summarized as follows:

1. The time interval τ is divided into "j" sub-intervals $\check{\tau}$.
2. At each sub-interval $\check{\tau}$, the dynamic force F_d^j is determined (according to the procedure outlined in Chapter 3).
3. At the same time, two additional functions are generated, namely: $\check{\tau}F_d^j$ and $\check{\tau}^2F_d^j$.
4. Then, the "j" discrete values of these three functions (i.e., F_d, tF_d and t^2F_d) are integrated numerically over the interval τ to give components of vector **Q**. (The cubic spline method of numerical integration [38], is used in this process).

4.1 Main Features of the Computer Program

The basic features of the computer program are as follows:

5. The program is written in FORTRAN language (double precision is used).
6. It is general for any beam or plane frame models with horizontal and vertical beam members (can be easily extended for any structure).
7. The program is general for any boundary conditions and constraints in the system.

8. Two different models of the Timoshenko beam finite element are used.
9. The program can be used to determine system natural frequencies and eigenvectors.
10. A static test can be performed, by computing static deflections (using global stiffness matrix) and comparing results with known exact solutions.
11. The transient vibration problem of the models is solved using time stepping scheme based on finite time formulation.
12. The program uses the following IMSL subroutines:
    a. EIGZS to determine eigenvalues/vectors
    b. LEQT2F as equation solver for static test
    c. LINV2F to invert matrix $[Z_{12}]_m$
13. The program employs 4-point Gaussian quadrature (for Model 1 & 2) and cubic spline (Model 3) as integrating procedures to evaluate components of generalized load vector.
14. The Runge-Kutta (4th order) method is used to solve journal centre equations of motion (Model 3).

4.2 The Computer Program Organization

The simplified schematic diagram of the computer program structure is shown in Fig. 4.1 and Fig. 4.2.

MAIN

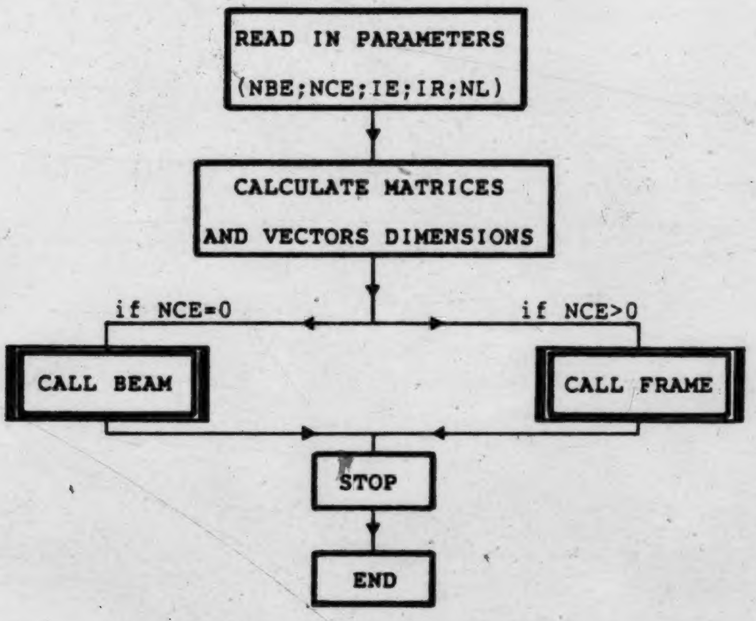
READ IN PARAMETERS
(NBE;NCE;IE;IR;NL)
CALCULATE MATRICES
AND VECTORS DIMENSIONS
if NCE=0
if NCE>0
CALL BEAM
CALL FRAME
STOP
END

NOTE! 1) Subroutines BEAM and FRAME are actually the main programs. The split MAIN-BEAM-FRAME is used to enable changing the dimensions of all global matrices and vectors, depending on a type and number of finite lements used.

2) NCE - a number of elements in column. All other variables' names are explained by comments cards in the program.

3) The main segments and several subroutines of the computer program are listed in Appendix A-3.

Fig. 4.1 Schematic diagram of the computer program (MAIN)

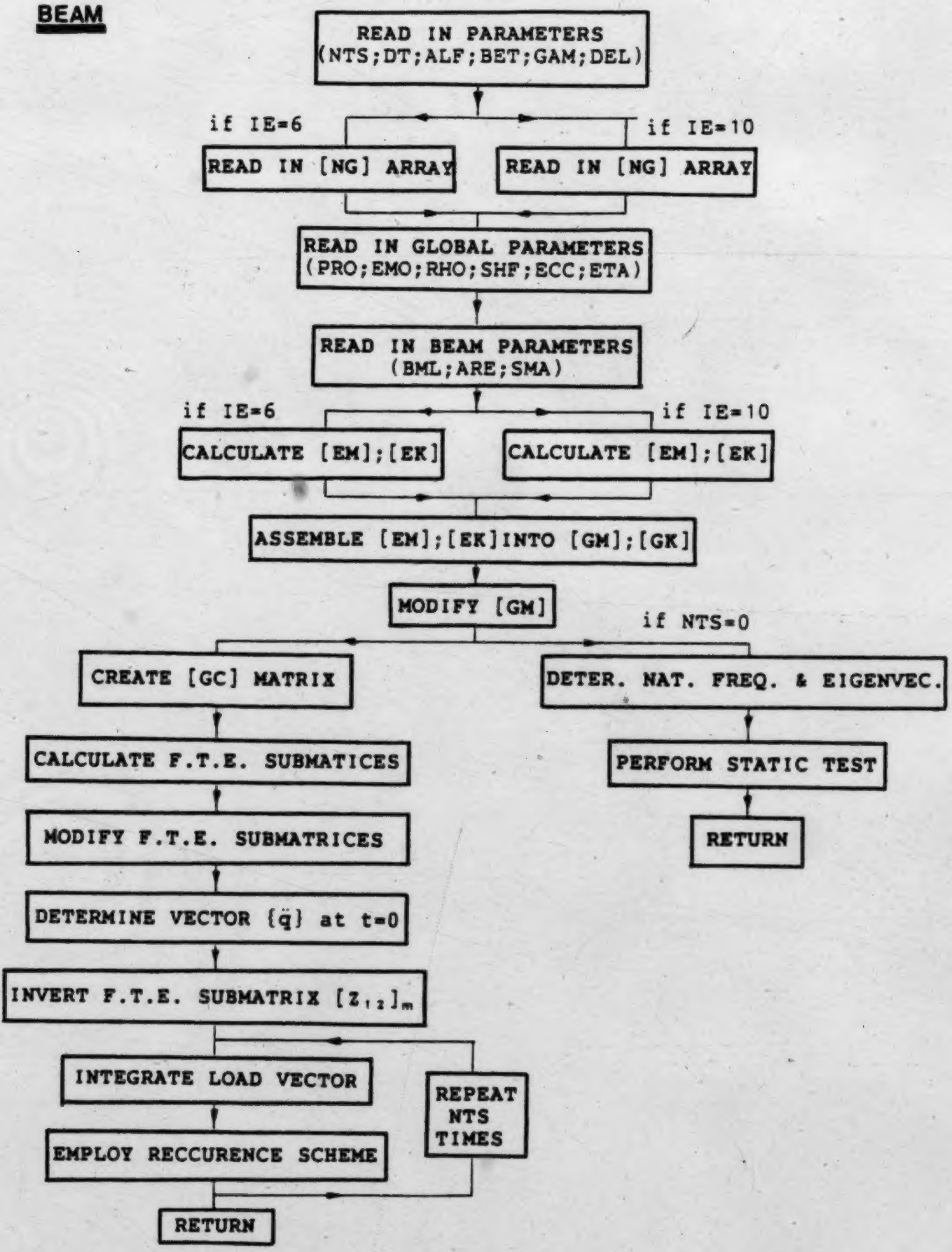
BEAM
READ IN PARAMETERS (NTS;DT;ALF;BET;GAM;DEL)
if IE=6
if IE=10
READ IN [NG] ARRAY
READ IN [NG] ARRAY
READ IN GLOBAL PARAMETERS (PRO;EMO;RHO;SHF;ECC;ETA)
READ IN BEAM PARAMETERS (BML;ARE;SMA)
if IE=6
if IE=10
CALCULATE [EM];[EK]
CALCULATE [EM];[EK]
ASSEMBLE [EM];[EK]INTO [GM];[GK]
MODIFY [GM]
if NTS=0
CREATE [GC] MATRIX
DETER. NAT. FREQ. & EIGENVEC.
CALCULATE F.T.E. SUBMATICES
PERFORM STATIC TEST
MODIFY F.T.E. SUBMATRICES
RETURN
DETERMINE VECTOR {q̈} at t=0
INVERT F.T.E. SUBMATRIX [Z₁₂]ₘ
INTEGRATE LOAD VECTOR
REPEAT NTS TIMES
EMPLOY RECCURENCE SCHEME
RETURN

Fig. 4.2 Schematic diagram of the computer program
(subroutine BEAM)

5. SIMULATION RESULTS AND DISCUSSION

In order to make the discussion of the results (presented herein in graphical form) general, all the parameters and variables appearing on plots are dimensionless. Two parameters are especially important in the following discussion, namely: α and β, defined as:

$$\alpha=\omega_s/\omega_0 \qquad \beta=T_1/\tau_0$$

For the sake of simplicity, the dynamic response of each model is examined by analyzing displacements only at the structure driving point (i.e. at the midspan of the beam).

5.1 Parametric Studies - Model 1

5.1.1 Preliminaries

The dynamic analysis of a structural system is usually preceded by determination of its natural frequencies. For Model 1, these frequencies depend on: (1) the supporting beam (i.e. its material, geometry and boundary conditions) and (2) the mass of the rotor. It is therefore of interest to know the effect of the rotor mass on the system natural frequencies. The natural frequencies of Model 1 are computed for different rotor to beam mass ratio with all other parameters of the system fixed. The first three frequencies are plotted in Fig. 5.1. As expected, an increase of the mass ratio decreases the natural frequencies, except for those of anti-symmetric modes, which are not affected. (Take, for instance, the second mode one indicated by "2" on the plot). Therefore, a fixed mass ratio η=Mr/Mb=0.1, representative of large turbomachine support system, is chosen for further analysis.

Fig. 5.2 shows build-up of the system vibration as a response to the exciting force generated by an accelerating unbalanced rotor starting from rest. Exactly the same response is plotted again, in Fig. 5.3, together with the "positive" envelope of maximum displacements. For clarity, only displacement envelopes are plotted on all further graphs. It should be noted that an envelope represents a series of points obtained from the numerical calculations. The shape of the curve, therefore, is not important since it depends on the approximation method chosen for connecting the associated data points.

Fig. 5.4 shows the relationship between displacement envelope and time for three different lengths of the supporting beam with, all other system parameters fixed. The plot is intended to show that the dynamic magnification factor (DLF) depends on the slenderness of the beam. In further analysis, only the beam shown in Fig. 3.3 (with slenderness factor κ=0.12) is considered.

5.1.2 Dynamic analysis

Response of an ideal system without damping is examined first. An interesting case is shown in Fig. 5.5, which will be discussed in detail. This graph shows displacement envelopes versus time for three different values of the parameter β (i.e., for three different rotor acceleration times). The rotor operating speed is set to be greater than the first natural frequency of the system (α=1.2).

Consider the case when β=45.0. Starting from zero, the displacement envelope increases slowly, but with a steadily increasing rate of change, following the increase of the rotor instantaneous speed, Ω. This rate of change reaches a maximum when the rotor speed approaches the fist critical frequency of the system ($\Omega=\omega_0$), indicated by "•" on the curve. Passing this point, the displacement envelope increases further until it reaches its maximum at non-dimensional time $t/\tau_0 \simeq 29.2$. (At this moment, the rotor instantaneous speed is still less than the operating speed ω_s, to be reached at time 45.0). After reaching its maximum value, the displacement envelope oscillates around a certain level with all the consecutive maxima slightly less than the first one. The pattern of this oscillation and its frequency, which depend on the rotor speed, stabilize after the rotor attains a constant operating angular velocity. For the fixed parameter α, as it is in the case being discussed, shortening the rotor acceleration time (β=25.0, 10.0) increases its acceleration rate. In comparing all three curves of this plot, it is evident that the maximum response amplitude and the level of the envelope oscillation are highly dependent upon the rotor acceleration rate. They become smaller when the acceleration rate increases, as does the difference between the maximum amplitude and the consecutive maxima of the envelope oscillation. It is also observed that the maximum amplitude does not occur at the critical frequency, and that a shift in its position from that point also depends on the rotor acceleration rate. When the acceleration rate is high enough (as it happens to be for β=10.0 on the graph), the maximum amplitude occurs some time after the rotor speed stabilizes at its operating level.

Fig. 5.6 shows the results of the analysis carried out for varying the parameter α (α=0.5,0.8,1.2,1.5) and constant β (β=30.0). It is clear from this graph that the dynamic response and the maximum amplitude of vibration are dependent on the level of the rotor operating speed, and whether it is below or above the critical frequency of the system. For example, consider the cases for α=0.5 and 0.8. Both the level and the amplitude of the envelope oscillation increase when the rotor speed approaches the natural frequency of the system. The level of this oscillation could also be predicted through consideration of a steady-state response analysis. It should be noted that varying the parameter α, when β is constant, changes not only the level of rotor operating angular velocity but also rate of its acceleration. It is, therefore, logical to compare the results for the cases $a=1.2$ and 1.5 of Fig. 5.6 to the previously discussed in detail results of Fig. 5.5. The results of Fig. 5.6 confirm once again that the maximum amplitude of vibration and the level of envelope oscillation decrease when the acceleration rate increases. Additionally, they show that the amplitude of the envelope oscillation becomes smaller for greater parameter a, i.e. when "the spread" between the rotor operating speed and the system critical frequency increases.

The analysis has proved so far that there is a pronounced effect of the rotor acceleration rate on the dynamic response of the system. To determine this effect more precisely, new dimensionless variables are introduced into the analysis, namely: the rotor acceleration rate through the critical frequency ξ, and the shift of the maximum amplitude of vibration σ, defined as:

$$\xi=\Omega_o/\omega_o{}^2 \qquad \sigma=\Omega_m/\omega_o$$

where: Ω_o is the rotor acceleration rate at the moment the rotor instantaneous speed passes through the first natural frequency of the system ($\Omega=\omega_o$), and Ω_m is the rotor instantaneous speed at the moment the response amplitude reaches its maximum.

The effect of the rotor acceleration rate through the critical frequency on the maximum amplitude of vibration is shown in Fig. 5.7. The effect of this acceleration on the shift of maximum amplitude from the critical frequency, is presented in Fig. 5.8. The first relationship (Fig. 5.7) demonstrates clearly that, for a fixed level of rotor operating speed (i.e. for constant parameter a), the greater the acceleration rate through the critical frequency the smaller the maximum amplitude of the system response. It also shows that, for the same values of this acceleration rate, the maximum amplitude is reduced by increasing the deviation of the rotor operating speed from the critical frequency, i.e. for greater parameter a. Fig. 5.8 shows that the shift in location of the maximum amplitude from the critical frequency increases for higher acceleration rates and/or for higher levels of the rotor operating speed. For the case when a=1.1, with the acceleration rate exceeding some critical value ($\xi > \approx 5.0 \cdot 10^{-3}$), the condition is met when the maximum amplitude occurs some time after the rotor speed has stabilized at its operating level. This is marked on the plot by a dotted line. (An example of response envelope, for such case, is shown in Fig. 5.5, curve for β=10.0).

The relationships presented in Figs. 5.7 and 5.8 include the effect of the rate of change of acceleration when the rotor instantaneous speed passes through the critical frequency. To eliminate this effect, the analysis is repeated once again, assuming this time that the forcing function is generated by an unbalanced rotor accelerating at a constant rate ($\dot{\Omega}$=constant). The results, for a fixed level of the rotor operating speed ($a=1.2$), are shown in Fig. 5.9. It is evident that an increase in the acceleration rate reduces the maximum amplitude of response and shifts it from the critical frequency. It is observed that, for very small values of the acceleration, the shift of the maximum amplitude ($\sigma=\Omega_m/\omega_0$) is slightly less than 1.0, which implies that the maximum amplitude occurs just before the instantaneous rotor speed reaches its critical frequency.

The effect of damping, always present in structural systems, is now examined. Fig 5.10 shows the relationship between the displacement envelope and time, for $a=0.8$, 1.1 and 1.2, $\beta=30.0$ and $\zeta=0.02$, where ζ is a damping factor in the first mode of the system natural vibration. The effect of damping on system dynamic response can be clearly seen by comparing curves (with equal values of parameter a) shown in Fig. 5.10 and Fig. 5.6. Consider first the case $a=0.8$ (that is, when the rotor operating speed is less than the first critical frequency). The response envelopes for the system with and without damping increase almost identically until they reach their maximum values. Then, for both cases, the envelope starts to oscillate about the same level which could be obtained from steady-state analysis. The effect of damping is to diminish the amplitude of this oscillation until it dies out completely. For the case with rotor operating speed greater than critical frequency, the effect of damping is much more pronounced. Comparing the results shown in Fig. 5.10 and Fig 5.6 once again (this time for $\alpha=1.2$), it is noted that the maximum amplitude of vibration is reduced by 29% (from 15.5 to 11.0), and the level of the envelope transient oscillation by 84% (from 12.5 to 2.0). For the same amount of damping in the system, the maximum amplitude and level of envelope transient oscillation depends on the rotor operating speed. This is clearly illustrated by curves (for $\alpha=1.1$ and 1.2) in Fig. 5.10.

Fig. 5.11 demonstrates the relationship between the maximum amplitude of vibration and the damping factor, for various levels of the rotor operating speed. The maximum amplitude of damped vibration is non-dimensionalized by dividing by the maximum amplitude of vibration of the undamped system subjected to the same excitation. It is observed that the maximum amplitude of vibration decreases with an increase in the amount of damping in the system. The effect of damping on reducing the response maximum amplitude becomes greater if the rotor operating speed is "closer" to the system natural frequency, that is for values of parameter α closer to 1.0.

5.1.3 Concluding remarks

The results obtained in this section are identical to those of Victor & Ellyin [5], and thus confirm the ability of the model to predict known results accurately. Several conclusions can be drawn from the results of numerical analysis of Model 1. These include:

1. The maximum amplitude of vibration of low-tuned foundation structures supporting rotating machinery occurs during the transients at start-up or shut-down operations.

2. The response maximum amplitude is dependent on: (1) the rotor acceleration rate through the critical frequency of the system, and (2) the deviation of the rotor operating speed from the critical frequency.
   a. The greater this acceleration, the smaller the maximum amplitude.
   b. The greater the deviation of the rotor operating speed, the smaller the maximum amplitude.

3. There is a shift in position of the maximum amplitude with respect to the critical frequency, dependent on the same parameters.
   a. The greater the rotor acceleration rate through the critical frequency, the greater the shift.
   b. The greater the deviation of the rotor speed from the critical frequency, the greater the shift.

4. The effect of structural damping is to subdue transient vibration to the level of steady-state

response, which depends on the rotor operating speed. The maximum amplitude of vibration decreases with an increase of the damping in the system. The effect of damping on this reduction becomes greater if the deviation of the rotor operating speed from the critical frequency is smaller.

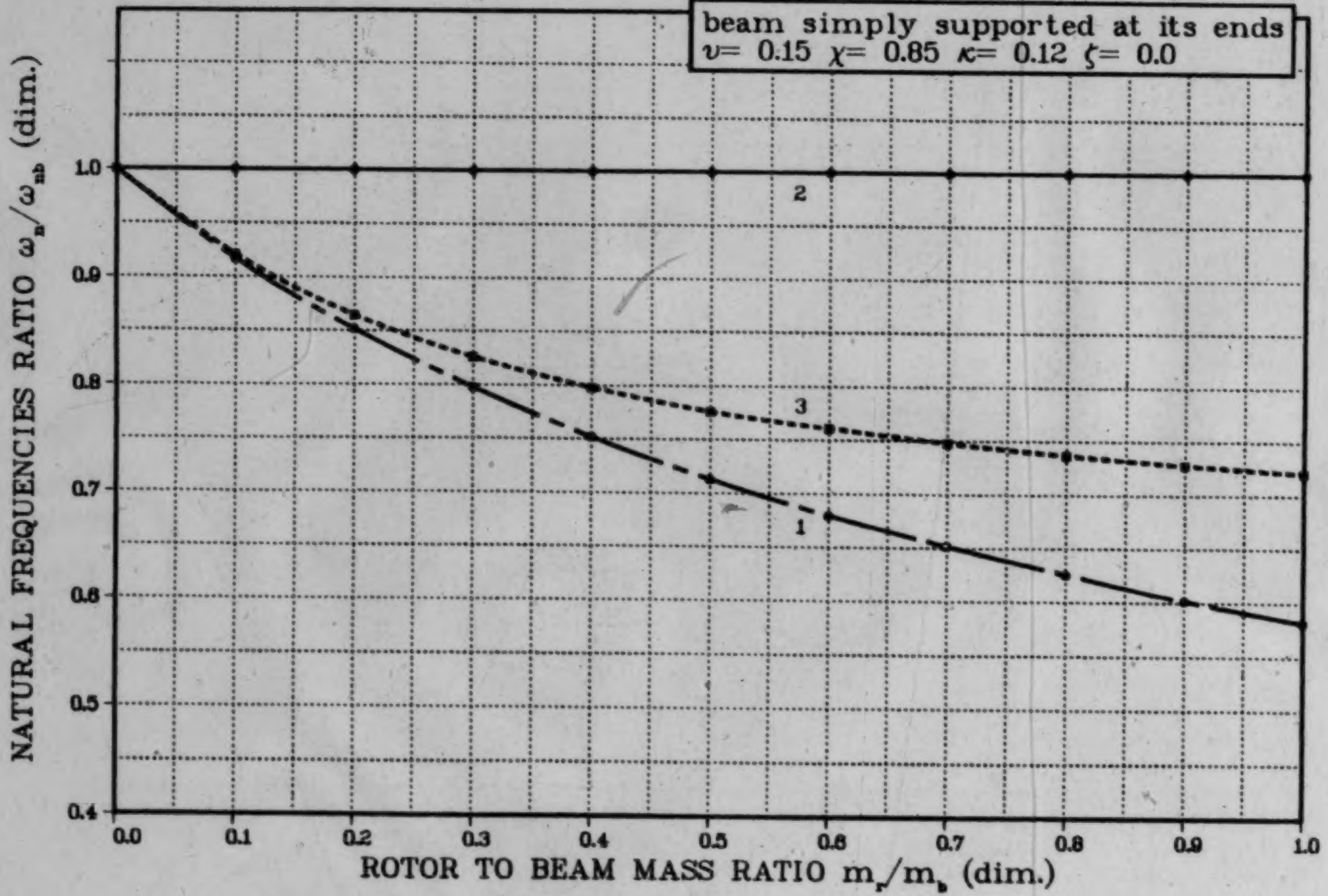

Fig. 5.1 Effect of rotor mass on the determination of system natural frequencies.

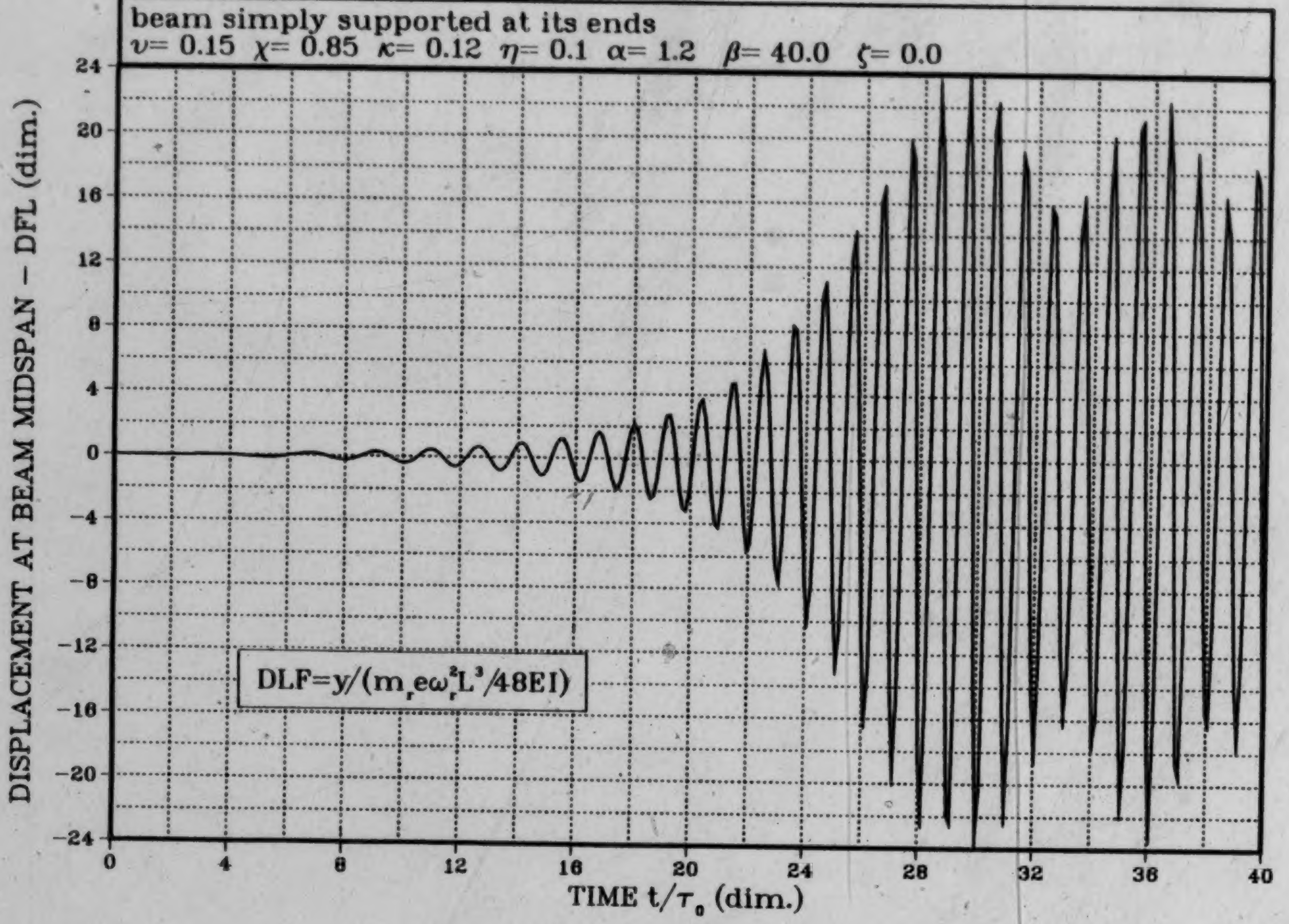

Fig. 5.2 Build-up of beam vibration in response to excitation of an unbalanced accelerating rotor.

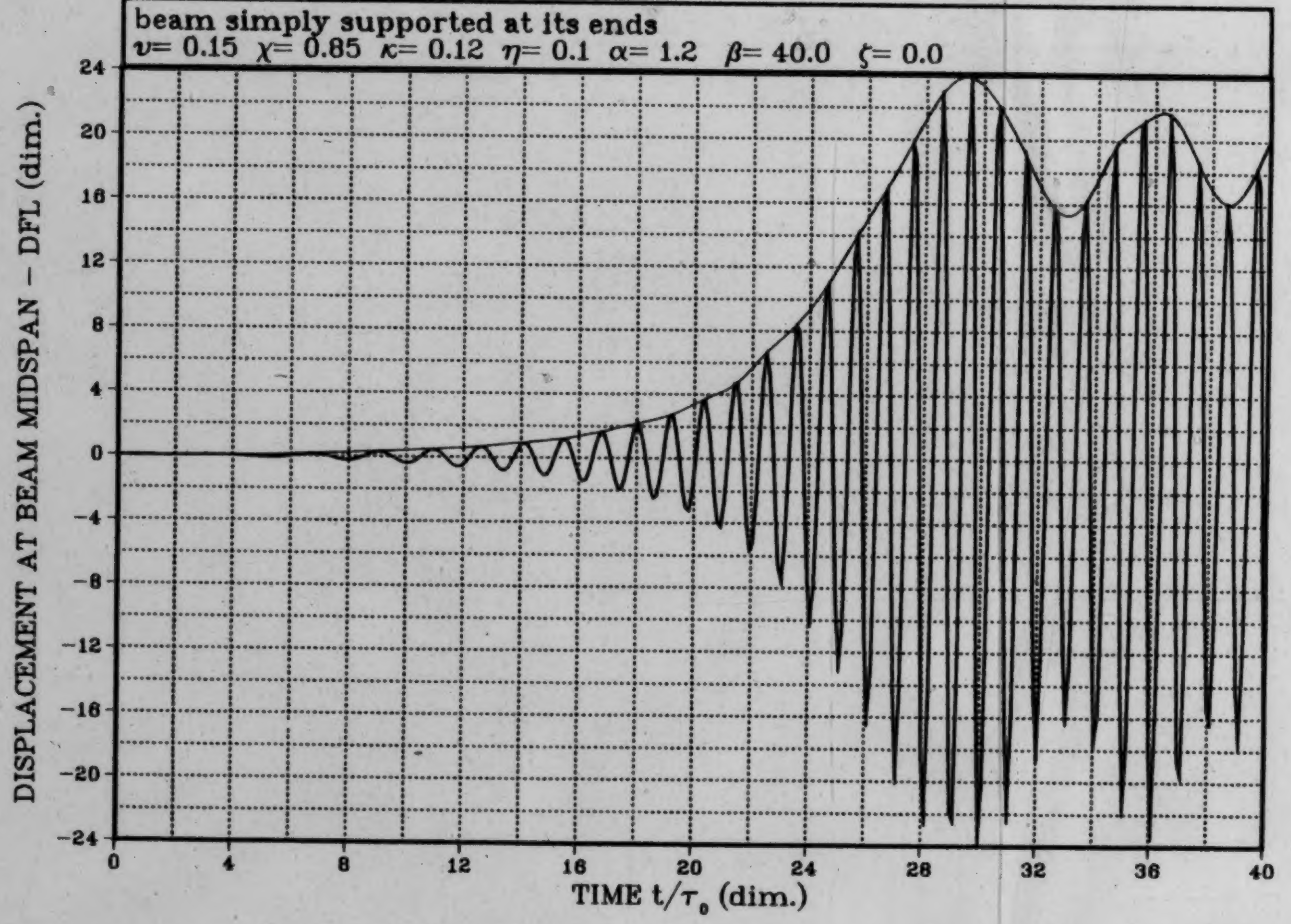

Fig. 5.3 Dynamic response of a beam, and an envelope of response maximum amplitudes.

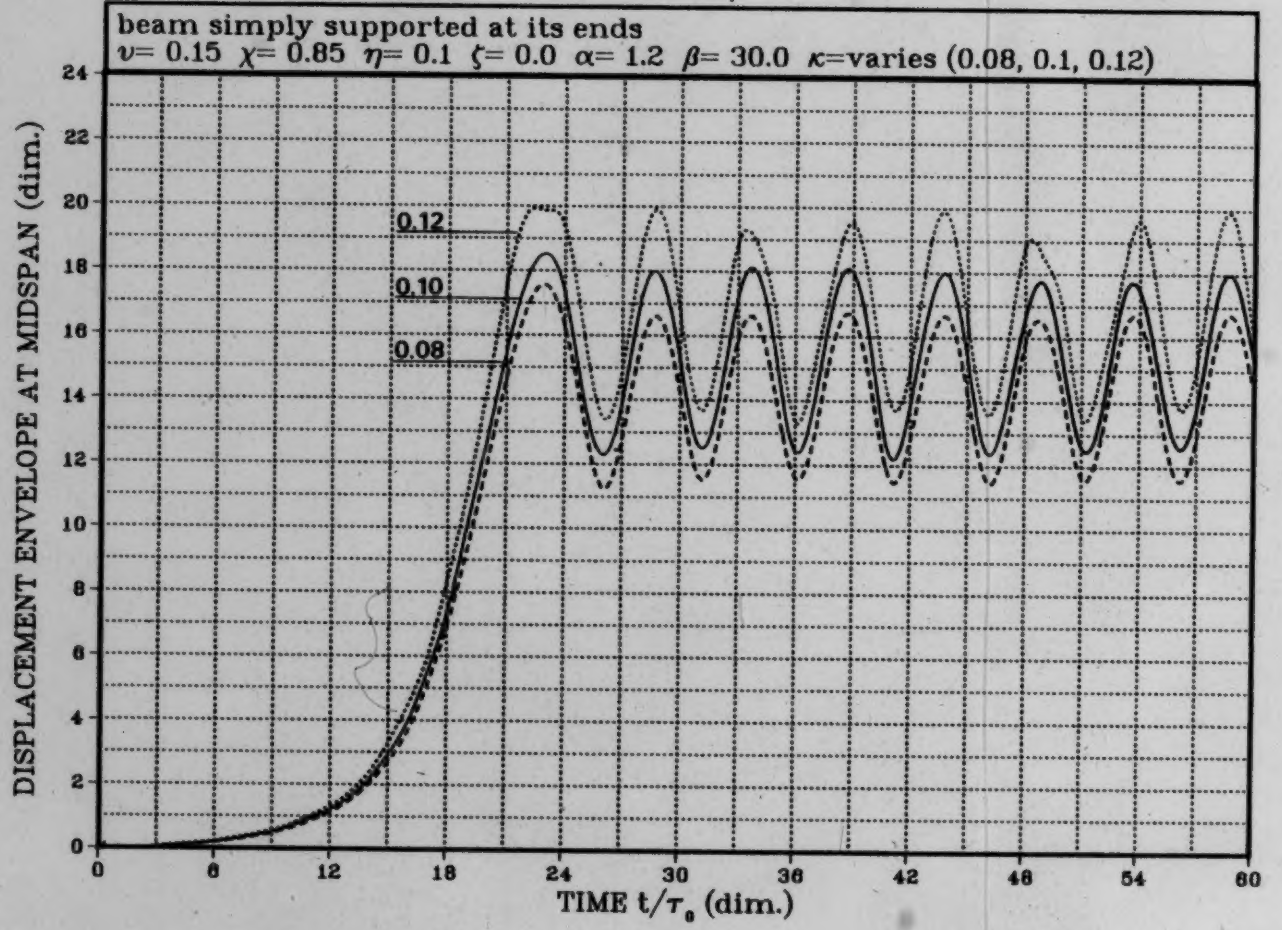

Fig. 5.4 Displacement envelopes versus time, for different values of beam slenderness parameter κ .

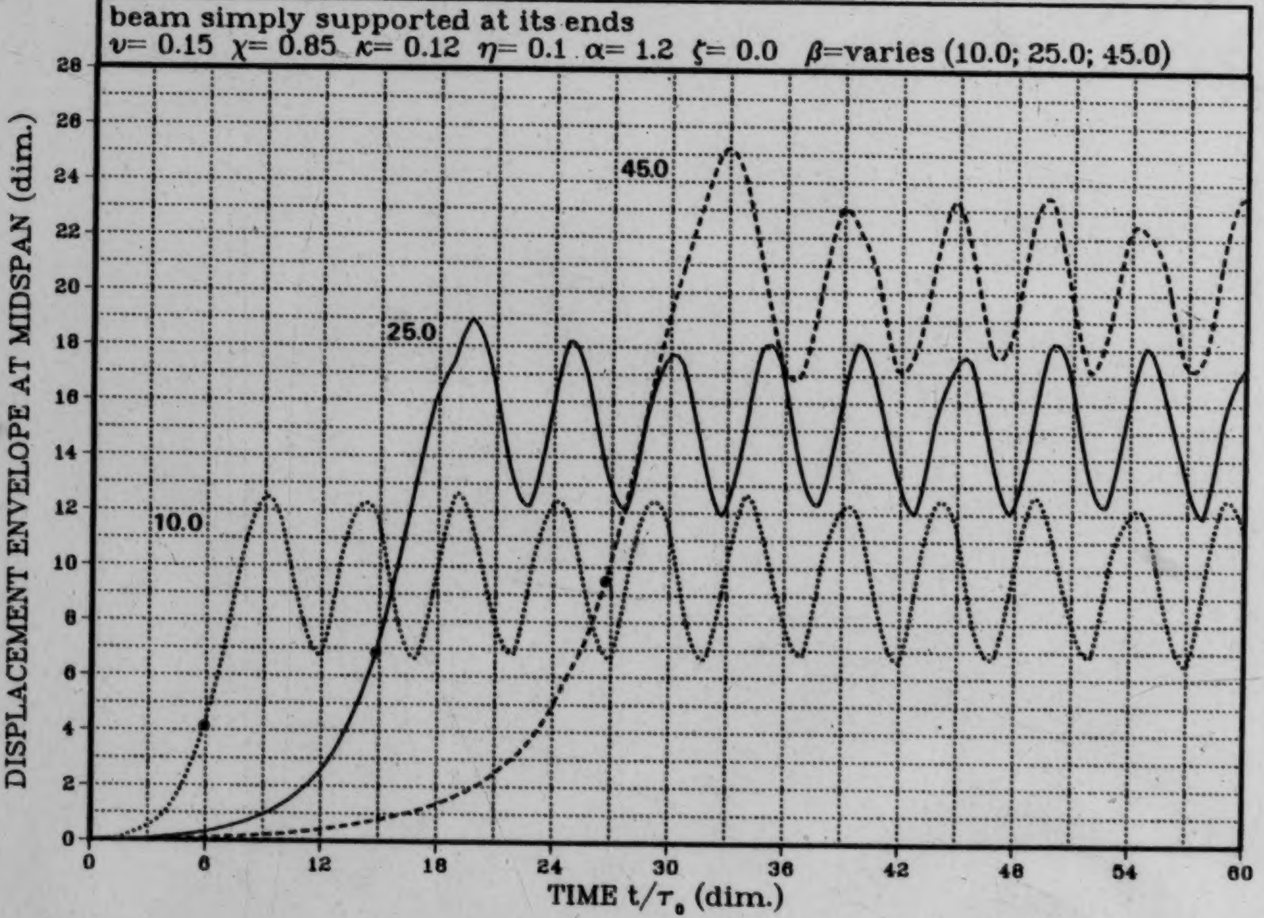

Fig. 5.5 Displacement envelopes versus time, for different values of rotor acceleration time parameter β .

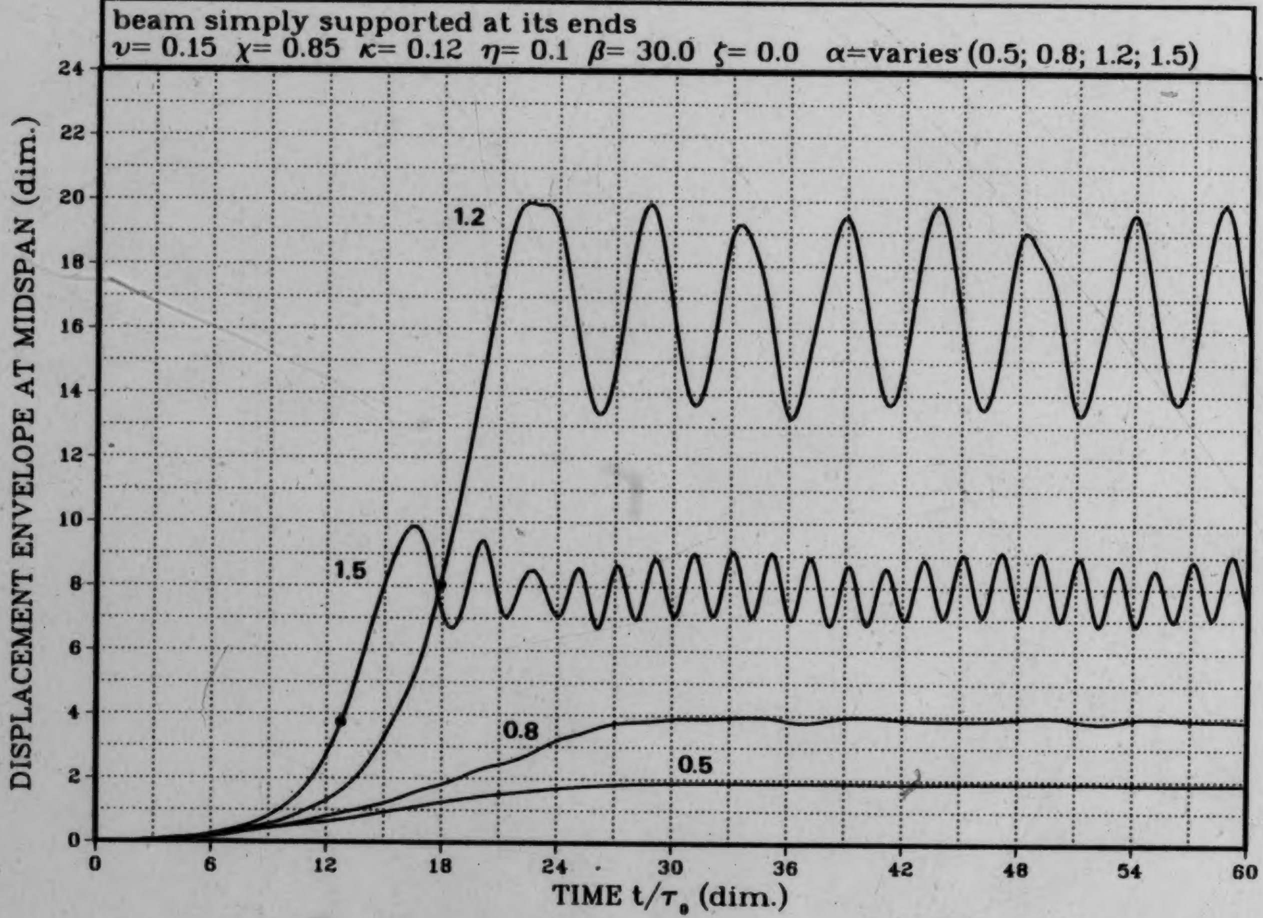

Fig. 5.6 Relationship between displacement envelope and time, for various values of rotor speed parameter α.

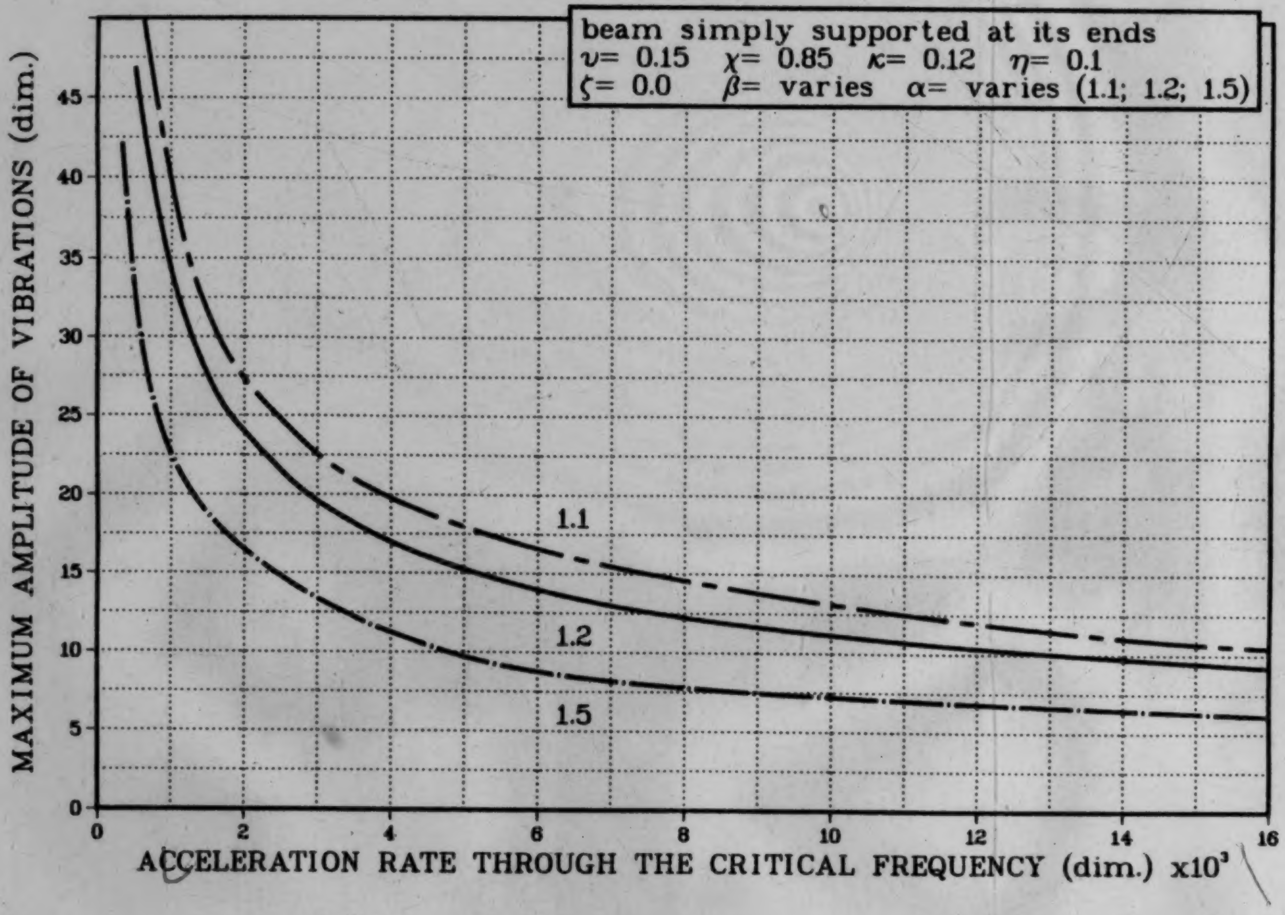

Fig. 5.7 Relationship between response maximum amplitude and rotor acceleration rate through the critical frequency, for different values of parameter a.

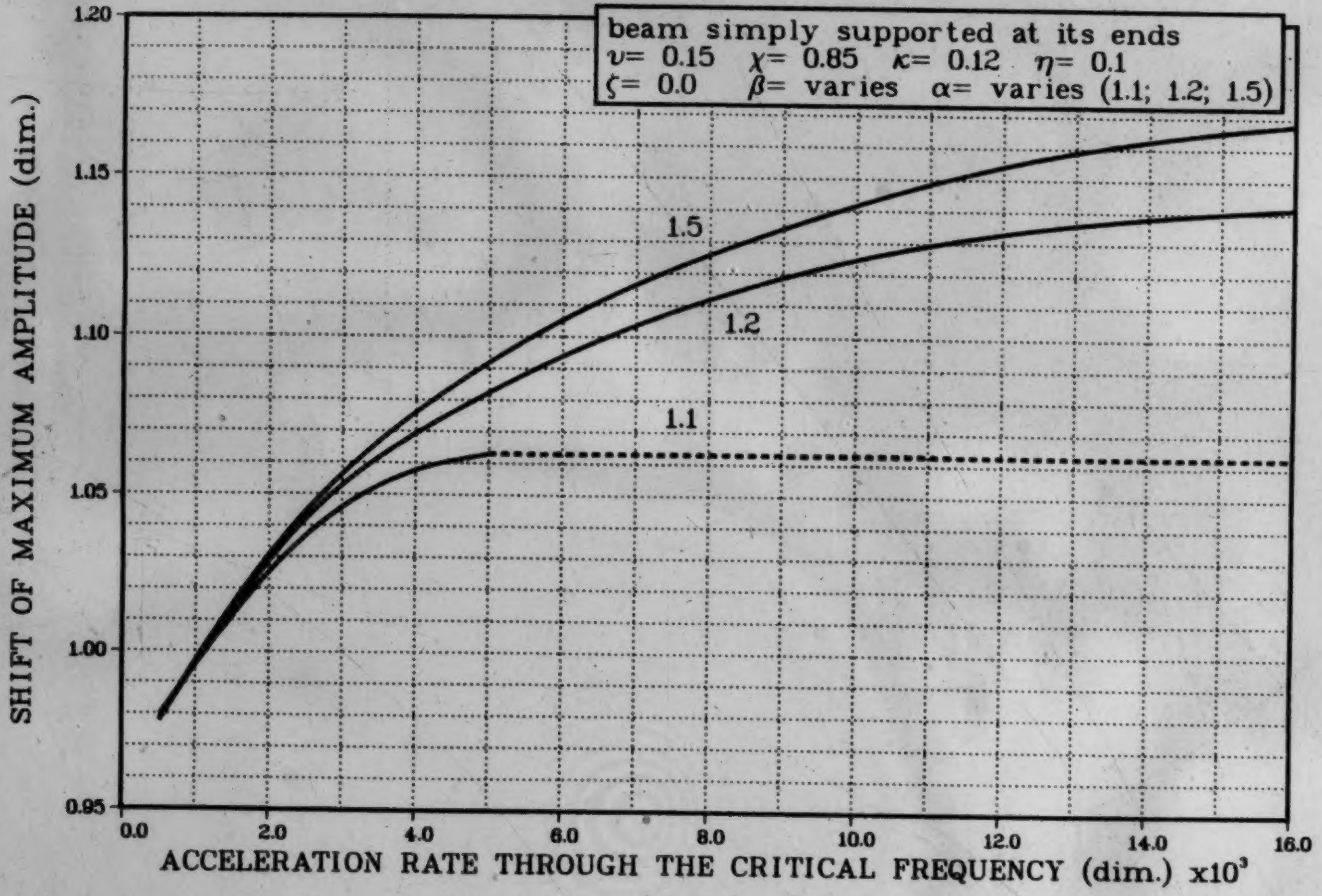

Fig. 5.8 Effect of rotor acceleration rate through the critical frequency on shift of maximum amplitude from the critical frequency, for different values of parameter α .

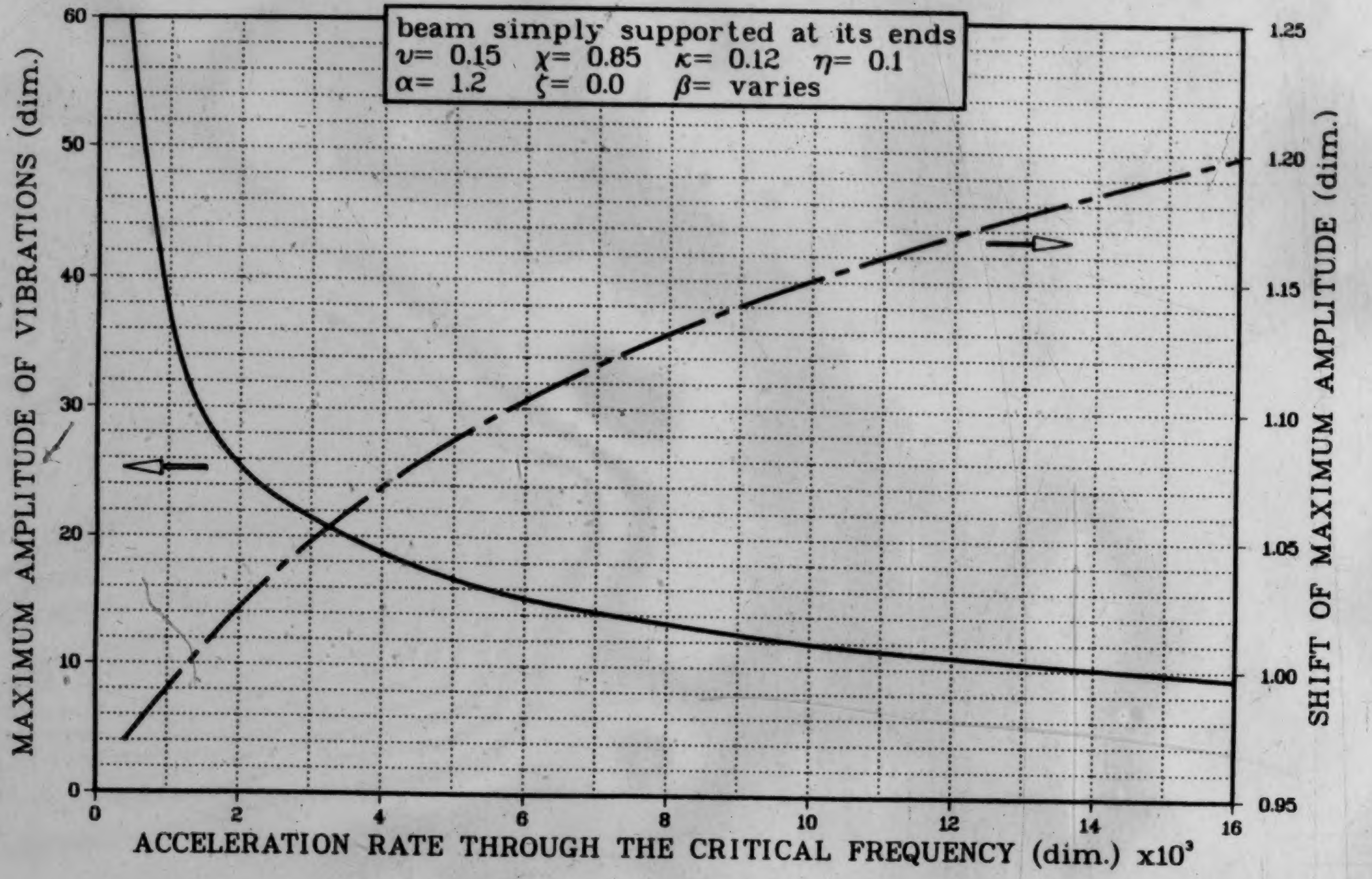

Fig. 5.9 Relationships between: (1) maximum amplitude of vibration and (2) shift in its position from the critical frequency and constant rotor acceleration rate.

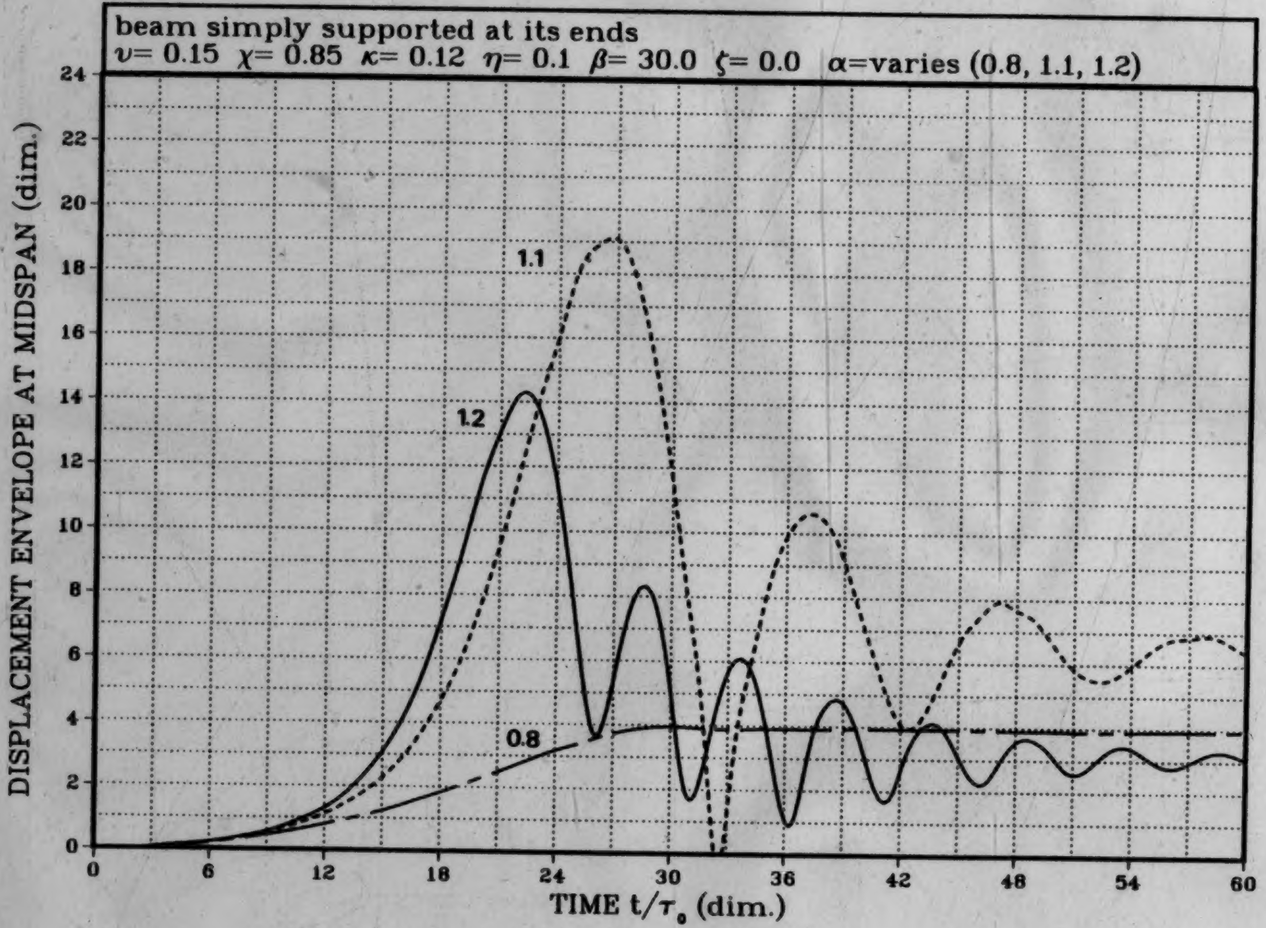

Fig. 5.10 Displacement envelopes versus time, for different values of rotor speed parameter α ; damping effect included.

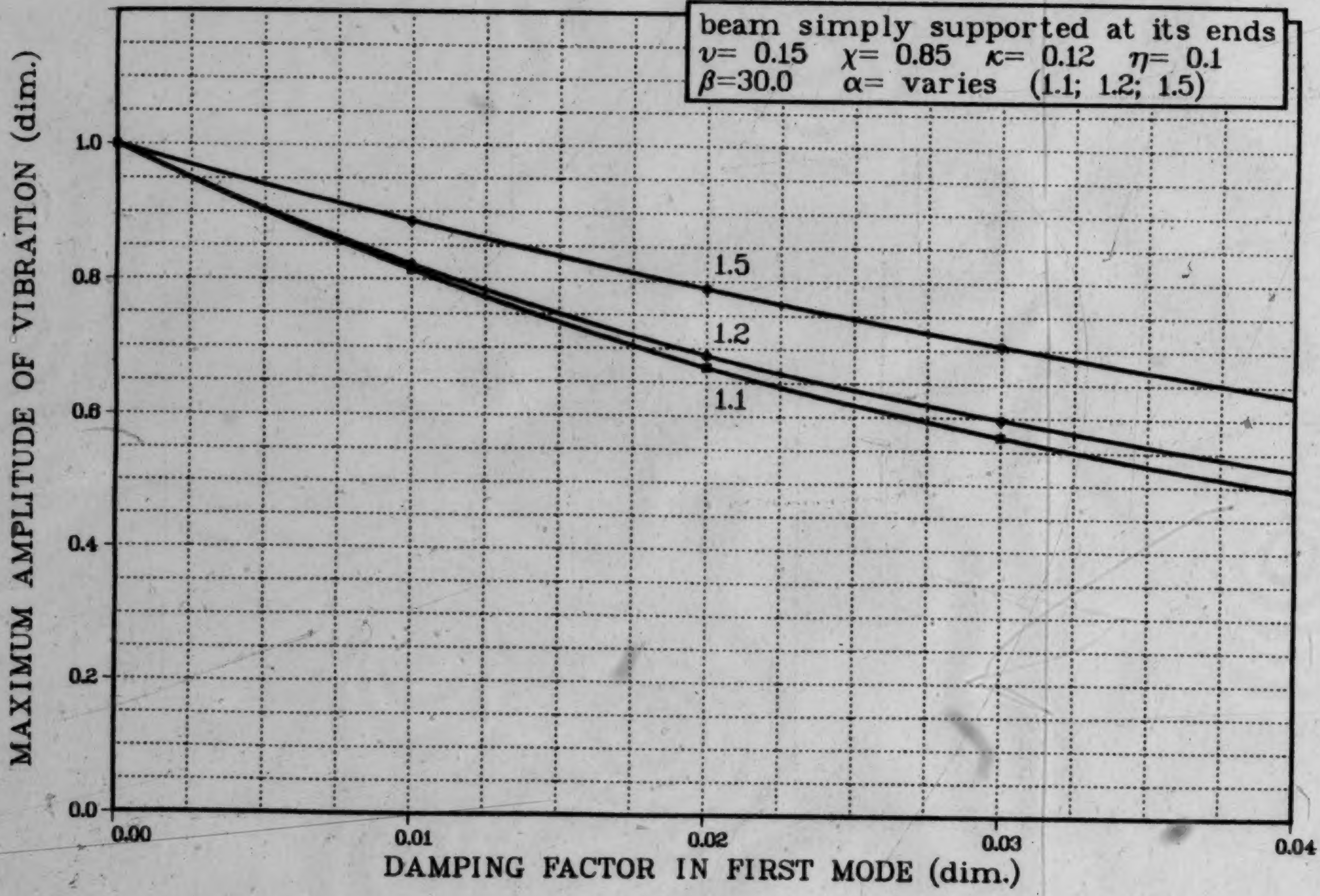

Fig. 5.11 Effect of damping on maximum amplitude of vibration, for different values of rotor speed parameter a .

5.2 Parametric Studies - Model 2

5.2.1 Preliminaries

As in the case of Model 1, the dynamic analysis of this model is also preceded by the determination of system natural frequencies. For a simply supported beam, once its material and boundary conditions are defined, the natural frequencies spectrum depends on one non-dimensional parameter κ. However, there is no such simple relationship for a framework. For a single bay portal frame (that is, for the simplest case of a framework), with clamped columns, the natural frequencies spectrum is a function of a group of several non-dimensional parameters [39]. Therefore, parametric studies of Model 2 cannot be generalized as easily as they can be for simple beams. To simplify the discussion, a new non-dimensional parameter ("frame parameter", γ), defined as $\gamma=\kappa_1/\kappa_2=\sqrt{I_1A_2/I_2A_1}\,L_2/L_1$, is brought into the analysis.

One of the main distinctions between the vibration of a beam and a framework is that in the latter case, the longitudinal motion is coupled with flexural motion. Fig. 5.12 shows the distribution of the lowest four natural frequencies of the single bay portal frame (shown in Fig. 3.5), as a function of the frame parameter γ. The natural frequencies are obtained by considering the axial-flexural coupling in the model. The frequencies of symmetric and asymmetric modes of vibration are indicated on the graph by "S" and "A", respectively. In order to simplify dynamic analysis of a framework, it is a common practice to neglect the axial deformation of its members and to take only flexural motion into consideration. This approximation is applied to the frame model. The resulting natural frequencies of the system are plotted in Fig. 5.13. For easy comparison of results , the lowest three natural frequencies of Figs. 5.12 and 5.13 are plotted together in Fig. 5.14. It is noted that as the frame parameter increases, the influence of axial deformation decreases, with flexural deflections eventually dominating the first three modes of vibration. However, a more detailed analysis indicates that the higher modes remain affected by axial vibration. As well, this approximation is not justified at all for small values of the frame parameter (clearly seen in Fig. 5.14). In view of the above, the axial-flexural coupling in the frame model is considered in the present analysis.

Fig. 5.15 shows the effect of the rotor to support frame mass ratio (η=Mr/Mf) on the determination of the lowest two natural frequencies of the system, for two different lengths of frame columns. This figure is intended to exemplify the reduction of natural frequencies for increasing ratio η, and to demonstrate that this effect depends on the frame geometry and mode of vibration. The lowest four natural frequencies of the system chosen for the dynamic analysis (γ=4.8) are plotted against the mass ratio, η, in Fig. 5.16. Once again a pronounced effect of this mass ratio on the system natural frequencies can be seen. In-depth analysis of this effect would require simultaneous examination of the system mode shapes of vibration, which is beyond the scope of this project. Further analysis was carried out for the fixed value of the mass ratio, $\eta=0.05$, representative of turbomachinery foundation systems.

5.2.2 Dynamic analysis

The displacements at the location of the driving force (i.e. at the midspan of the beam) versus time are plotted in Fig. 5.17. Displacements in horizontal and vertical directions are marked on the graph by "X", and "Y", respectively. The displacements in both these directions are non-dimensionalized by dividing their absolute values by the same quantity- y_s. Where y_s is the maximum static deflection at the midspan of the beam due to a vertical load equal to $Mr \cdot e \cdot \omega_s^2$ applied at this point. The rotor operating speed is set to be beyond the fourth natural frequency of the system, i.e $\alpha=\omega_s/\omega_4=1.2$. As illustrated in Fig. 5.12, the fourth natural frequency for this specific model ($\gamma=4.8$) is of the symmetric mode of vibration. The frame chosen for the dynamic analysis has a short stubby beam and relatively long and slender columns. As a result of this geometric configuration and the specific frequency of the forcing function, the response of the system (at the driving point) is dominated (in the y-direction) by flexural vibration. The motion of this point in the x-direction is more complex, due to superposition of the columns' flexural and the beam's axial vibration, which results in "beat" frequencies. The maximum displacement envelopes, for the same response, are shown in Fig. 5.18. The instant when the instantaneous rotor speed passes consecutive critical frequencies of the system is indicated on the curve by "•". There are four such points, described by "1A", "2S", "3A", and "4S", where "A" and "S" stand for asymmetric and symmetric modes of vibration, respectively. It is observed that at the beginning of the transient period, the enevelope of maximum displacements in the vertical direction rises very slowly. For $t/\tau_0 <\simeq 2.0$, the response is dominated by vibration in the x-direction. When the instantaneous rotor speed passes the third natural frequency, the vibration in the y-direction begins to build up more rapidly. Eventually, both the maximum amplitude of vibration and level of envelope oscillation in the vertical direction become several times greater than in horizontal direction. Therefore it is logical to focus attention on the response envelope in the y-direction, for this particular model.

Fig. 5.19 shows the displacement envelopes versus time for a fixed level of rotor operating speed (α=1.1) and various rotor acceleration times T_1, (β=3.0,4.0,5.0). The results, obtained for a fixed rotor acceleration time (β=5.0) and different levels of rotor operating speed

(α=1.1,1.2,1.3), are presented in Fig. 5.20. Careful examination of the curves shown in these two figures indicates that the patterns of the envelope oscillation are identical to those presented in Figs. 5.5 and 5.6 (for Model 1). Evidently, the maximum amplitude of vibration and its shift from the critical frequency are both dependent on the level of rotor operating speed, α, and the rotor acceleration time, β. It is observed that this dependency has exactly the same character as the one already discussed in detail in Section 5.1.2. It is obvious that the resulting general relationships between the maximum amplitude of vibration (and its shift) and the rotor acceleration rate through the critical frequency of the system are, for this model, similar to those shown in Figs. 5.7, 5.8 and 5.9 (that is, for Model 1). Therefore, because they are "costly" (i.e., many runs of a computer program are required to generate data points), these general relationships are not plotted for Model 2.

The effect of damping on the system response is shown in Fig. 5.21. The level of rotor operating speed and its acceleration time are fixed (α=1.1, β=5.0), with the displacement envelopes obtained for ideal (ζ=0.0) and damped (ζ=0.1) systems. The effect of damping is clearly seen and, since it is identical to Model 1, no detailed discussion is presented.

An interesting case is shown in Fig. 5.22. Here, the rotor operating speed is set to pass the third natural frequency of the system, which for this model is of asymmetric mode of vibration (see Fig. 5.12). As a result, the dynamic response of this specific model is dominated by vibration in the horizontal ("X") direction.

5.2.3 Concluding remarks

The following conclusions may be drawn from the results of the numerical analysis of Model 2:

1. The proposed method for transient analysis proves to be equally suitable for frameworks as it is for simple beam.

2. The dynamic behavior of a framework, as a model of foundation structure, is far more complex than the response of a simple beam.

3. Results of dynamic analysis of frameworks, even for similar types of structures, cannot be generalized since the dynamic response may differ qualitatively, depending on the specific model geometry.

4. For a specific framework, as a model of a low-tuned structure supporting rotating machinery, all the conclusions (i.e. regarding the maximum amplitude of vibration and the shift in its position, as well as the effect of damping on the system response) drawn

from the analysis of Model 1 (Section 5.1.3) are also valid.

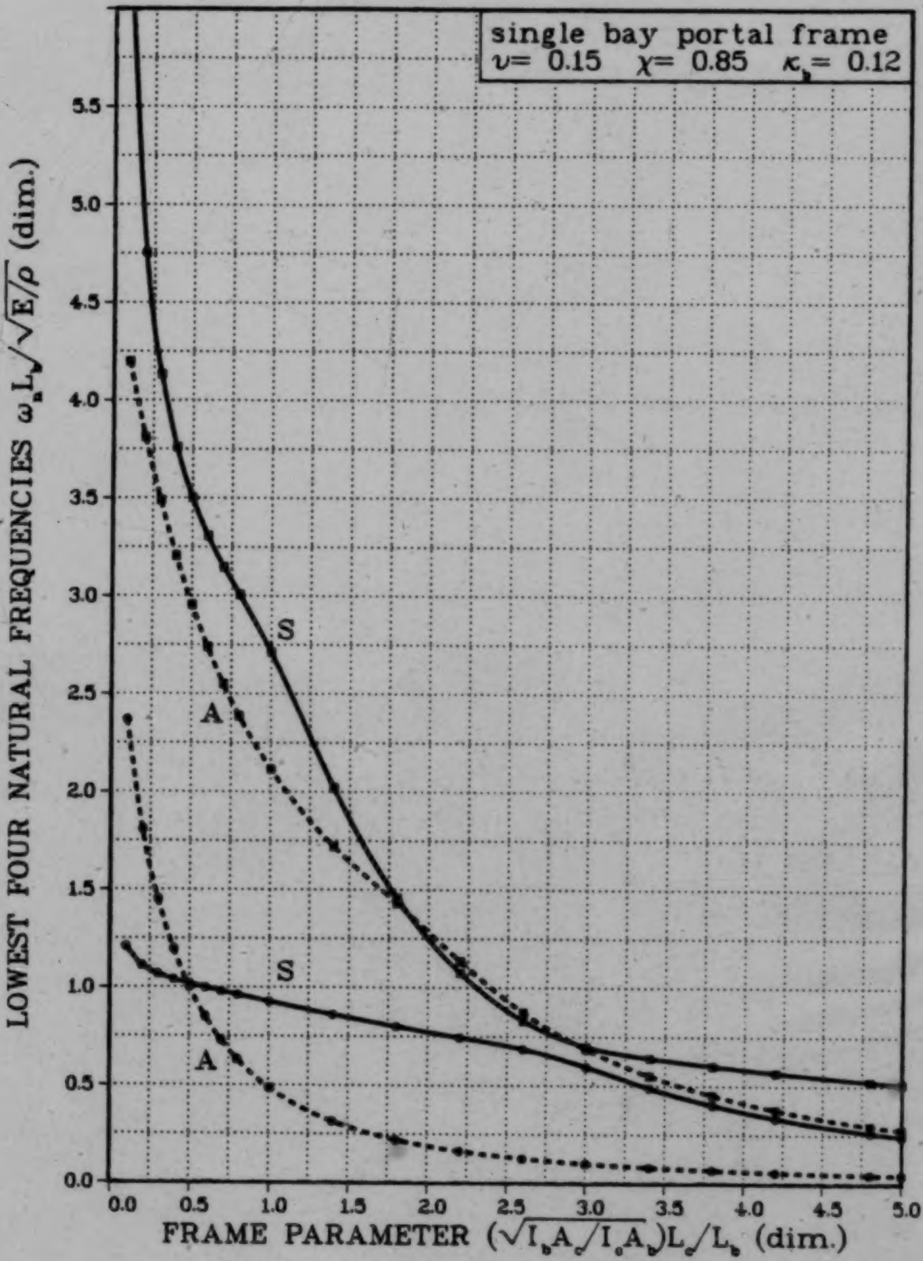

Fig. 5.12 Effect of frame parameter on natural frequencies of a portal frame; axial deformation in beams considered.

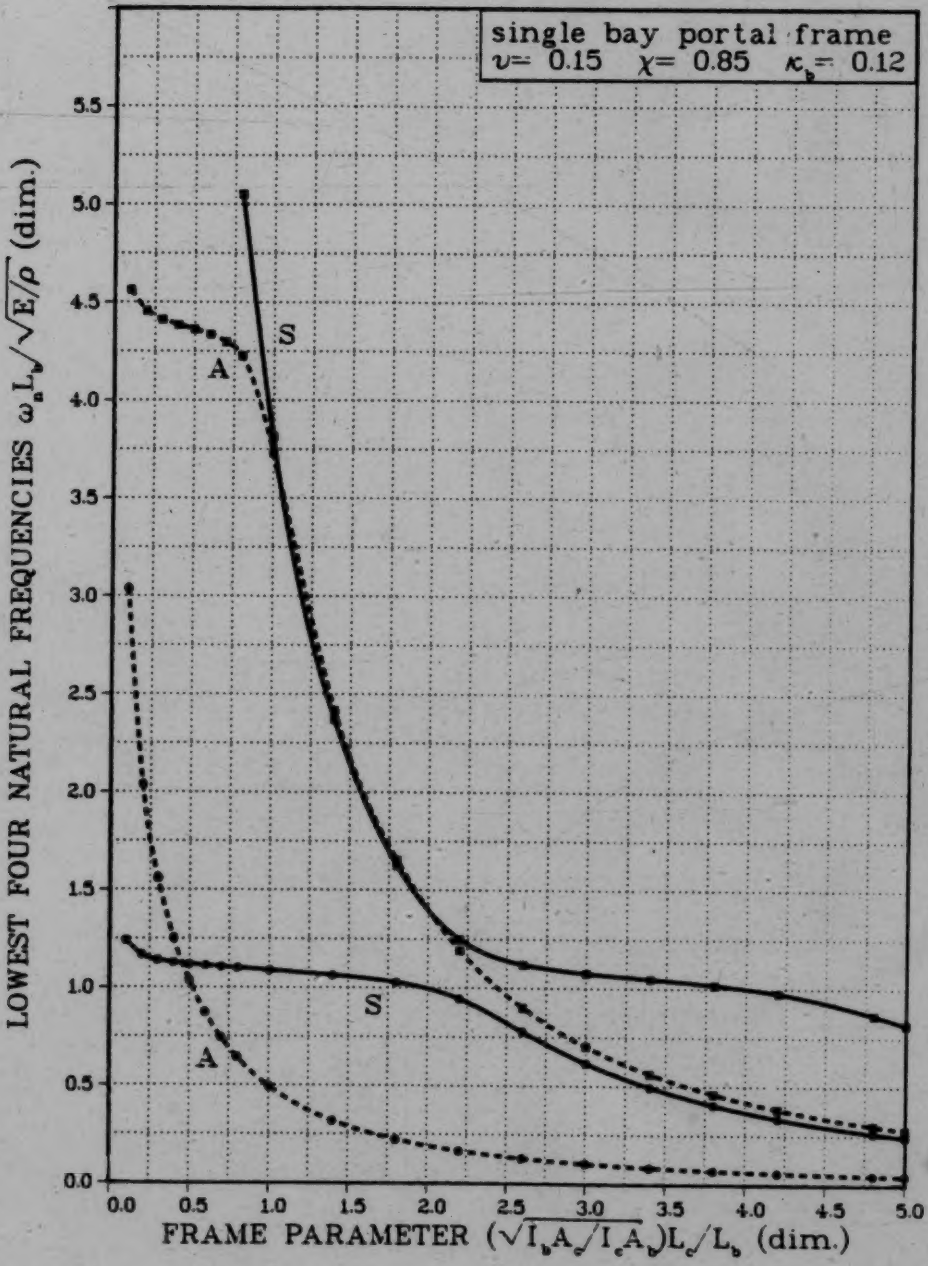

Fig. 5.13 Effect of frame parameter on natural frequencies of a portal frame; axial deformation in beams neglected.

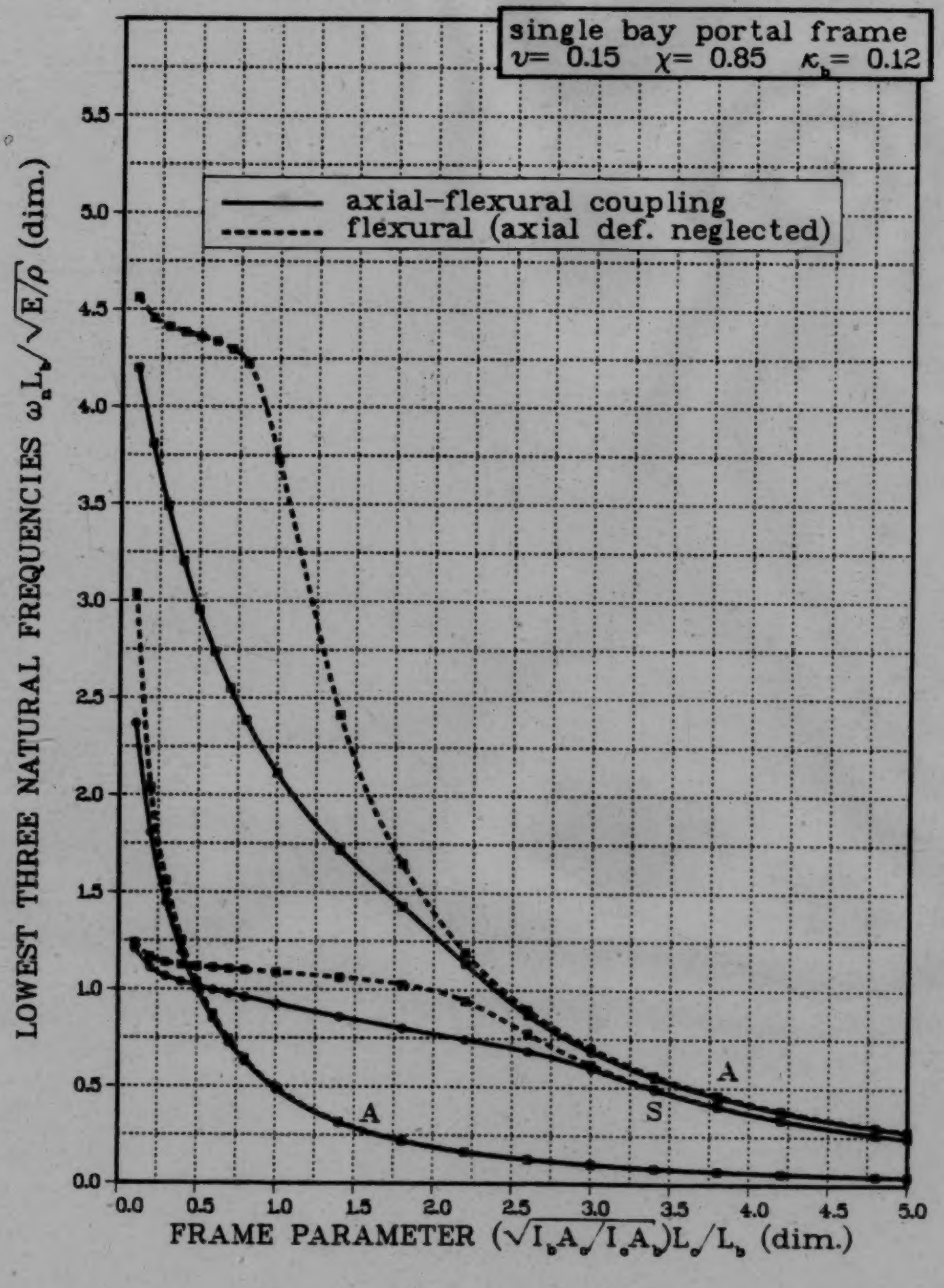

Fig. 5.14 Comparison of lowest three natural frequencies of a portal frame.

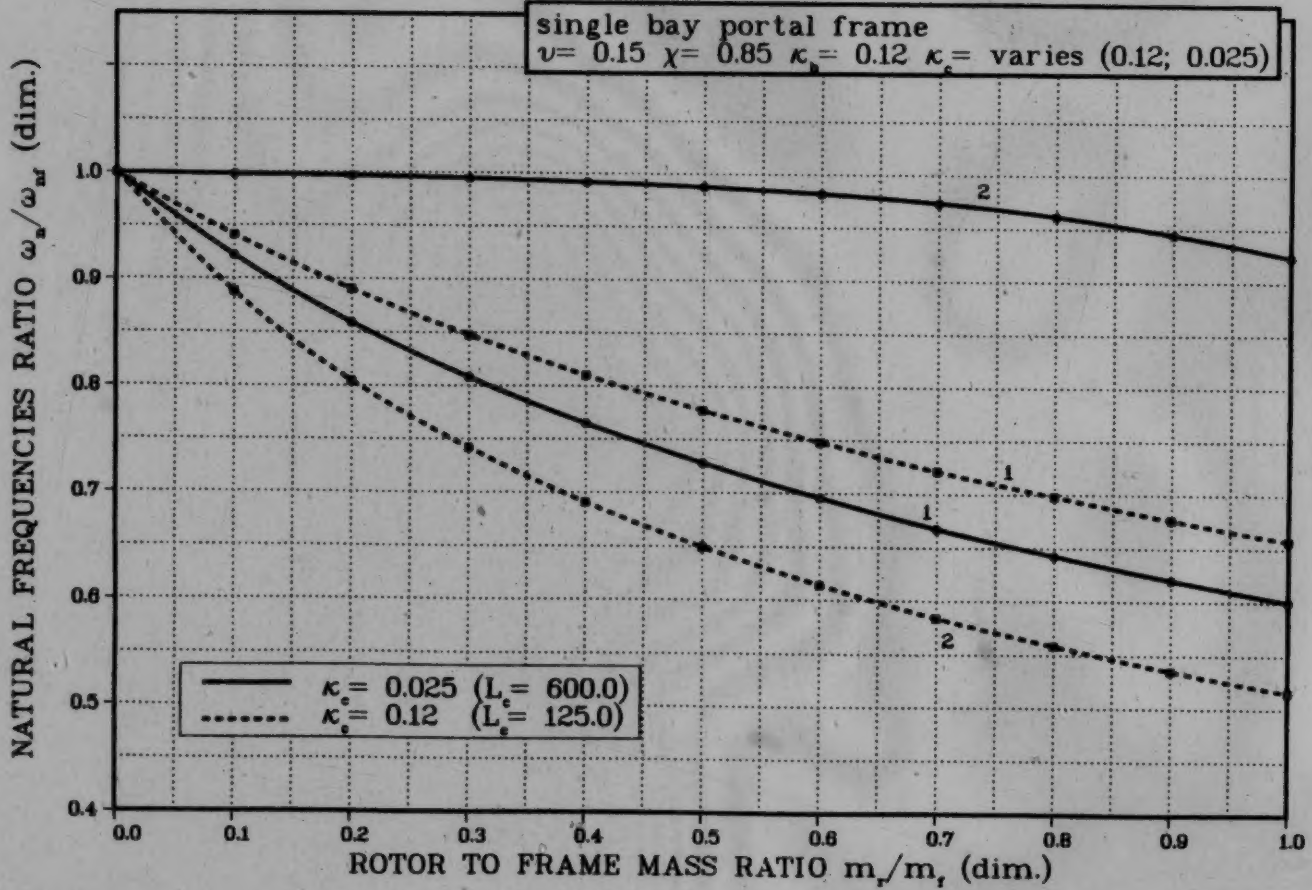

Fig. 5.15 Effect of rotor mass and frame geometry on system's lowest two natural frequencies.

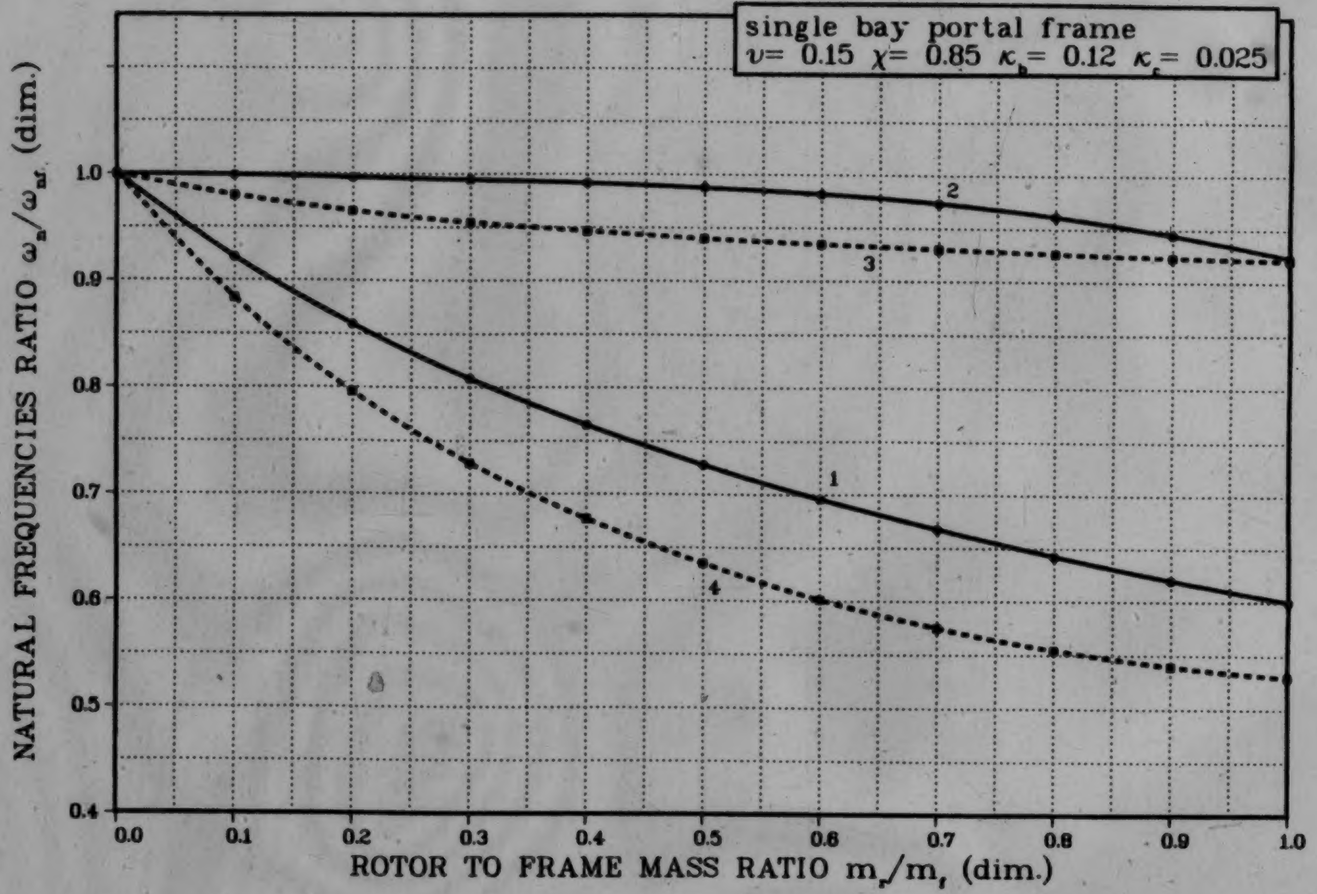

Fig. 5.16 Effect of rotor mass on lowest four natural frequencies of a portal frame.

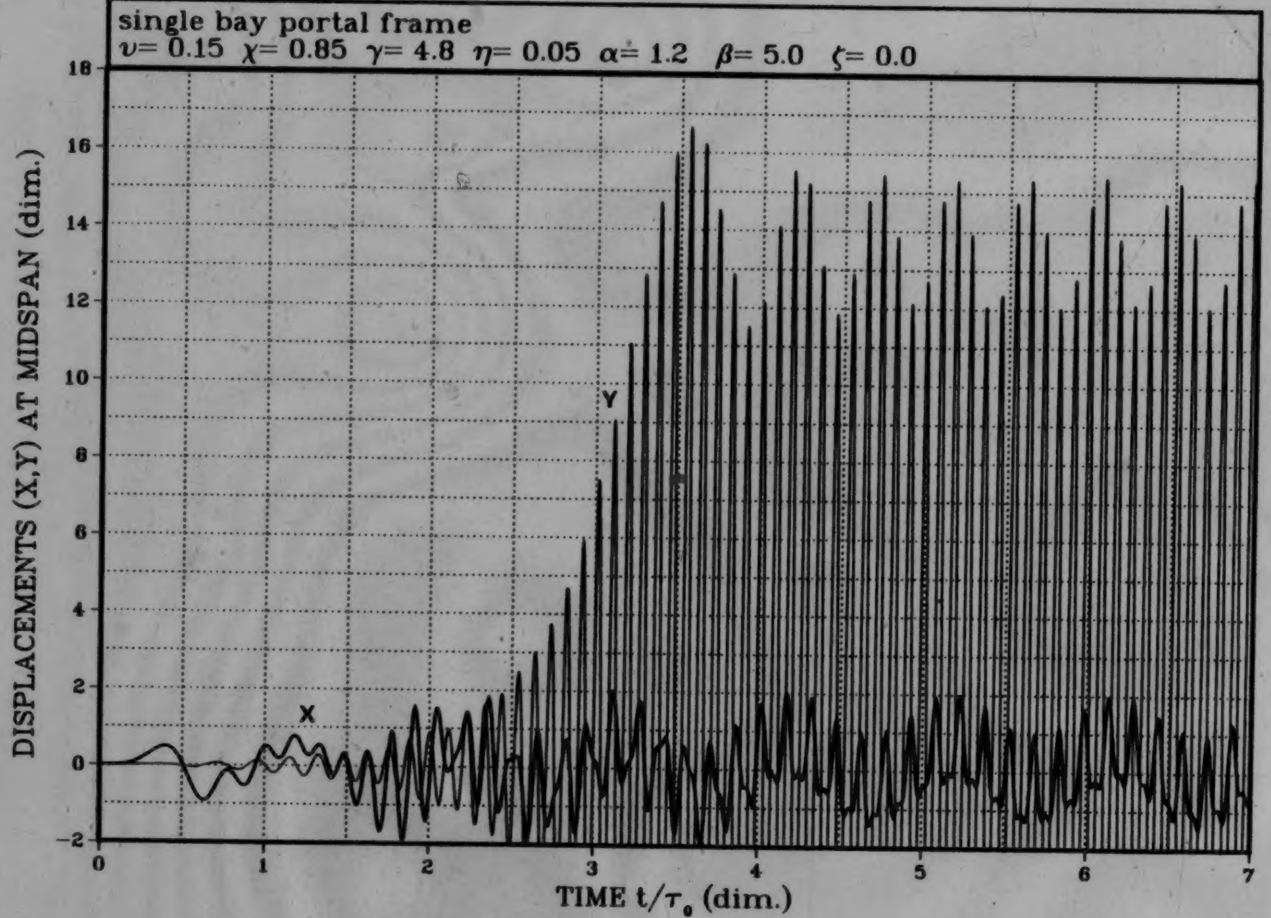

Fig. 5.17 Displacements in horizontal ("X") and vertical ("Y") directions at frame's driving point versus time.

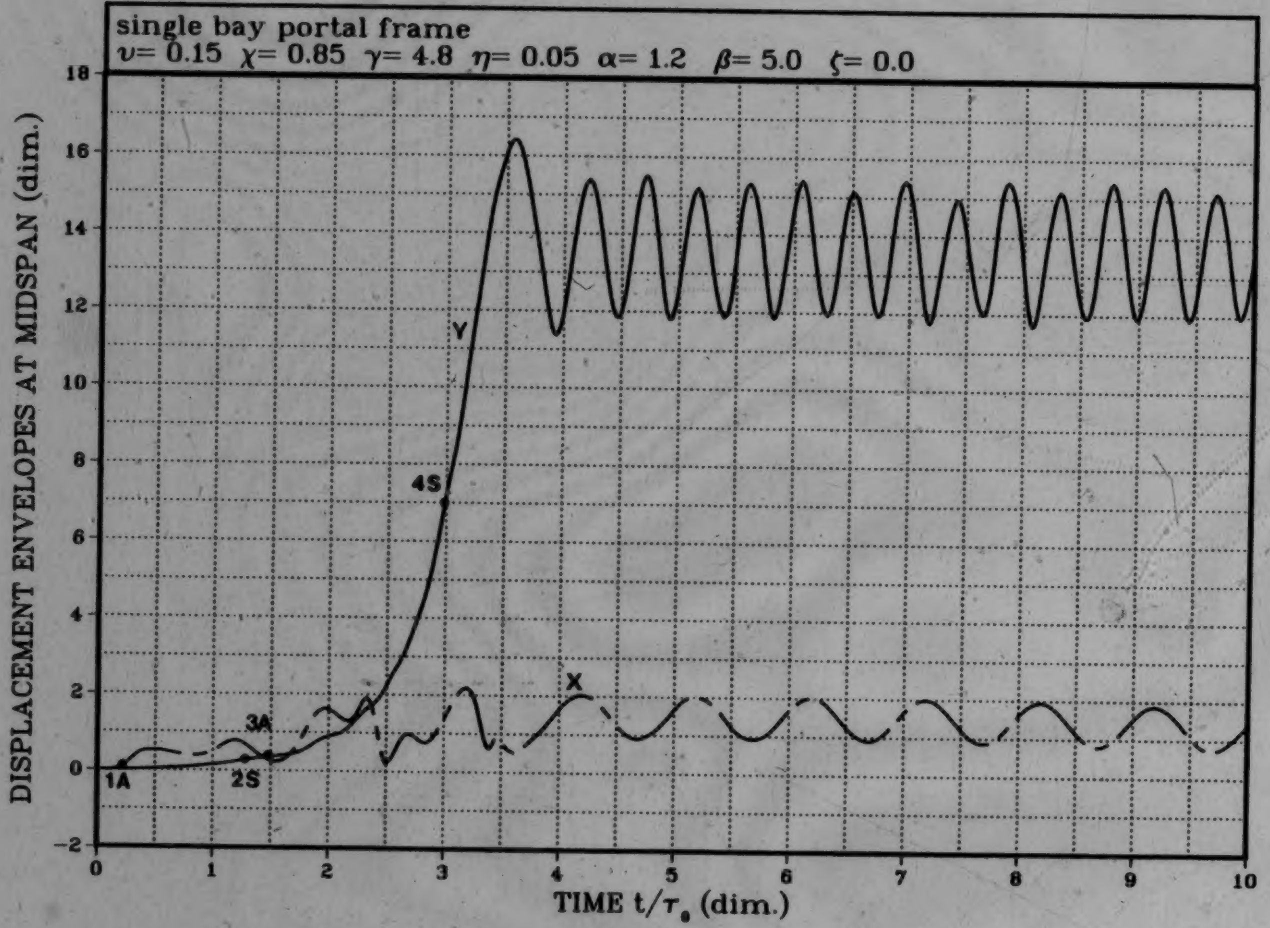

Fig. 5.18 Envelopes of response amplitudes at frame's driving point versus time.

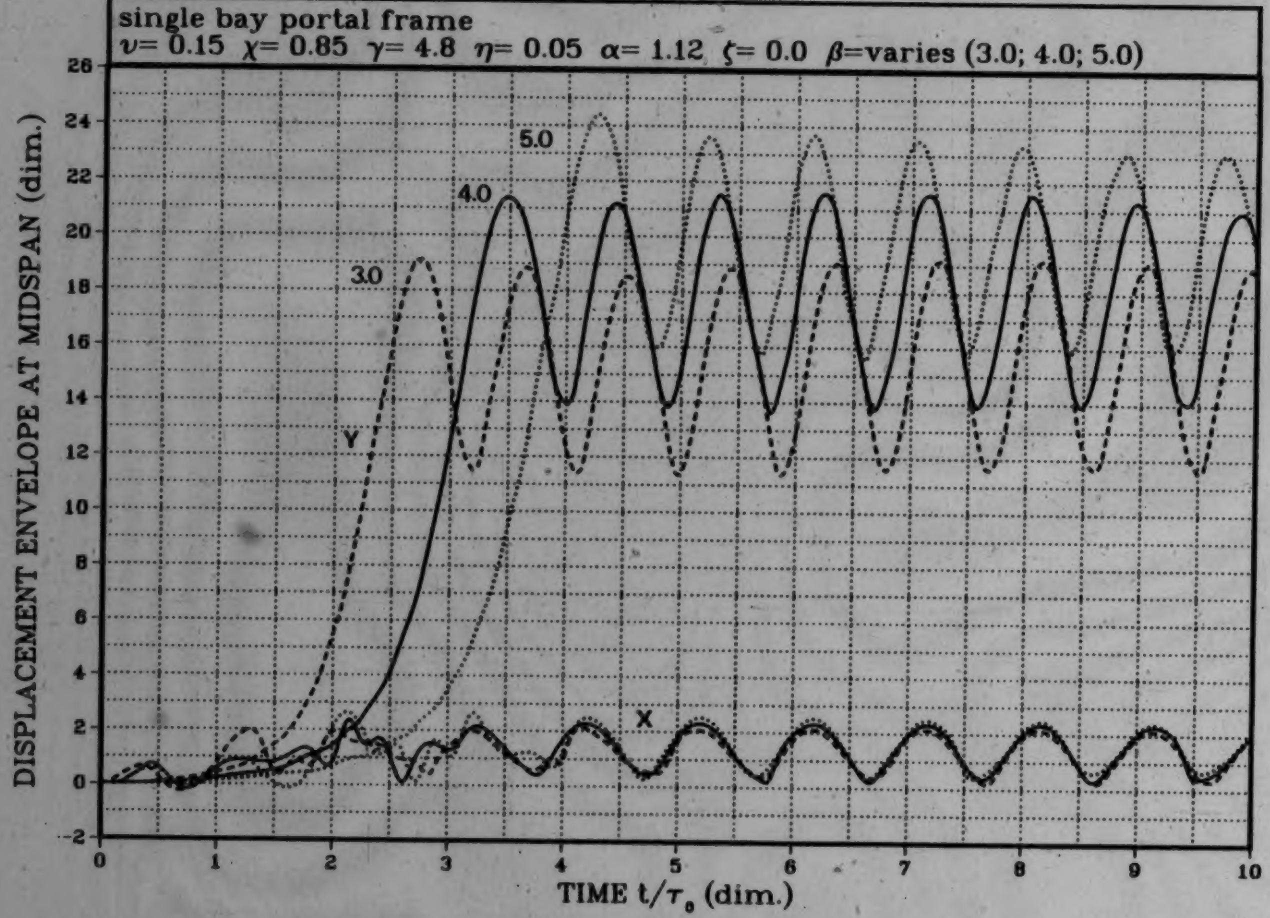

Fig. 5.19 Displacement envelopes versus time, for different values of rotor acceleration time parameter β.

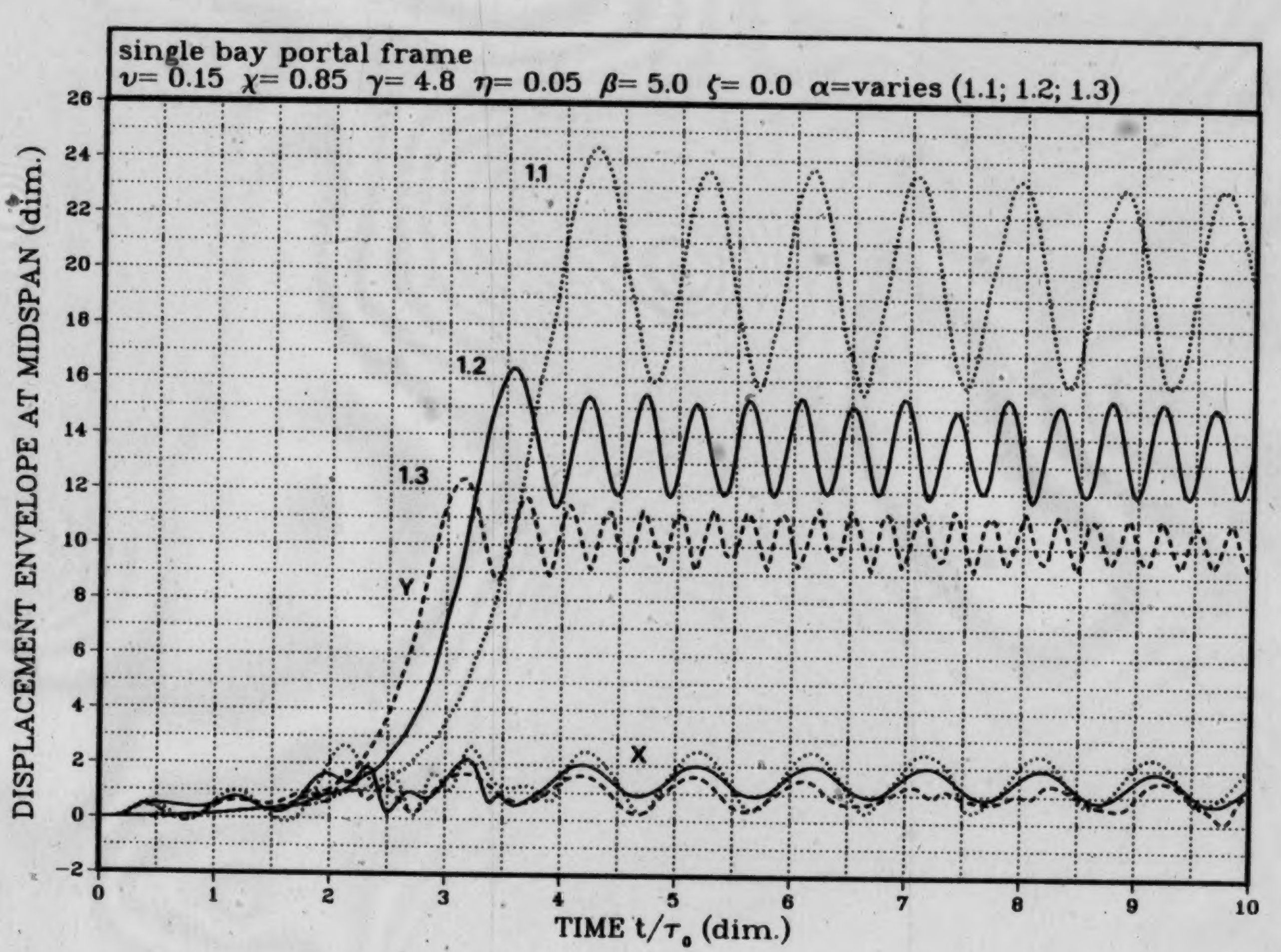

Fig. 5.20 Relationships between displacement envelope and time, for various values of rotor speed parameter α.

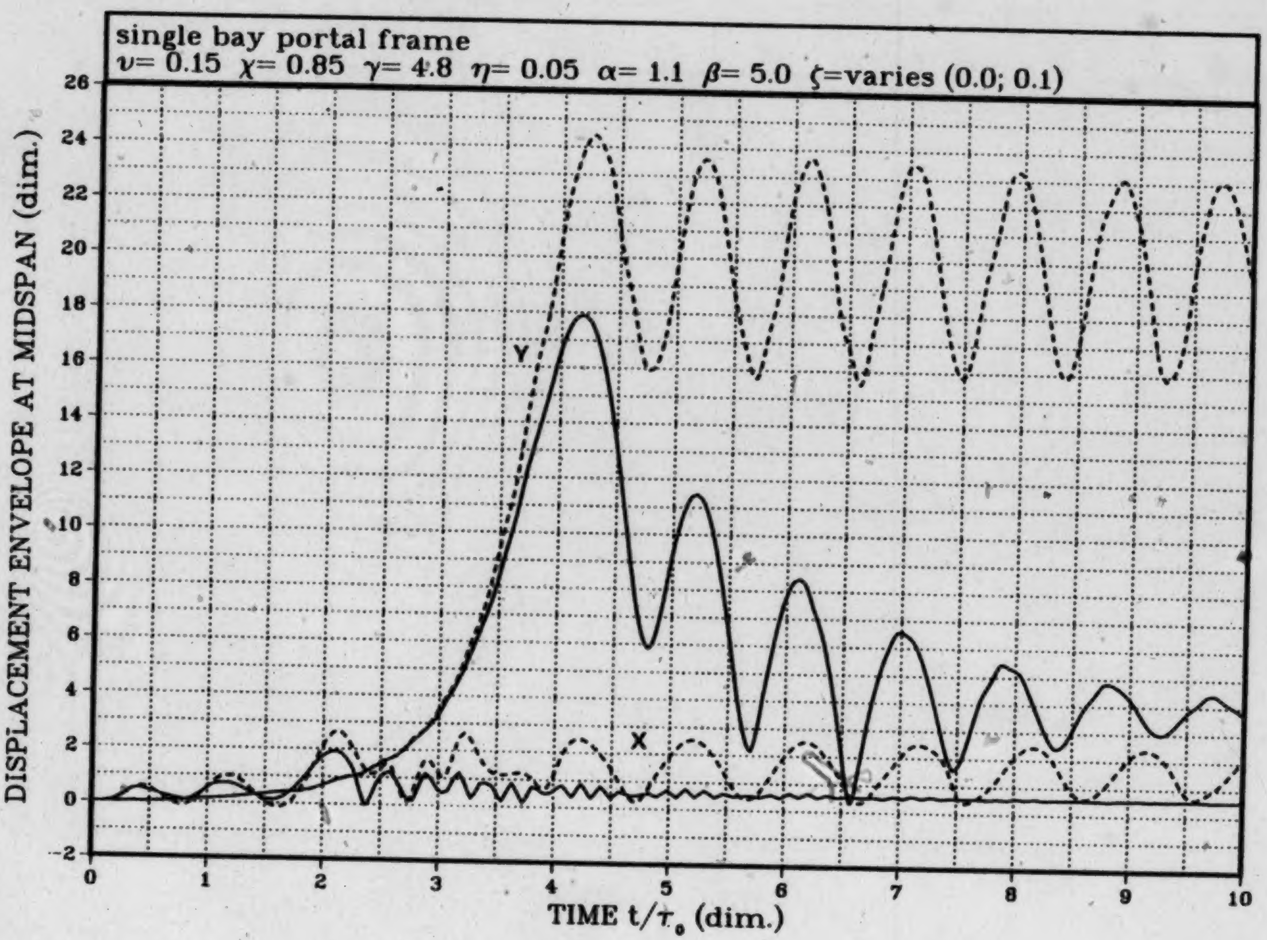

Fig. 5.21 Displacement envelopes versus time, for system with and without damping and for fixed values of parameters α and β.

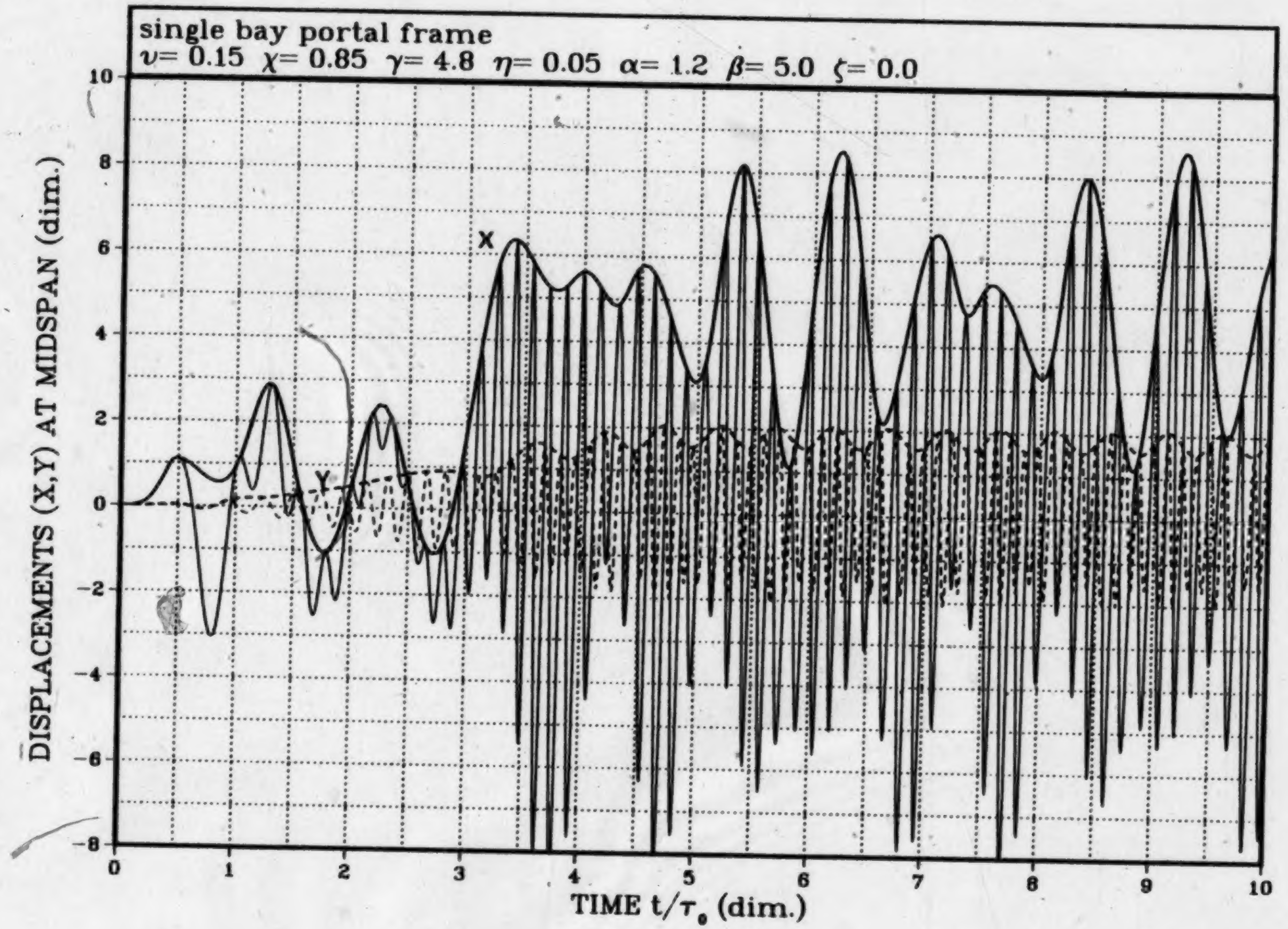

Fig, 5.22 Displacements at frame's driving point versus time, with rotor operating speed set to pass the third natural frequency.

5.3 Parametric Studies - Model 3

5.3.1 Preliminaries

At any given constant angular speed of an ideal (perfectly balanced) rotor, the journal centre is in a stationary equilibrium and the total oil-film pressure force equals the static load on the bearing. However, when the rotor has an unbalance, the centre of the rotating journal is in motion describing a closed orbit about this equilibrium position. Due to this motion, additional pressures are set up in the lubricant film acting on the journal as dynamic forces over and above the static force. These dynamic forces, as mentioned in Section 3.4.2, are a complicated function of ϵ_0, ϵ, $\dot{\epsilon}$, ψ and $\dot{\psi}$, where $\epsilon_0=f(\mu,L,R,C,W,\omega)$ is described by eqs. (3.15) and (3.17). This means that for specific rotor-bearing configuration and speed, the dynamic forces depend on both amplitude and velocity of the journal centre motion, i.e. on the journal centre orbit.

Fig. 5.23 shows whirl loci of the journal centre for $\epsilon_0=0.4$ and $g/C\omega_s^2=0.25$, being typical for a rotor-bearing system of a relatively small high-speed turbogenerator[10]. The orbits are obtained by integrating equations of motion (3.7) for two different values of the rotor unbalance parameter, (e/C=0.1 and 0.2). The pronounced effect of rotor unbalance on the journal centre motion and, consequently, on oil-film dynamic forces is obvious from this figure. In the dynamic analysis of previous models (that is with rigid bearings), the magnitude of the rotor unbalance was unimportant, since it had no effect on the displacement envelopes[11]. The results shown in Fig. 5.23 indicate, however, that this magnitude will play a very important role in the analysis of the present model.

---

[10] Specific bearing system parameters used in the numerical calculations are taken from commercially operating turbogenerator (Wabamun Power Plant, Alberta, Canada), with the service speed 3600 RPM.

Under dynamic conditions the bearing oil film behaves as a spring-damping system. By employing a conventional linear analysis[12] of the journal bearing, it can be shown that the oil-film "stiffness" and "damping" properties depend on the bearing geometry, the lubricant viscosity, the static load on the bearing and, most importantly, on the rotor speed. As a result of these dynamic properties, the oil-film plays a dominant role in attenuating or amplifying the excitation force due to the rotor unbalance. These effects are very complex in nature, involving a great number of independent parameters, and their detailed discussion is beyond the scope of this project[13].

---

[11] Note that the displacement envelopes are normalized with respect to static deflections due to centrifugal force $Mr \cdot e\omega_1^2$.

[12] Linear analysis of the journal-bearing system is very well documented. See, for example, [24-28].

[13] An interested reader is referred to specialized papers concerned with stability of the rotor-bearing system. For example [33-34].

5.3.2 Dynamic analysis

Fig. 5.24 shows the relationship between displacement envelope and time for the model with: (1) journal bearing, and (2) rigid bearing. Except for parameters associated with the bearing, all other system parameters are identical for both cases. The curves illustrate the results of the analysis carried out for the specific rotor-bearing system with the operating speed of 3600 RPM. The first natural frequency of the supporting beam selected for this analysis gives $a=\omega_s/\omega_0=1.2$. The rotor acceleration time is set so that the rotor service speed is reached at the non-dimensional time equal to 20.0, ($\beta=20.0$). Due to the reasons explained in Section 3.4.3, transient analysis of these models starts with a rotor having an initial speed ω_i (set to be 1000 RPM in this case). Therefore, transient analysis has to be preceded by initial calculations (time t=0) to establish the journal centre position and velocity for model (1), and dynamic forces transmitted to the supporting beam for both models. Applying these initial forces to the beam, being at time t=0 in static equilibrium, results in shock excitation which causes some irregularities in the system dynamic response during a short initial period. Therefore, displacement envelopes shown in Fig. 5.24 do not start at t=0.

Comparison of the curves indicates that the dynamic response of the system has practically the same general character for both models considered. However, magnitudes of the maximum amplitude of vibration and levels of envelope oscillation differ considerably. It should be pointed out that the absolute value of the rotor unbalance is identical in both models, and consequently, the response is normalized with respect to the same value. Hence, it is concluded that the force due to the rotor unbalance is magnified by the bearing oil film. It is also noted that the magnitude of the envelope oscillation after the rotor speed has stabilized at the operating level is almost the same for both cases. This suggests that the steady-state bearing transmissibility is close to 1.0 and, consequently, that the force magnification occurs during the transient period.

Fig. 5.25 shows transient orbits of the journal centre, for this specific case, following the rotor coming up from the initial to the operating speed. High rotor acceleration rate at the beginning of the motion causes rapid increase in the rotor speed and, accordingly, fast growth of the orbit amplitude. With the steadily decreasing acceleration rate these changes become smaller for each consecutive cycle of journal motion and, eventually, the journal centre describes the steady-state orbit. From this illustration the effect of changing rotor speed on journal centre motion is apparent. From the remarks made earlier it follows that the dynamic bearing force and oil-film flexibility and damping have to change accordingly.

For the particular case studied the change of bearing dynamic forces with time is demonstrated in Fig. 5.26. Both forces (i.e. journal bearing and rigid bearing forces) are normalized with respect to the same value of maximum centrifugal force due to the rotor unbalance ($Mr \cdot e\omega_s^2$). Both nonlinearity of the oil-film force, and the change of transmissibility with time is noted. To better visualize the dynamic transmissibility of the oil-film, a force magnification factor is defined as a peak-to-peak magnitude ratio of journal bearing force to rigid bearing force. This magnification factor versus time is plotted in Fig. 5.27. The relationship manifests full agreement with the conclusions drawn from the analysis of the system response presented in Fig. 5.24.

The effect of damping on the response is demonstrated in Fig. 5.28. The displacement envelopes for the model with the journal bearing and with the rigid bearing are plotted both for ideal and damped systems. It is noted that the levels of the damped transient envelope oscillation for both these models lie close to each other. This can be expected, since the steady-state oil-film force magnification factor is less than 1.1, as shown in Fig. 5.27.

To appreciate the effect of the rotor unbalance on the system response, the analysis was repeated for the rotor unbalance parameter $e/C=0.1$ with all other system parameters unchanged. The transient motion of the journal centre is shown in Fig. 5.29. Comparing the results presented in Figs. 5.29 and 5.25, it becomes obvious that transient orbits of the journal centre are highly dependent on the magnitude of the rotor unbalance. The smaller this unbalance, the smaller the amplitude of the journal orbit and, obviously, the smaller the magnitude of the dynamic bearing forces. However, no conclusions regarding the dependency of the bearing transmissibility on the rotor unbalance can be drawn from this figure. To do this, the instantaneous peak-to-peak force magnification factor is calculated. The results are shown in Fig. 5.30. It is clear that for the given rotor-bearing system parameters, the oil-film transmissibility depends on not only the rotor instantaneous speed but also on the rotor unbalance. Moreover, there seems to be no unique relationship between the transmissibility and the magnitude of the oil-film dynamic force. Finally, the system response envelope versus time, for e/C=0.1 and 0.2, are plotted in Fig. 5.31. It is observed that the maximum amplitude of vibration and the level of envelope oscillation are both higher for the smaller rotor unbalance. This does not come as a surprise, remembering that the response is normalized[14] with respect to two different values, and since the transmissibility is higher for e/C=0.1 as illustrated in Fig. 5.30. It should be stressed however that the absolute system vibration levels decrease with a reduction in the rotor unbalance.

---

[14] The curves represent the dynamic load factor as shown in Fig. 5.2.

Fig. 5.32 shows the results of the analysis carried out for varying the rotor acceleration time parameter β (β=20.0, 30.0, 40.0) and all other system parameters fixed. The results illustrate that the maximum amplitude of vibration and its shift from the system critical frequency are both dependent on the rotor acceleration time, that is also on the rotor acceleration rate through the critical frequency. It is noted that the character of this relationship is identical to that previously discussed in connection with the analysis of Model 1 and 2. (See Figs. 5.5 and 5.19). This implies that the conclusions of Section 5.1.3 regarding the dependency of the system response on the rotor acceleration rate through the critical frequency and on the rotor operating speed are, in general, irrespective of the type of bearing in the system.

The analysis carried out so far dealt with the bearing-rotor system parameters typical for a small turbogenerator. Larger units operate generally at lower speeds and with higher static loads on bearings. Both these parameters, as discussed in Section 3.4.2, have an essential effect on the dynamic performance of the journal bearing. It is therefore of interest to investigate the dynamic response of the system with considerably different parameters. Consequently, further discussion is concerned with some of the results obtained for ϵ_0=0.7 and $g/C\omega_s^2$=1.0, being typical of a medium-sized turbogenerator rotor [7]. The rotor operating speed for this model is 1800 RPM.

Fig. 5.33 shows a family of steady-state journal centre orbits obtained for different values of rotor unbalance. It is noted, comparing the curves shown in Figs. 5.33 and 5.23 (for the corresponding values of rotor unbalance), that non-linear effects are more pronounced for greater ϵ_0. Transient orbits of the journal centre for the rotor accelerating from the initial speed of 500 RPM and with the rotor unbalance parameter e/C=0.4 is presented in Fig. 5.34. The effect of changing rotor speed on the orbit amplitude is well illustrated. The change in position of the "instantaneous" steady-state journal centre can be easily traced as it "moves" upwards following an increase in the rotor speed and, consequently, in the bearing load carrying capacity.

The dynamic response of the system to unbalance excitation, for the models with journal bearings and with rigid bearings, is shown in Fig. 5.35. The rotor speed parameter and acceleration time parameter are α=1.2 and β=20.0, respectively. While the general character of the system response remains the same for both models, the maximum amplitude of vibration, the level of envelope oscillation, and the amplitude of this oscillation are greatly increased for the model with journal bearings. This implies that the journal bearing transmissibility, for this specific case, is much higher than 1.0. More importantly, the increased magnitude of the envelope oscillation infers that the transmissibility remains high even after the rotor speed has stabilized at its operating level.

Fig. 5.36 illustrates the relationship between displacement envelope and time for the same rotor-bearing system and a different supporting beam (α=0.8). The results presented are obtained for the rotor unbalance parameter e/c=0.1 and 0.4 and for the models with journal bearings and with rigid bearings. The curves indicate that the system response is typical for high-tuned supporting structures subjected to unbalanced excitation, as discussed in detail in Section 5.1.2. They also imply that the transmissibility is higher for the smaller rotor unbalance.

Fig. 5.37 shows the peak-to-peak force magnification factor plotted against time, for e/c=0.1 and 0.4. These relationships fully confirm the predictions deduced from the analysis of the results presented in Figs. 5.35 and 5.36.

5.3.3 Concluding remarks

The following major conclusions are drawn from the results of the numerical analysis of Model 3:

1. The proposed method of solution for the transient response analysis of structures supporting rotating machinery is readily adaptable for complex models of the forcing function.

2. The dynamic response of the system is highly dependent on the rotor-bearing system parameters.

3. A generalization of overall trends in the system response as a result of the system parameters alteration, as, for example, lubricant viscosity, static load, radial clearance et cetera, is extremely difficult due to a large number of independent parameters involved.

4. Dynamic properties of journal bearing depend on the region of bearing operation on design maps (ϵ_o, $g/C\omega_s^2$) and they change during transient period with rotor speed.

5. The magnitude of the rotor unbalance has a significant effect on the system response. This effect is dependent on a specific rotor-bearing system and varies with the instantaneous rotor speed.

6. For any given system parameters, the dynamic response is dependent on the level of the rotor operating speed and its acceleration rate through the system critical frequency. The conclusions regarding this dependency, as well as the effect of damping on the system response, drawn from the analysis of Model 1 (See Section 5.1.3) are general regardless of a type of bearing in the system.

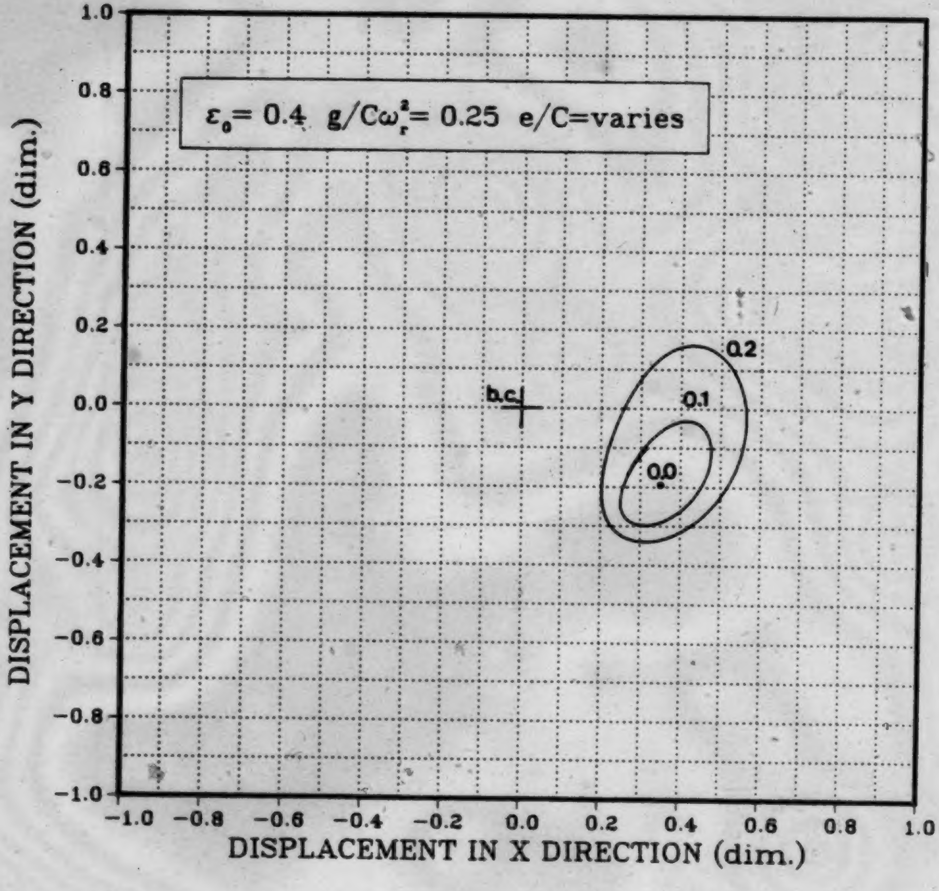

Fig. 5.23 Effect of rotor unbalance on steady-state whirl orbit of journal centre.

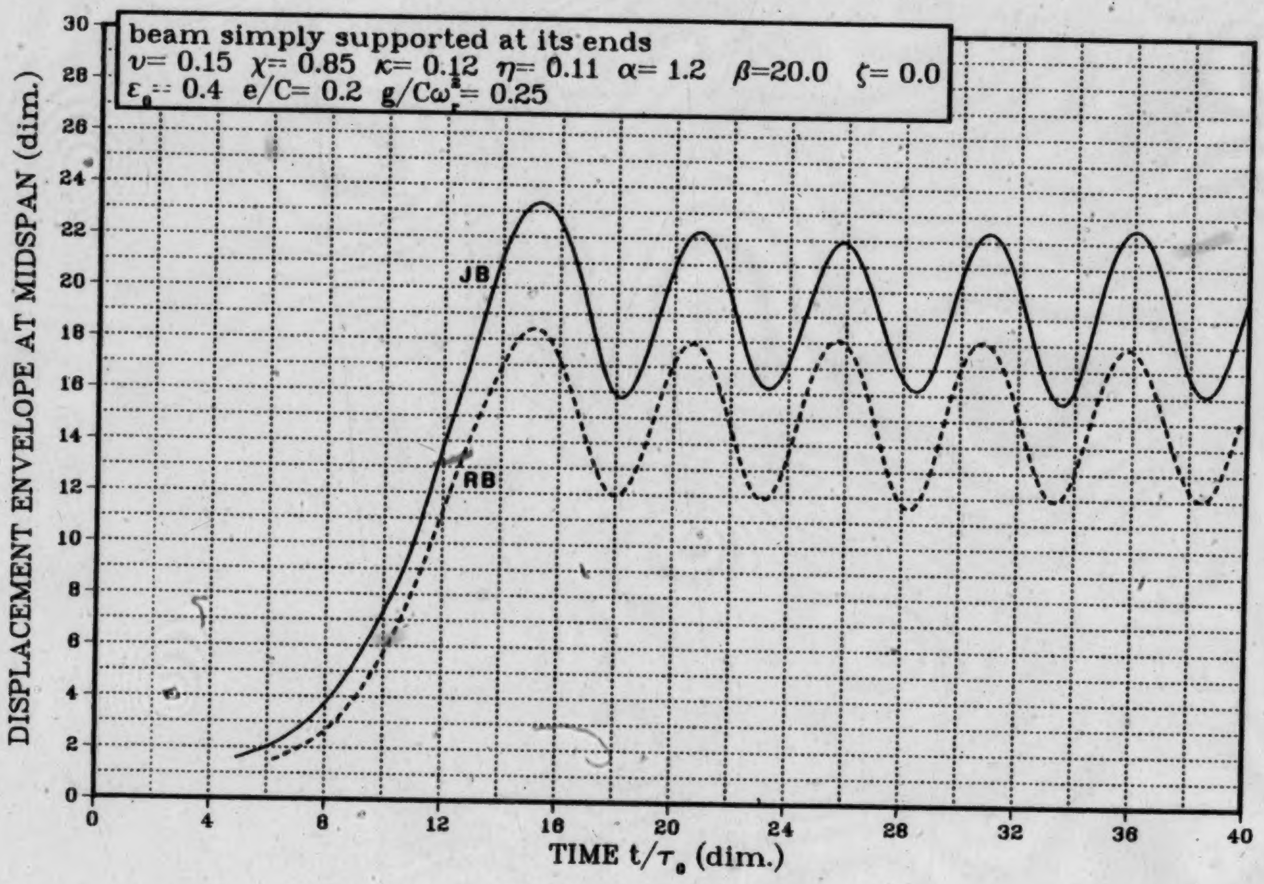

Fig. 5.24 Displacement envelopes versus time for model with: (1) journal bearing (JB), and (2) rigid bearing (RB).

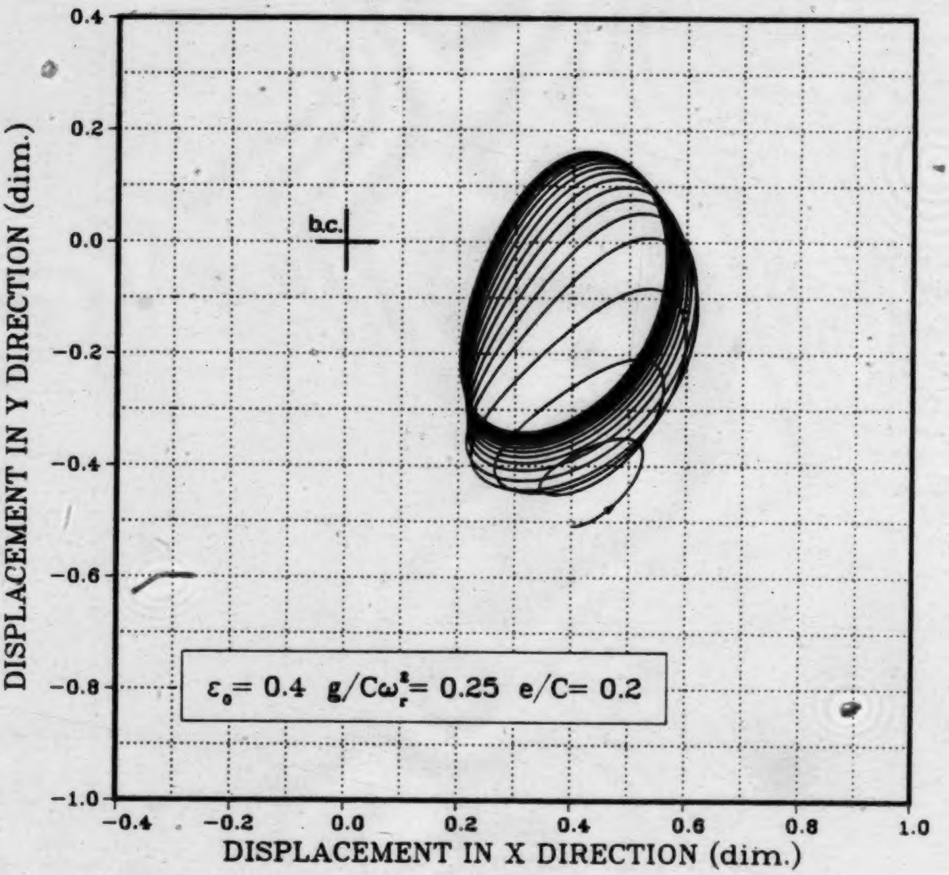

Fig. 5.25 Transient whirl orbit of journal centre due to rotor acceleration, for rotor unbalance parameter $e/C=0.2$.

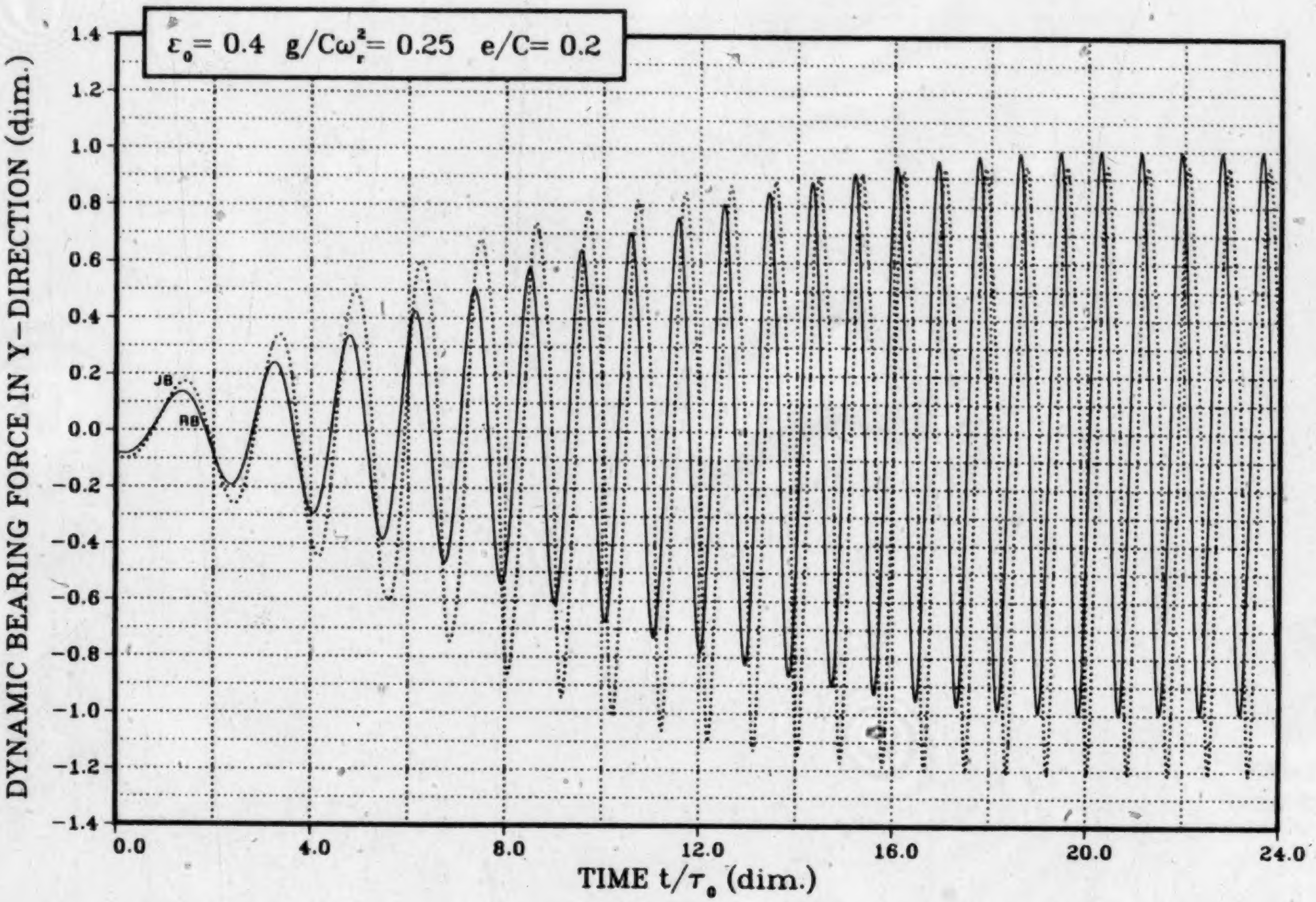

Fig. 5.26 Comparison of dynamic bearing forces for: (1) journal bearing, and (2) rigid bearing.

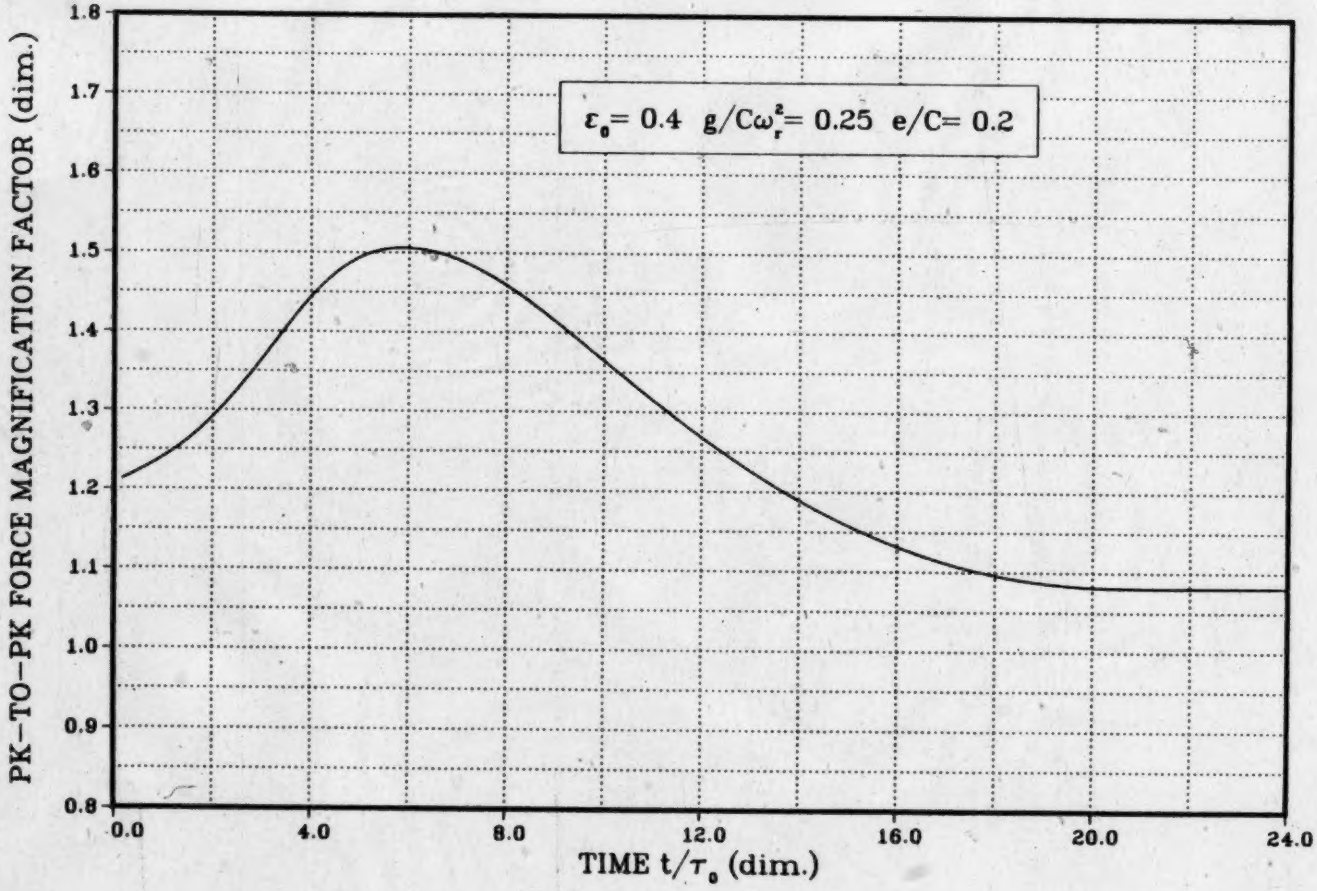

Fig. 5.27 Oil-film force magnification factor in journal bearing versus time.

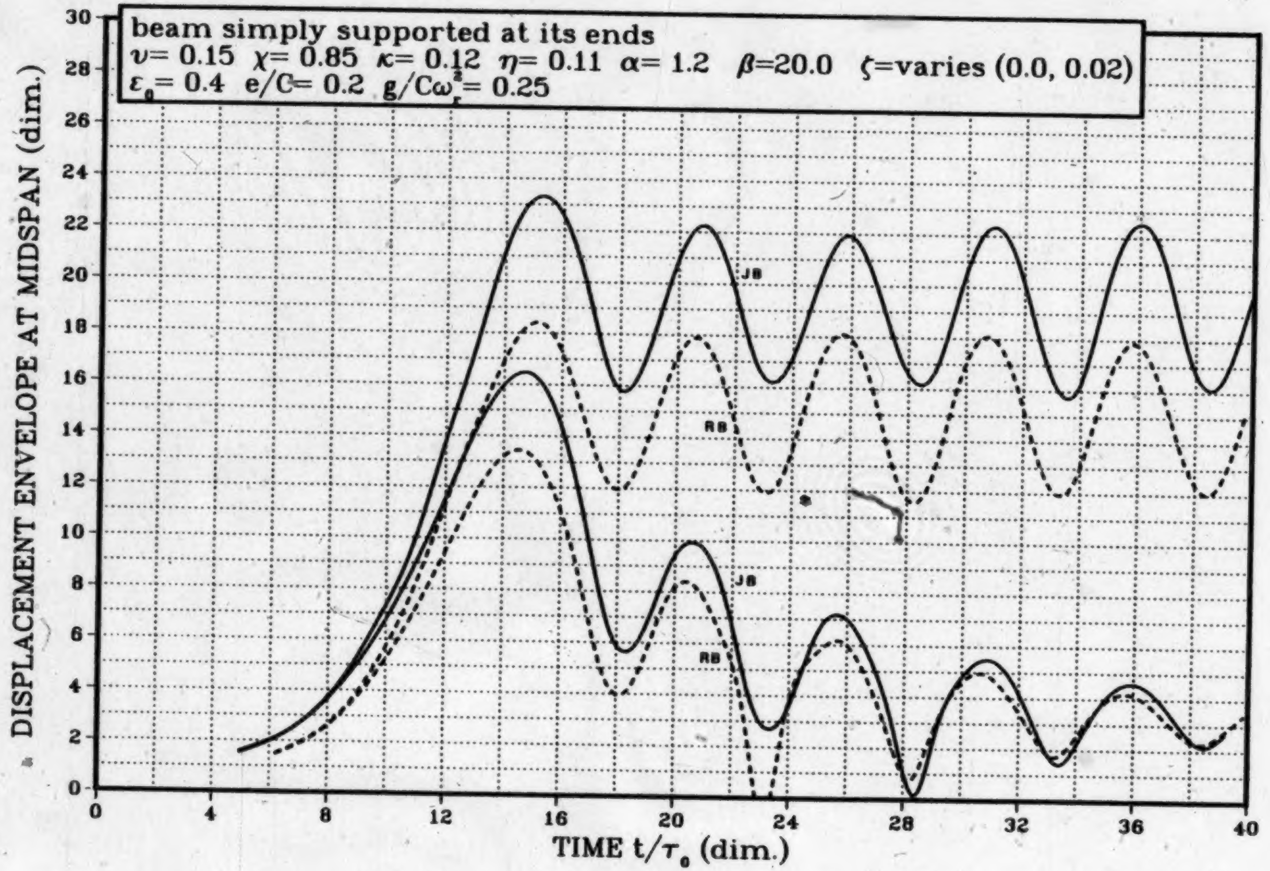

Fig. 5.28 Comparison of damping effect on system response for model with: (1) journal bearing (JB), and (2) rigid bearing.

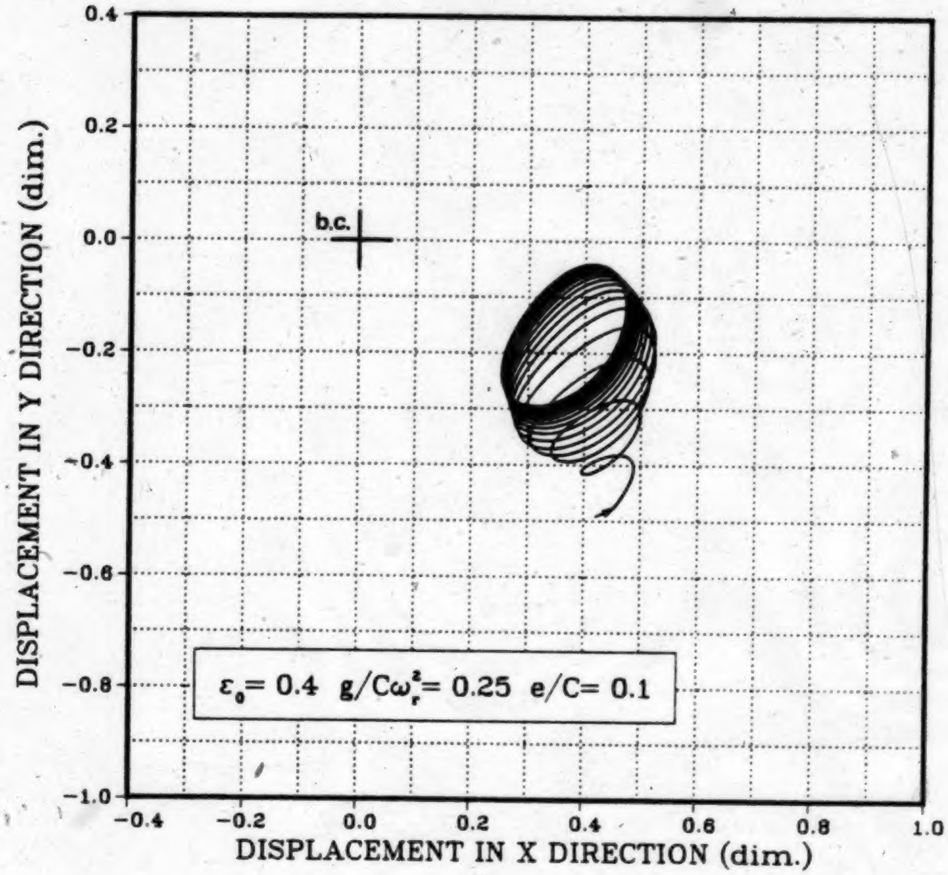

Fig. 5.29 Transient whirl orbit of journal centre due to rotor acceleration, for rotor unbalance parameter e/C=0.1.

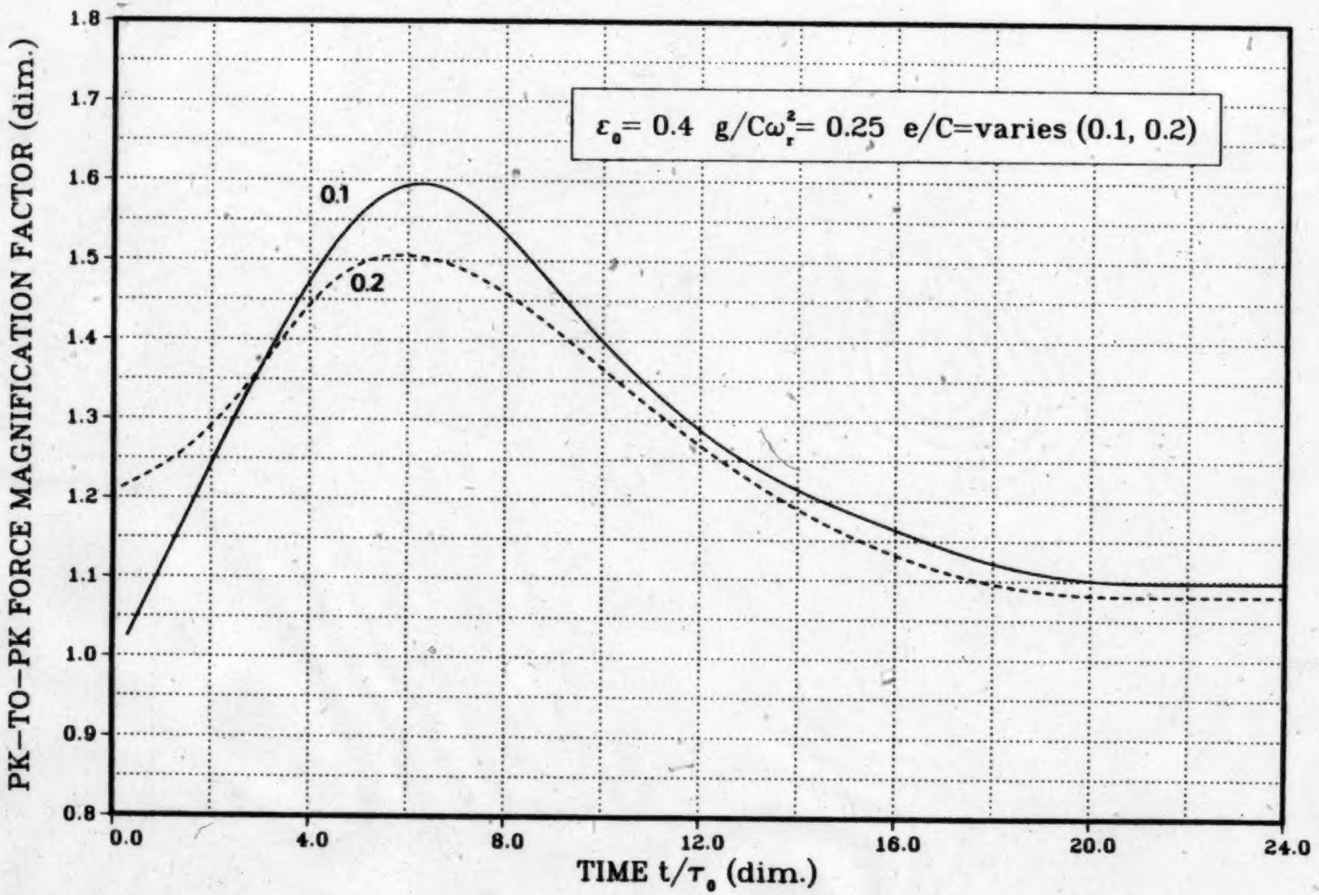

Fig. 5.30 Effect of rotor unbalance on oil-film force magnification factor.

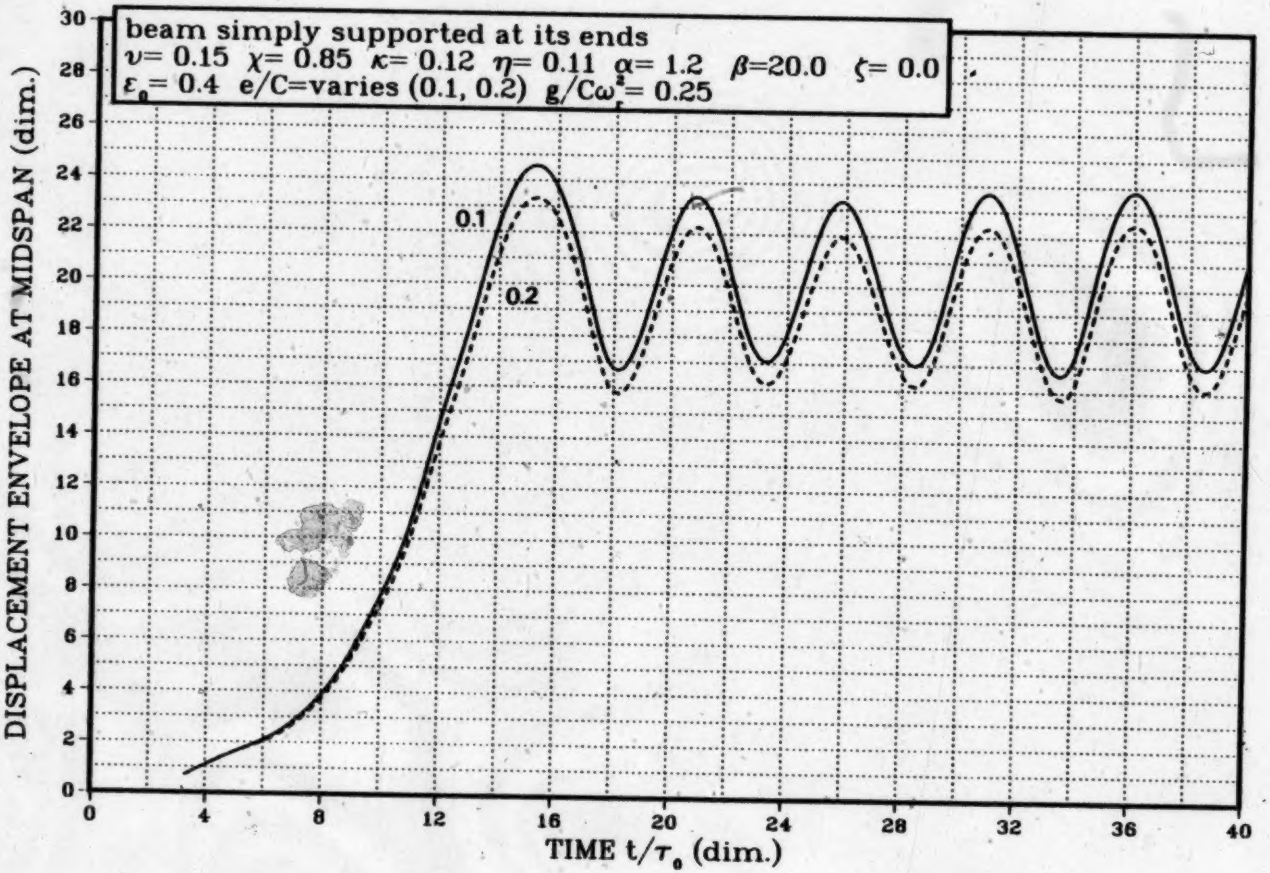

Fig. 5.31 Displacement envelope versus time, for two different values of rotor unbalance parameter (e/C=0.1, 0.2).

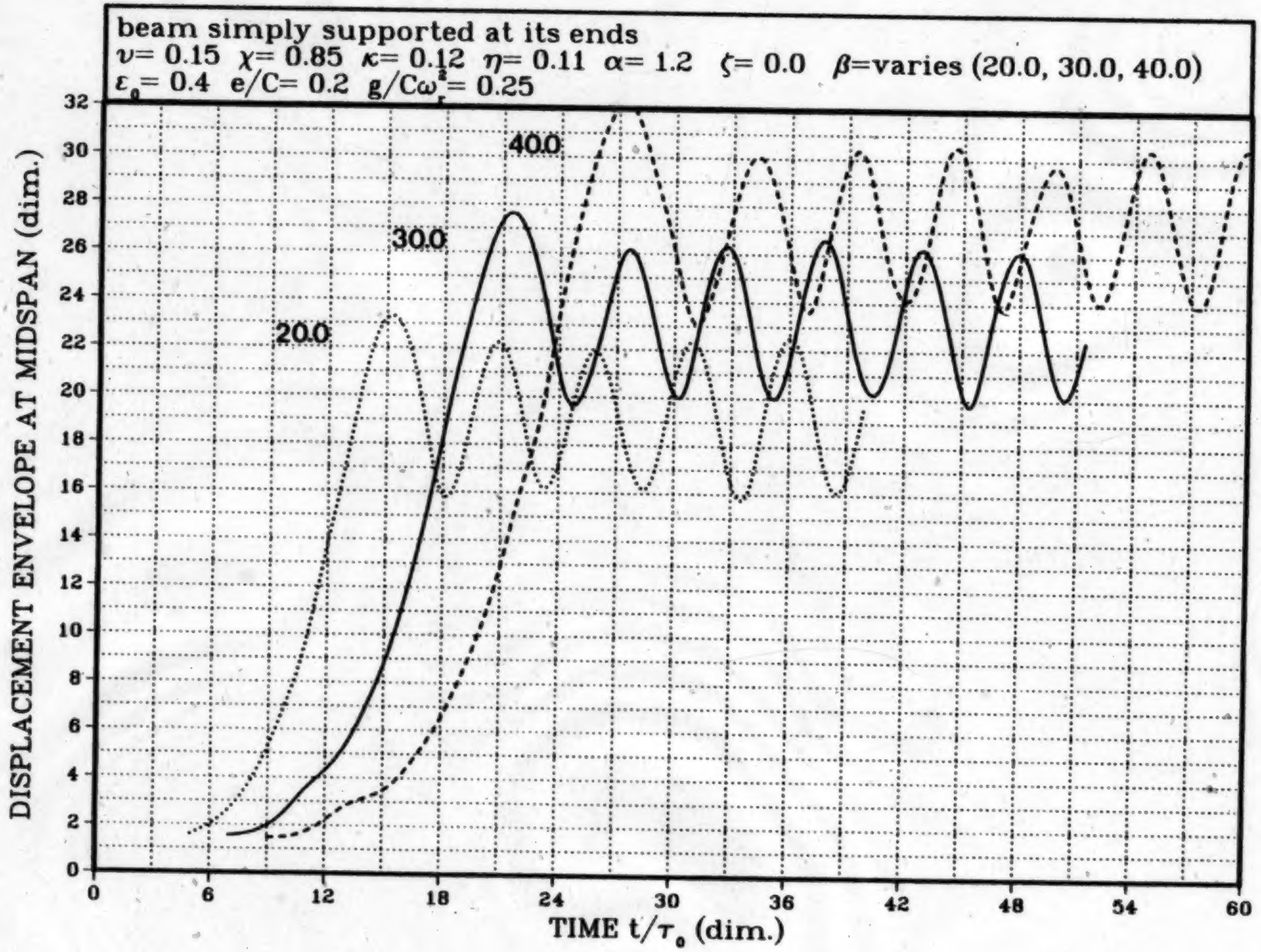

Fig. 5.32 Displacement envelope versus time for different values of rotor acceleration time parameter β.

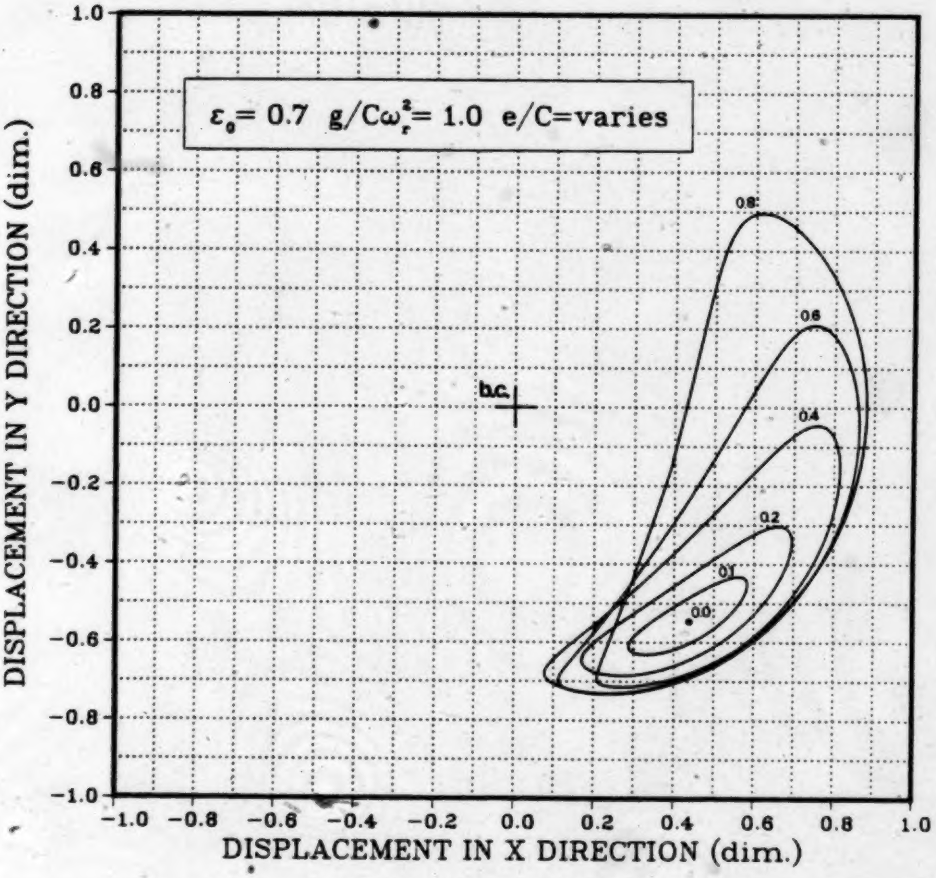

Fig. 5.33 Family of journal centre whirl loci for different values of rotor unbalance parameter e/C.

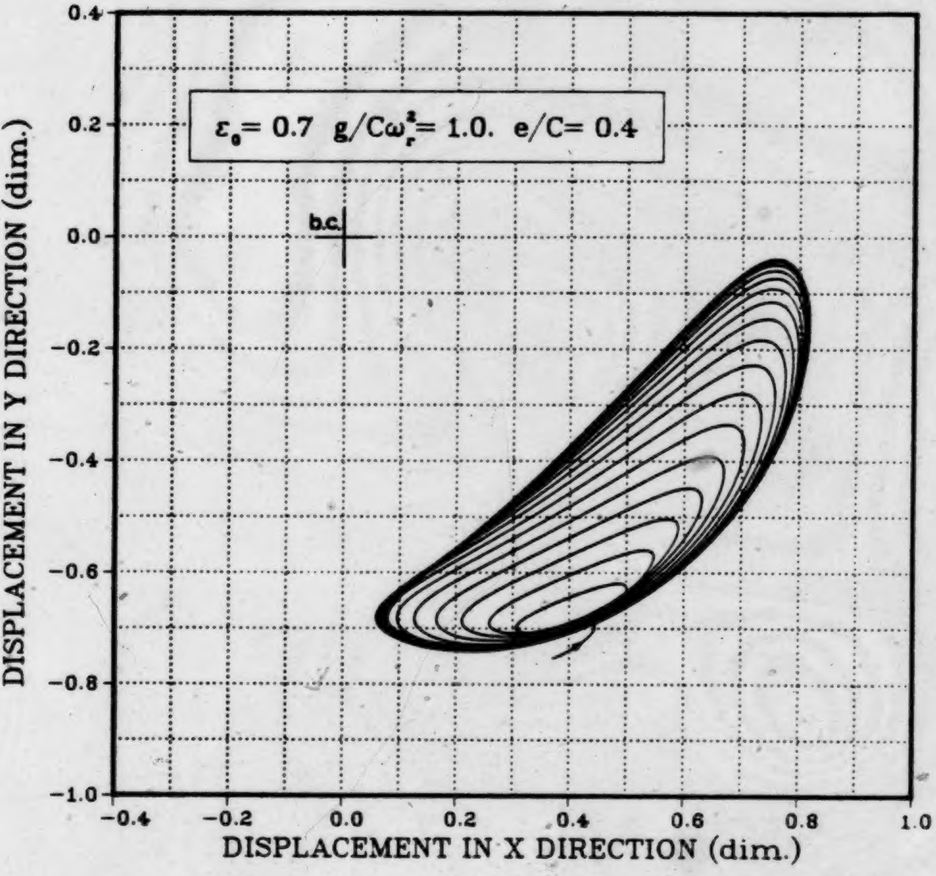

Fig. 5.34 Transient whirl orbit of journal centre due to unsteady rotor angular velocity.

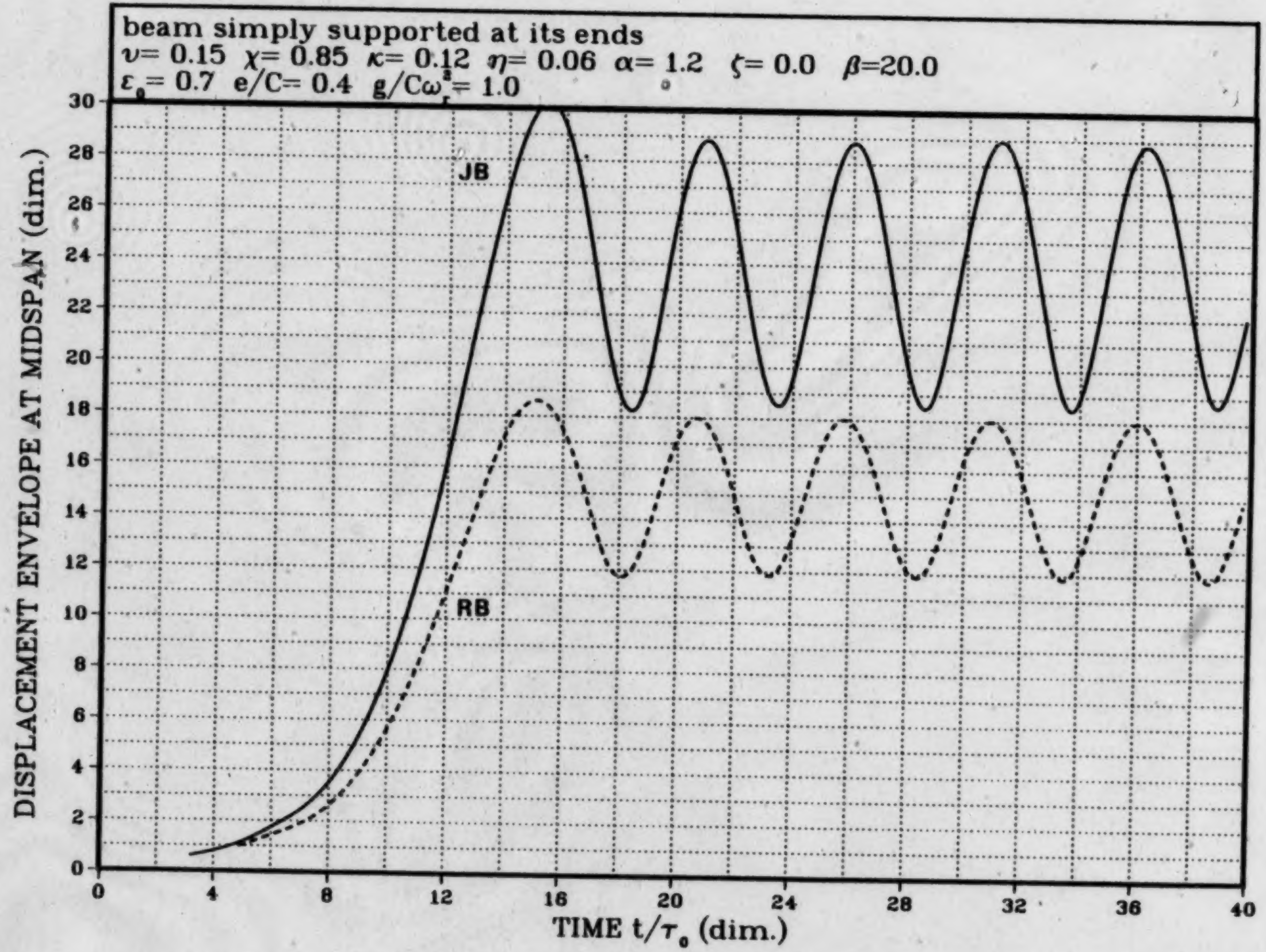

Fig. 5.35 Displacement envelope versus time for model with: (1) journal bearing (JB), and (2) rigid bearing (RB).

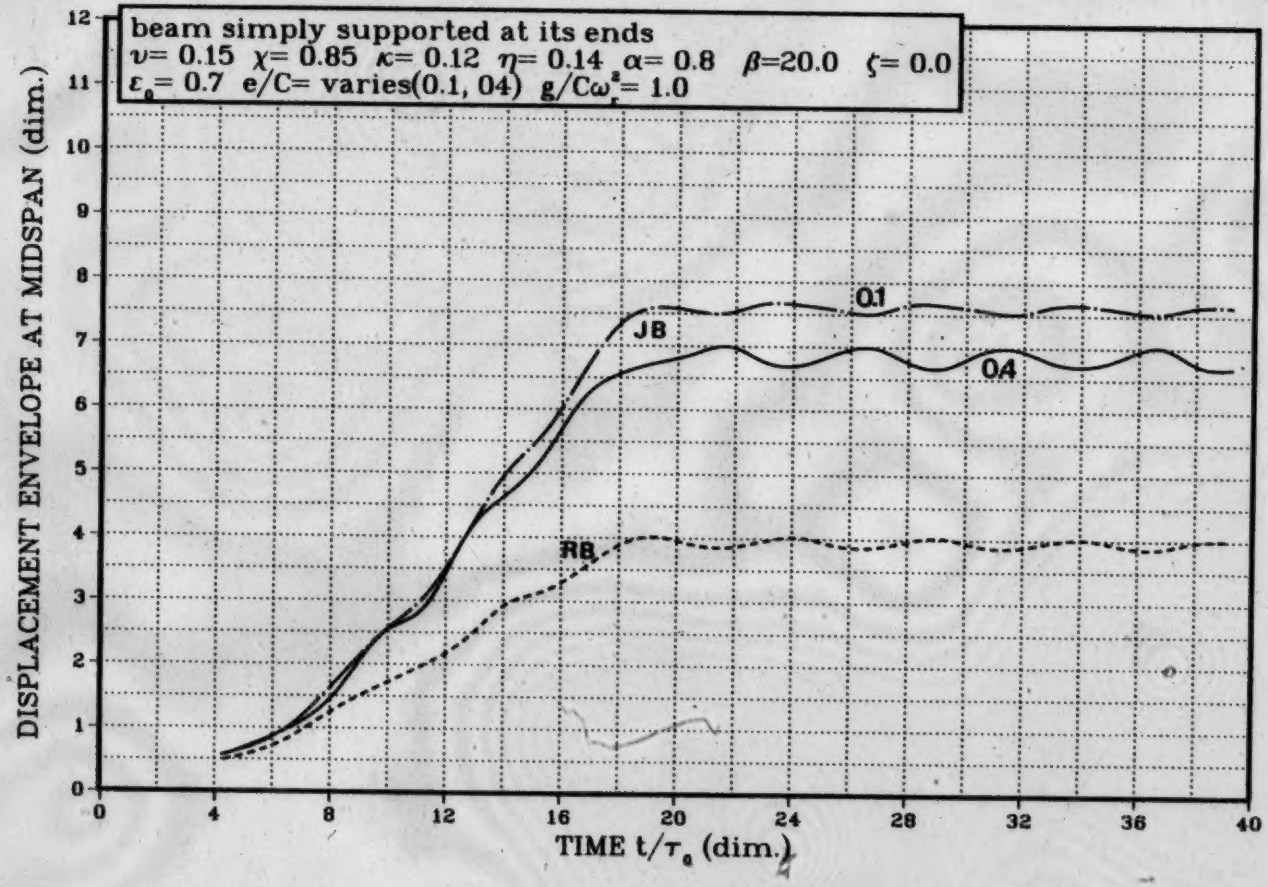

Fig. 5.36 Effect of rotor unbalance on system dynamic response for rotor speed parameter =0.8, for model with: (1) journal bearing, and (2) rigid bearing.

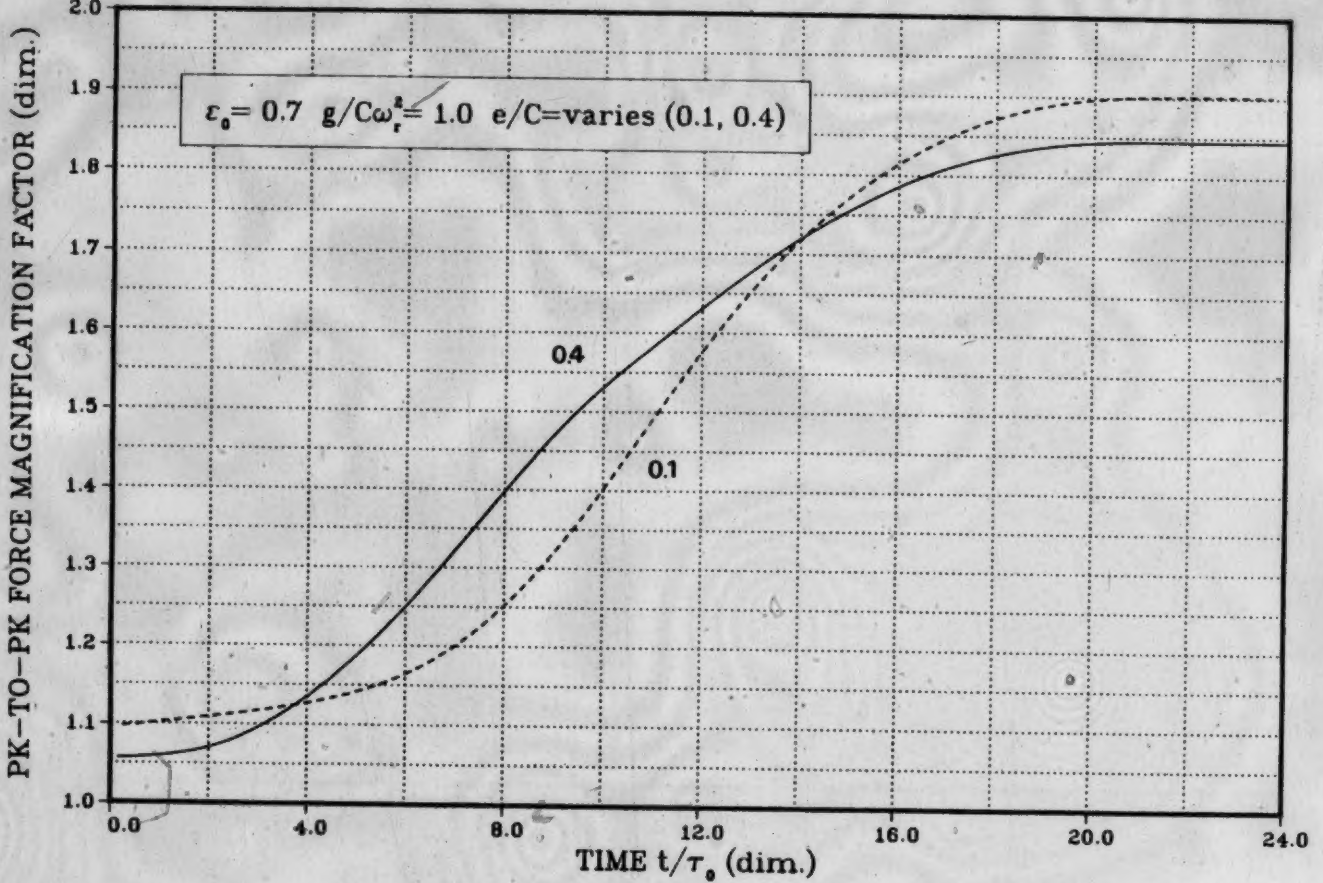

Fig. 5.37 Oil-film force magnification factor versus time, for two different values of rotor unbalance parameter e/C=0.1,0.4

6. CONCLUSIONS AND RECOMMENDATIONS

A numerical investigation was carried out mainly to verify the proposed method of solution and to establish its usefulness for the specific type of problem. Both the results and the simplicity in obtaining them demonstrate that the method of solution based on finite time formulation is very convenient for the transient analysis of machine-foundation interacting systems. The study shows that the method is suitable for any system regardless of structure and/or forcing function complexity.

General conclusions, drawn from the numerical analysis of each of the models considered, regarding dynamic behavior of the system are given in the sections immediately following the discussion of the results. Perhaps the most important conclusion being that the maximum amplitude of vibration of low-tuned structures supporting rotating machinery occurs during the transient period of the rotor coming up to speed and that it is highly dependent on the rotor acceleration rate through the critical frequency of the system. This maximum amplitude cannot be predicted by the classical steady-state analysis. Therefore, the transient response analysis, as the most inclusive approach to the system dynamic analysis, should be employed in the present-day design practices of low-tuned foundations.

Models chosen for this study were simple ones. They proved to be adequate for a qualitative analysis concerned mainly with the determination of general relationships and trends in the dynamic behavior of the system. It should be stressed that more accurate models would not alter the general conclusions drawn from this study. However, for a quantitative analysis of the system response, the use of much more elaborate models would be required. That means realistic modelling of three dimensional foundations, multiple bearings flexible rotor systems, bearing pedestals, seals, et cetera. While such a comprehensive approach to the problem is very desirable and possible with the analytical and technological tools available today, it is not always practical. The analysis would be extremely difficult due to the further increase in the number of independent parameters involved and because of a drastic increase in the size of the problem followed immediately by many numerical difficulties. Moreover, in many instances the cost of transient analysis, involving the repetition of tedious calculations for a great number of time steps may simply prohibit the use of rigorous analysis of the system. As a result there will always be a need for intermediate models and methods allowing for a simplified analysis of the system.

It is suggested that the method of solution presented in this study constitutes a very encouraging basis for further development. It would be interesting, for example, to determine effects of changing bearing geometry and lubrication system parameters on the system transient response. The method can also be used to obtain information on system stability, response to impact loading, and so on. Before such efforts are undertaken, thorough studies are required to determine the numerical accuracy and stability of the method.

REFERENCES

1. Ellyin,F., "Dynamic Behaviour and Design of Turbo-Generator Support System",Proc.,Seventh Machinery Dynamics Seminar, Edmonton,October 1982,National Research Council of Canada

2. Suzuki,S.I., "Dynamic Behaviour of a Beam Subjected to a Force of Time-Depenedent Frequency", Journal of Sound and Vibration, Vol. 57, 1978, pp. 59-64

3. Suzuki,S.I., "Dynamic Behaviour of a Beam Subjected to a Force of Time-Depenedent Frequency (continued)", Journal of Sound and Vibration, Vol. 60, 1978, pp. 417-422

4. Suzuki,S.I., "Dynamic Behaviour of a Beam Subjected to a Force of Time-Depenedent Frequency (Effects of Solid Viscosity and Rotary Inertia)", Journal of Sound and Vibration, Vol. 62, 1979, pp. 157-164

5. Victor,F., and Ellyin,F., "Acceleration of Unbalanced Rotor Through the Resonance of Supporting Structure", ASME Journal of Applied Mechanics, Vol. 48, 1981, pp. 419-424

6. Dubois,G.B., and Ocvirk,F.W., "Short Bearing Approximation for Full Journal Bearings", N.A.C.A. Report 1157, 1953

7. Holmes,R., "Non-Linear Performance of Turbine Bearings", Journal of Mechanical Engineering,Vol. 12, No.6,1970, pp. 377-380

8. Holmes,R., "Vibration and Its Control in Rotating Systems", Dynamics of Rotors, Symposium Lyngby,Denmark, August 1974

9. Donea,J. , et al, "Advanced Structural Dynamics", Applied Science Publishers Ltd., London, England, 1980

10. Strang,G., and Fix,G.J., "An Analysis of the Finite Element Method", Prentice-Hall, Englewood Cliffs, N.J., 1973

11. Zienkiewicz,O.C., "The Finite Element Method", McGraw-Hill, UK, 1977

12. Archer, J.S., "Consistent Matrix Formulation for Structural Analysis Using Finite Element Techniques", American Institute of Areonautical and Astronautics Journal, Vol.3 1965, pp. 1910-1918

13. Davis,R., Henshell, R.D., and Warburton,G.B., "A Timoshenko Beam Element", Journal of Sound and Vibration, Vol. 22(4) 1972, pp. 475-587

14. Kapur, K.K., "Vibrations of a Timoshenko Beam, Using Finite

Element Approach", Journal of the Acoustical Society of America, Vol. 42, 1966, pp.1058-1063

15. Carnegie,W., Thomas,J., and Dokumaci,E.,"An Improved Method of Matrix Displacement Analysis in Vibration Problems", The Aeronautical Quarterly, Vol. 20, 1069, pp. 321-332

16. Nickell,R.E., and Secor, G.A., "Convergence of Consistently Derived Timoshenko Beam Finite Elements", International Journal for Numerical Methods in Engineering, Vol.5, 1972 pp. 243-253

17. Dawe, D.J., "A Finite Element for the Vibration Analysis of Timoshenko Beams", Journal of Sound and Vibration, Vol.60 1978, pp. 11-20

18. Abbas,B.A.H., and Thomas,J., "The Second Frequency Spectrum of Timoshenko Beams", Journal of Sound and Vibration,Vol. 51(1), 1977, pp.123-137

19. Thomas, J., and Abbas, B.A.H., "Finite Element Model for Dynamic Analysis of a Timoshenko Beam", Journal of Sound and Vibration, Vol. 41(3), 1975, 291-299

20. Thomas,D.L., Wilson,J.M., and Wilson,R.R., "Timoshenko Beam Finite Elements", Journal of Sound and Vibration, Vol. 31 1973, pp.315-330

21. Akella, S., and Craggs, A., "An Accurate Timoshenko Beam Element", Department Report No. 32, 1982, Department of Mechanical Engineering, The University of Alberta, Canada

22. Bathe, K.J., and Wilson, E.L., "Numerical Methods in Finite Element Analysis", Prentice-Hall, Englewood Cliffs, N.J., 1976

23. Ehrich, F. and Childs, D., "Self-Excited Vibration in High-Performance Turbomachinery", ASME Mechanical Engineering, Vol. 106(5), May 1984, pp. 66-79

24. Holmes, R., "The Vibration of a Rigid Shaft on Short Sleeve Bearings", Journal of Mechanical Engineering for Science, Vol. 2(4), 1960, pp. 337-341

25. Lund, J.W., and Sternlicht,B., "Rotor-Bearing Dynamics with Emphasis on Attenuation", ASME, Journal of Basic Engineering, Vol. 84(4), 1962, pp.491-502

26. Lund, J.W., and Orcutt, F.K., "Calculations and Experiments on the Unbalance Responce of a Flexible Rotor", ASME, Journal of Engineering for Industry, Vol. 89, No. 4, 1967 pp. 785-796

27. Lund, J.W.,and Saibel, E.,"Oil Whip Whirl Orbits of a Rotor

in Sleeve Bearings",ASME,Journal of Engineering for Industry, Vol. 89(4), 1967, pp. 813-823

28. Sternlicht, B., and Lewis,P.,"Vibration Problems with High-Speed Turbomachinery", ASME, Journal of Engineering for Industry, Vol. 90(1), 1968, 174-186

29. Ruhl, R.L.,and Booker,J.F.,"A Finite Element Model for Distributed Parameter Turborotor Systems", ASME, Journal of Engineering for Industry, Vol. 94(1), 1972, pp. 126-132

30. Lund, J.W., "Modal Response of a Flexible Rotor in Fluid-Film Bearings", ASME, Journal of Engineering for Industry May 1974, pp.525-533

31. Lund, J.W., "Stability and Damped Critical Speeds of a Flexible Rotor in Fluid-Film bearings", ASME, Journal of Engineering for Industry, Vol. 96(2), 1974, pp. 509-517

32. Kirk, R.G., and Gunter, E.J., "Transient Response of Rotor-Bearing Systems", ASME, Journal of Engineering for Industry, May 1974, pp.682-693

33. Hahn, E. J. ",The Excitability of Flexible Rotors in Short Sleeve Bearings", ASME, Journal of Lubrication Technolgy, May 1975, pp. 105-115

34. Myers, C.J., "Bifurcation Theory Applied to Oil Whirl in Plain Cylindrical Bearings", ASME, Journal of Applied Mechanics, Vol. 51, June 1984, pp. 244-250

35. Pinkus, O.,and Sternlicht, B., "Theory of Hydrodynamic Lubrication", McGraw-Hill, New York, 1961

36. Gross, W.A., et al., "Fluid Film Lubrication", John Wiley & Sons, New York, 1980

37. Gerald, C.F., "Applied Numerical Analysis", Addison-Weslay Toronto, 1980

38. Forsythe, G.E.,and Malcolm, M.A.,and Moler, C.B., "Computer Methods for Mathematical Computations", Prentice-Hall, Englewood Cliffs, N.J., 1977

39. Blevins, R.D.,"Formulas for Natural Frequency and Mode Shape", Van Nostrand Reinhold, N.Y., 1979

APPENDIX A-1: Nomenclature

{ }	denotes column vector (nx1)
[ ]	denotes square matrix (nxn)
$[\ ]^T$	denotes transpose of square matrix (nxn)
$[\ ]^{-1}$	denotes reciprocal of square matrix (nxn)
A	cross-sectional area
a,b	constants
b,1	subscripts, refer to beam
[C]	damping matrix
C	radial clearence in journal-bearing system
c,2	subscripts, refer to column
E	modulus of elasticity
e	rotor mass eccentricity
e_j	eccentricity of journal centre
f	subscript, refers to frame
{F}	external load vector
G	shear modulus
g	gravitational constant
h	oil-film thickness, $h=C(1+\epsilon\cos\theta)$
[I]	identity matrix
I	second moment of cross-sectional area
i	counter ($i=1,2,3,\ldots$)
[K]	stifness matrix
K	shear coefficient
k	cross-sectional radius of gyration, $k=\sqrt{I/A}$
L	length (beam/column/bearing)

[M]	mass matrix
m ,Mr	rotor mass
N_i	shape (interpolation) functions
p	oil-film pressure
P,Q	generalized forces
P_n	centrifugal force due to rotor imbalance
P_1^d, P_2^d	oil-film dynamic forces
$q, \dot{q}, \ddot{q}$	nodal displacement, velocity and acceleration
S_m	modified Sommerfeld Number
t	time
Δt	time interval (time step)
T_1	rotor acceleration time
u	nodal displacement (axial) in beam element
V	shear force
w	nodal displacement (transversal) in beam element
W	rotor weight
x_m	displacement (horizontal) at beam midspan
y_m	displacement (vertical) at beam midspan
[Z]	matrix of finite time formulation

* * *

a	rotor speed parameter (frequency ratio), $a=\omega_s/\omega_0$
β	rotor acceleration time parameter, $\beta=T_1/\tau_0$
γ	frame geometry parameter, $\gamma=\sqrt{I_1A_2/I_2A_1}\,L_2/L_1$
ϵ	journal eccentricity ratio, $\epsilon=e_j/C$

ε_0	eccentricity of static journal centre
ζ	damping factor
η	rotor to support mass ratio
θ	cross-sectional rotation (in Thimoshenko beam)
θ	circumferential coordinate (in journal-bearing)
θ_1,θ_2	limits of oil-film positive pressure
κ	beam slenderness factor, $\kappa=k/L$
μ	viscosity
ν	Poisson's ratio
ξ	rotor acceleration (through the critical frequency) parameter, $\xi=\dot{\Omega}_0/\omega_0{}^2$
π	constant, $\pi=3.1415927...$
ρ	density
σ	shift of maximum amplitude of vibration, $\sigma=\dot{\Omega}_m/\omega_0$
τ	time interval (time step)
$\check{\tau}$	time sub-interval
τ_0	system first natural period
ϕ	bending slope
χ	shear coefficient (on graphs only)
ψ	shear slope (in Timoshenko beam element)
ψ	attitude angle (in journal-bearing system)
ω,ω_s	rotor operating (service) speed
ω_r	rotor operating speed (on graphs only)
ω_i	rotor initial speed
ω_0	system first natural frequency
ω_n	natural frequency of the n-th mode of vibration

Ω	rotor angular travel
$\dot{\Omega},\ddot{\Omega}$	instantaneous rotor speed and acceleration rate
$\ddot{\Omega}_o$	rotor acceleration rate through the critical freq.
$\dot{\Omega}_m$	instantaneous rotor speed at the instant the response amplitude reaches its maximum

APPENDIX A-2: Timoshenko beam elements' matrices

Simple Timoshenko Beam Element
(Davis, at al; [13])

(a) element stiffness matrix:

$$[EK] = a\begin{bmatrix} k_1 & 0 & 0 & -k_1 & 0 & 0 \\ & k_2 & k_3 & 0 & -k_2 & k_3 \\ & & k_4 & 0 & -k_3 & k_5 \\ & & & k_1 & 0 & 0 \\ & \text{symmetric} & & & k_2 & -k_3 \\ & & & & & k_4 \end{bmatrix}$$

where:

$\phi = 12EI/GKAL^2$

$a = EI/(1+\phi)L^3$

$k_1 = AE/La$

$k_2 = 12$

$k_3 = 6L$

$k_4 = (4+\Phi)L^2$

$k_5 = (2-\phi)L^2$

(b) element mass matrix

$$[EM] = \beta \begin{bmatrix} m_1 & 0 & 0 & m_2 & 0 & 0 \\ & m_3 & m_4 & 0 & m_5 & -m_6 \\ & & m_7 & 0 & m_6 & m_8 \\ & & & m_1 & 0 & 0 \\ & \text{symmetric} & & & m_3 & m_4 \\ & & & & & m_7 \end{bmatrix}$$

where:

$\beta = \rho AL/(1+\phi)^2$

$\gamma = I/AL^2$

$m_1 = \rho AL/3\beta$

$m_2 = m_1/2$

$m_3 = 13/35+7\phi/10+\phi^2/3+6\gamma/5$

$m_4 = L(11/210+11\phi/120+\phi^2/24+\gamma/10-\gamma\phi/2)$

$m_5 = 9/70+3\phi/10+\phi^2/6-6\gamma/5$

$m_6 = L(13/420+3\phi/40+\phi^2/24-\gamma/10+\gamma\phi/2)$

$m_7 = L^2(1/105+\phi/60+\phi^2/120+2\gamma/15+\gamma\phi/6+\gamma\phi^2/3)$

$m_8 = L^2(-1/140-\phi/60-\phi^2/120-\gamma/30-\gamma\phi/6+\gamma\phi^2/6)$

Complex Timoshenko Beam Element
(Akella & Craggs, [21])

(a) element stiffness matrix:

$$[EK] = \delta \begin{bmatrix} k_1 & 0 & 0 & 0 & 0 & -k_1 & 0 & 0 & 0 & 0 \\ & k_2 & k_3 & -k_4 & k_5 & 0 & -k_2 & k_3 & -k_4 & -k_5 \\ & & k_6 & -k_7 & k_8 & 0 & -k_3 & k_9 & -k_7 & -k_{10} \\ & & & k_{11} & -k_{12} & 0 & k_4 & -k_7 & -k_{13} & k_{12} \\ & & & & k_{14} & 0 & -k_5 & k_{10} & -k_{12} & -k_{15} \\ & & & & & k_1 & 0 & 0 & 0 & 0 \\ & & & & & & k_2 & -k_3 & k_4 & k_5 \\ & & \text{symmetric} & & & & & k_6 & -k_7 & -k_8 \\ & & & & & & & & k_{11} & k_{12} \\ & & & & & & & & & k_{14} \end{bmatrix}$$

where:

$\delta = GKA/L$

$k_1 = E/GK$

$k_2 = 6/5$

$k_3 = 3L/5$

$k_4 = L/10A$

$k_5 = L^2/10I$

$k_6 = 3L^2/10+6EI/5GKA$

$k_7 = L^2/20A$

$k_8 = L^2/20I+EL/10GKA$

$k_9 = 3L^2/10-6EI/5GKA$

$k_{10} = L^3/20I-EI/10GKA$

$k_{11} = 4L^2/30A^2$

$k_{12} = L^3/120IA$

$k_{13} = k_{11}/4$

$k_{14} = L^4/120I^2+2EL^2/15IGKA$

$k_{15} = L^4/120I^2+EL^2/30IGKA$

(b) element mass matrix:

$$[EM] = \sigma \begin{bmatrix} m_1 & 0 & 0 & 0 & 0 & m_2 & 0 & 0 & 0 & 0 \\ & m_3 & m_4 & -m_5 & m_6 & 0 & m_7 & -m_8 & m_9 & m_6 \\ & & m_{10} & -m_{11} & m_{12} & 0 & m_8 & -m_{13} & m_{14} & m_{15} \\ & & & m_{16} & -m_{17} & 0 & -m_9 & m_{14} & -m_{18} & -m_{17} \\ & & & & m_{19} & 0 & m_6 & -m_{15} & m_{17} & m_{20} \\ & & & & & m_1 & 0 & 0 & 0 & 0 \\ & & & & & & m_3 & -m_4 & m_5 & m_6 \\ & & \text{symmetric} & & & & & m_{10} & -m_{11} & -m_{12} \\ & & & & & & & & m_{16} & k_{17} \\ & & & & & & & & & m_{19} \end{bmatrix}$$

where:

$\sigma = \rho AL$

$m_1 = 1/3$

$m_2 = 1/6$

$m_3 = 13/35$

$m_4 = 17L/280$

$m_5 = 11L/210A$

$m_6 = L^2/240I$

$m_7 = 9/70$

$m_8 = 11L/280$

$m_9 = 13L/420A$

$m_{10} = 17L^2/1260+13I/35A$

$m_{11} = 57L^2/5040A$

$m_{12} = 11L^3/10080I+11L/210A$

$m_{13} = L^2/90-9I/70A$

$m_{14} = L^2/112A$

$m_{15} = 11L^3/10080I-13L/420A$

$m_{16} = L^2/105A^2$

$m_{17} = 9L^3/10080AI$

$m_{18} = L^2/140A^2$

$m_{19} = L^4/10080I^2+L^2/105AI$

$m_{20} = L^4/10080I^2-L^2/140AI$

APPENDIX A-3: Computer program listing

The following is the computer program listing (in FORTRAN code) consisting of the main segments (TRANSFB, BEAM and FRAME) and several subroutines. The schematic diagrams of TRANSFB and BEAM are shown in Figs. 4.1 and 4.2. There are considerable number of comments cards included in the program. It is hoped that these comments cards together with the above mentioned diagrams and the theoretical discussion presented in Chapters 2, 3 and 4 should make the program self-explanatory.

```
         C
         C
         C       program name: TRANSFB
         C
         C       +++++++++++++++++++++++++++++++++++++++++++++++++
         C       +               TRANSIENT RESPONSE              +
         C       +  OF SIMPLE BEAM  OR PORTAL FRAME AS MODELS OF +
         C       +  LOW-TUNED STRUCTURE SUPPORTING AN UNBALANCED +
         C       +              ACCELERATING ROTOR               +
         C       +                    * * *                      +
         C       +              DIRECT INTEGRATION               +
         C       +     OF SYSTEM EQUATION OF MOTION USING        +
         C       +  A  RECCURENCE  SCHEME  BASED  ON FINITE TIME +
         C       +             ELEMENT  FORMULATION              +
         C       +                    * * *                      +
         C       +        FINITE TIMOSHENKO BEAM ELEMENT         +
         C       +   (SIMPLE OR COMPLEX) IS USED TO APPROXIMATE  +
         C       +  ELASTIC AND INERTIAL PROPERTIES OF STRUCTURE +
         C       +                    * * *                      +
         C       +           DETERMINATION OF SYSTEM             +
         C       +     NATURAL FREQUENCIES AND/OR EIGENVECTOR    +
         C       +               AND STATIC TEST                 +
         C       +++++++++++++++++++++++++++++++++++++++++++++++++
         C
         C
0001            REAL*8  M(50,50),K(50,50),C(50,50),DD(50)
0002            REAL*8  AA(1275),BB(1275)
0003            REAL*8  E(10,10)
0004            REAL*8  Z(150,150),V(150,150)
0005            REAL*8  WV0(150),WV1(150),WV2(150),Q(150)
0006            REAL*8  WK(23000)
         C
0007            INTEGER NG(20,10)
         C
         C
         C          NE  - total number of elements in the structure
         C          NBE - number of elements in the beam
         C          NCE - number of elements in each column
         C          IE  - number of D.O.Fs per element
         C          IR  - number of D.O.Fs of constrained structure
         C          NL  - nodal no. of applied load; vertical comp.
         C          NG  - array; elemments' nodal numbers in global
         C                numbering system; considering constraints
         C                and boundary conditions of the system
         C
         C
0008            READ(5,1000)NBE,NCE,IE,IR,NL
0009            IT=3*IR
0010            NE=NBE+NCE*2
0011            ISM=IR*(IR+1)/2.0+0.5
0012            MWK=IT**2+3*IT
0013            IF( NCE .NE. 0) GO TO 10
```

University of Alberta

```
0014          CALL BEAM(NBE,NE,IE,IR,IT,NL,ISM,MWK,M,K,C,E,AA,
             +                    BB,DD,WK,NG,Z,V,Q,WV0,WV1,WV2)
0015       10 CALL FRAME(NBE,NCE,NE,IE,IR,IT,NL,ISM,MWK,M,K,C,
             +               E,AA,BB,DD,WK,NG,Z,V,Q,WV0,WV1,WV2)
0016     1000 FORMAT(5I6)
0017          STOP
0018          END
        C
        CC
        CCC   The following subroutine is actually the main pro-
        CCC   gram. The split MAIN-BEAM was introduced to enable
        CCC   changing dimensions of global matrices and vectors
        CCC   depending on a number of D.O.F. in the system. The
        CCC   BEAM  subroutine  differs  slightly for each model
        CCC   considered. The version for Model 3 is as follows:
        CC
        C
0001          SUBROUTINE  BEAM(NBE,NE,IE,IR,IT,NL,ISM,MWK,M,K,C,
             +                   E,AA,BB,DD,WK,NG,Z,V,Q,WV0,WV1,WV2)
        C
0002          REAL*8  M(IR,IR),K(IR,IR),C(IR,IR),E(IE,IE)
0003          REAL*8  Z(IT,IT),V(IT,IT),BB(30),CC(30)
0004          REAL*8  WV0(IT),WV1(IT),WV2(IT),Q(IT),WK(MWK)
0005          REAL*8  ALP,BET,GAM,T0,DT,TA,T,PI,OM0
0006          REAL*8  BML,EL,EMO,SMO,ARE,SMA,RHO,PRO,GKA,SHF
0007          REAL*8  MR,ECC,OMI,OMR,OMT,OMS,OMA,F1,F2,F3
        C
0008          REAL*8  UC,WT,MC,ME,PAR,EPS,PSI,VEP,VPS,DX,PYI
0009          REAL*8  TX(30),PX(30),PY(30),VIS,BL,BR,RC
0010          REAL    LAST
        C
0011          INTEGER NG(NE,IE)
        C
        C     E   - temporary element (mass or stiffness) matrix
        C     M   - consistent mass matrix of constrained system
        C     K   - consistent stiffness matrix of const. system
        C     C   - system  damping  matrix  (C = ALF*M + BET*K)
        C
0012          READ(5,1001)NDT,DT,ALP,BET,GAM
        C
        C     NDT - number of time steps
        C     DT  - time step
        C     ALP-  constant in Rayleigh's  proportional damping
        C     BET - constant in Rayleigh's  proportional damping
        C     GAM - rotor acceleration time parameter
        C
0013          WRITE(6,1107)
0014          WRITE(6,1114)
        C
        C     If simple Timoshenko beam (6 D.O.F.) used goto 453
        C
0015          IF(IE .EQ. 6) GO TO 453
```

```
      WRITE(6,1115)
      GO TO 454
  453 WRITE(6,1116)
  454 CONTINUE
      WRITE(6,1100)NE,NBE,NCE
      WRITE(6,1111)IE,IR,IT,NL
      WRITE(6,1106)
C
C     Read in NG array, storing element nodal numbers in
C     global  numbering  system.  If complex  Timoshenko
C     beam finite element (10 D.O.F.) used go to 551.
C
      IF(IE .EQ. 10) GO TO 551
      READ(5,1000)((NG(I,J),J=1,IE),I=1,NE)
      WRITE(6,1101)((NG(I,J),J=1,IE),I=1,NE)
      GO TO 552
  551 READ(5,2000)((NG(I,J),J=1,IE),I=1,NE)
      WRITE(6,2101)((NG(I,J),J=1,IE),I=1,NE)
  552 CONTINUE
      WRITE(6,1105)
C
C     Read in beam material constants  and  shear factor
C     PRO - Poisson's ratio
C     EMO - elasticity modulus
C     RHO - density
C     SHF - cross-sectional shape (shear) cofficient
C
      READ(5,1002)PRO,EMO,RHO,SHF
      PI=3.141592654D+00
      SMO=0.5*EMO/(1.0+PRO)
      RHO=RHO/386.16
C
C     Read in beam geometry parameters & mass of a rotor
C     BML - beam total length
C     ARE - cross-sectional area
C     SMA - second moment of cross-section area
C     MR  - rotor mass
C
      READ(5,1002)BML,ARE,SMA,MR
      EL=BML/NBE
      WRITE(6,1102)PRO,EMO,RHO,SHF,BML,ARE,SMA
      GKA=SMO*SHF*ARE
C
C     Initialize global M and K matrices.
C
      DO 10 I=1,IR
         DO 10 J=1,IR
            M(I,J)=0.0
   10       K(I,J)=0.0
C
C     Call routine to  evaluate  complex (TM544) element
C     stiffness matrix. If simple element used  goto 661
```

University of Alberta

```
        C
0043          IF(IE .EQ. 6) GO TO 661
0044          CALL KCTMBM(EL,GKA,ARE,EMO,SMA,E)
0045          GO TO 662
0046      661 CALL KSTMBM(EL,GKA,ARE,EMO,SMA,E)
0047      662 CONTINUE
        C
        C     Call assemblage routine (looping for  total number
        C     of elements in a beam) to get system stiff. matrix
        C
0048          DO 12 NK=1,NBE
0049       12    CALL ASSZW(E,NK,IE,NE,IR,K,NG)
        C
        C     Call routine to  evaluate  complex (TM544) element
        C     mass matrix. If simple element used go to 663.
        C
0050          IF(IE .EQ. 6) GO TO 663
0051          CALL MCTMBM(EL,ARE,SMA,RHO,E)
0052          GO TO 664
0053      663 CALL MSTMBM(EL,GKA,ARE,EMO,SMA,RHO,E)
0054      664 CONTINUE
        C
        C     Assemble elements' mass matrices into system's one
        C
0055          DO 14 NK=1,NBE
0056       14    CALL ASSZW(E,NK,IE,NE,IR,M,NG)
        C
        C     Read in journal-bearing system parameters
        C     VIS - lubricant viscosity
        C     BL  - length of a bearing
        C     BR  - radius of a bearing
        C     RC  - radial clearence
        C     UC  - normalized rotor unbalance (e/C)
        C
0057          READ(5,1002)VIS,BL,BR,RC,UC
0058          ECC=RC*UC
0059          RBM=MR/(BML*ARE*RHO)
0060          WRITE(6,1122)MR,ECC,RBM
        C
        C     Read in parameters
        C     OMO - system first natural frequency
        C     OMR - rotor oparating (service) speed
        C     OMI - rotor initial speed
        C     HOM - system highest natural frequency
        C
0061          READ(5,1002)OMO,OMR,OMI,HOM
0062          OMR=OMR*PI/30.0D+00
0063          DEL=OMR/OMO
0064          YO=(MR*ECC*OMR**2*BML**3)/(48.0*EMO*SMA)
0065          TO=(PI*2.0D+00)/OMO
0066          TN=2.0*PI/HOM
0067          TA=GAM*TO
```

University of Alberta

```
0068              ZET=DT/TN
          C
          C       Read in  number of time steps (IP) for calculation
          C       of oil-film dynamic forces  and initial conditions
          C       IP  - number of time sub-intervals
          C       EPS - journal centre eccentricity
          C       PSI - attitude angle
          C       VEP - journal centre radial velocity
          C       VPS - journal centre tangential velocity
          C       PYI - vertical component of initial dynamic  force
          C
0069              READ(5,1001)IP,EPS,PSI,VEP,VPS,PYI
0070              WT=MR*386.16D+00
0071              MC=MR*RC
0072              ME=MC*UC
0073              VIS=VIS/6.894757D+03
0074              PAR=VIS*BL**3*BR/(RC**2*2.0D+00)
0075              RSP=OMR*60.0/(2.0*PI)
0076              SMN=PAR*OMR/(WT*2.0)
0077              STP=OMR*(RC/386.16)**0.5
0078              NDT2=TA/DT+1.5
0079              DT=TA/(NDT2*1.0D+00)
0080              NDT=NDT2+TA/DT+1.5
0081              DX=DT/(IP*1.0D+00)
0082              IP=IP+1
0083              WRITE(6,1108)DT,NDT,ALP,BET,GAM,DEL
0084              WRITE(6,1123)OMO,TO,HOM,TN,ZET,OMR,TA
0085              WRITE(6,1125)OMI
0086              OMI=OMI*PI/30.0D+00
          C
          C       Evaluate system proportional damping  matrix  from
          C       global mass and stiffness matrices
          C
0087              DO 30 I=1,IR
0088                 DO 30 J=1,IR
0089           30       C(I,J)=ALP*M(I,J)+BET*K(I,J)
0090          655 CONTINUE
          C
          C       Call subroutines to create submatrices of a finite
          C       time formulation, and then  modify them to include
          C       effect of rotor acceleration in its linear  motion
          C       (due to beam vibration) on forcing function.
          C
0091              CALL FTZ12(IR,IT,DT,M,C,K,Z)
0092              Z(NL,NL+IR)=Z(NL,NL+IR)+MR
0093              Z(NL+IR,NL)=Z(NL+IR,NL)-MR
0094              Z(NL+IR,NL+IR)=Z(NL+IR,NL+IR)+MR*DT
0095              Z(NL+2*IR,NL)=Z(NL+2*IR,NL)-MR*DT
0096              Z(NL+2*IR,NL+IR)=Z(NL+2*IR,NL+IR)+0.8*MR*DT**2
0097              Z(NL+2*IR,NL+2*IR)=Z(NL+2*IR,NL+2*IR)+MR*DT**3/60.
0098              IDGT=0
          C
```

University of Alberta

```
C     Invert modified finite time formulation matrix Z12
C
      CALL LINV2F(Z,IT,IT,V,IDGT,WK,IER)
      DO 35 I=1,IT
         DO 35 J=1,IT
   35       Z(I,J)=V(I,J)
      CALL FTZ11(IR,IT,DT,M,C,K,V)
      V(NL,NL+IR)=V(NL,NL+IR)-MR
      V(NL+IR,NL)=V(NL+IR,NL)+MR
      V(NL+2*IR,NL)=V(NL+2*IR,NL)+MR*DT
      V(NL+2*IR,NL+IR)=V(NL+2*IR,NL+IR)+0.2*MR*DT**2
      V(NL+2*IR,NL+2*IR)=V(NL+2*IR,NL+2*IR)+MR*DT**3/60.
C
C     Determine vector of nodal acceleration at time t=0
C     to enable starting procedure for reccurence scheme
C
      DO 50 I=1,IT
         Q(I)=0.0
   50    WVO(I)=0.0
      DO 60 I=1,IR
   60    WV1(I)=0.0
      WV1(NL)=PYI
      IDGT=0
      IRHS=1
      CALL LEQT2F(M,IRHS,IR,IR,WV1,IDGT,WK,IER)
      DO 70 I=1,IR
   70    WVO(IT-IR+I)=WV1(I)
C
C     Direct integration of a system equations of motion
C     (using time-stepping scheme) and printing  out the
C     results  which,  for  the  sake  of simplicity, is
C     limited only to displacement envelope at a midspan
C     of a beam. Subroutine FORCE determines dynamic oil
C     film force (vertical component, Fy)  at each of IP
C     time sub-intervals and subroutine SPLINT evaluates
C     required integrals.
C
      NPT=0
      PREV=-0.1
      LAST=0.0
      T=0.0D+00
      WRITE(6,3300)SMN,STP,UC,RSP,WT,PAR
      WRITE(6,1109)
      DO 80 L=1,NDT
         IF(L .LE. NDT2) MAR=2
         IF(L .GT. NDT2) MAR=3
         CALL FORCE(T,DX,IP,TA,EPS,PSI,VEP,VPS,OMR,OMI,M
     &              WT,MC,ME,PAR,TX,PX,PY,OMT,OMS,OMA)
         CALL SPLINT(IP,DX,TX,PY,BB,CC,F1,F2,F3)
         Q(NL)=F1
         Q(NL+IR)=F2
         Q(NL+2*IR)=F3
```

University of Alberta

```
            CALL MMULT(V,WV0,IT,IT,1,WV1)
            DO 85 I=1,IT
   85          WV2(I)=Q(I)-WV1(I)
            CALL MMULT(Z,WV2,IT,IT,1,WV0)
            IF(LAST .GT. PREV .AND. LAST .GT. WV0(NL))GO TO
     +                                                    977
            GO TO 978
  977       TIME=T-DT
            NPT=NPT+1
            X=TIME/T0
            Y=LAST/Y0
            WRITE(6,1110)NPT,TIME,LAST,X,Y
  978       PREV=LAST
            LAST=WV0(NL)
   80 CONTINUE
      NPT=999
      WRITE(6,1110)NPT
C
 1000 FORMAT(6I5)
 2000 FORMAT(10I5)
 1001 FORMAT(I6,5D20.8)
 1002 FORMAT(9D20.8)
 1100 FORMAT(1X,'Total number of finite elements used',
     +       8X,'=',I3/
     +       1X,'Number of finite elements in beam   ',
     +       8X,'=',I3/
     +       1X,'Number of finite elements in column ',
     +       8X,'=',I3/)
 1101 FORMAT(1X,6I5)
 2101 FORMAT(1X,I3,9I5)
 1102 FORMAT(1X,'Poisson  ratio                  =',F19.5/
     +       1X,'Young  modulus                  =',F19.5/
     +       1X,'Density                         =',F19.5/
     +       1X,'Shape factor                    =',F19.5//
     +       1X,'Total beam length               =',F19.5/
     +       1X,'Beam cross-section area         =',F19.5/
     +       1X,'Beam second moment of area      =',F19.5/)
 1104 FORMAT(1X,'System 1st natural frequency=',F19.5/
     +       1X,'System 1st natural period   =',F19.5/
     +       1X,'System highest frequency    =',F19.5/
     +       1X,'System shortest period      =',F19.5)
 1105 FORMAT(1X/16X,'STRUCTURE AND MATERIAL PROPERTIES'/
     +       16X,'---------------------------------'/)
 1106 FORMAT(1X/1X,'Array NG(NE,IE):'/
     +  '+','________________'/)
 1107 FORMAT(1X/16X,'FORCED VIBR.   TRANSIENT SOLUTION'/
     +      '+',15X,'____________   __________________'/
 1108 FORMAT(1X,'Time step                         =',F19.5/
     +       1X,'No. of time steps                 =',I13/
     +       1X,'Alpha                             =',F19.5/
     +       1X,'Beta                              =',F19.5/
     +       1X,'Gamma                             =',F19.5/
```

University of Alberta

```
     +        1X,'Delta                              =',F19.5/)
 1109 FORMAT(12X,'TIME',6X,'DEFLECTION',8X,'TIME/TO',
     +       9X,'DRFactor'/
     +       12X,'----',6X,'----------',8X,'-------',
     +       9X,'--------'//)
 1110 FORMAT(1X,I3,5X,F8.4,5X,E11.5,5X,F10.3,5X,F10.3)
 1111 FORMAT(1X,'Number of degree of freedom per',
     +        1X,'element      =',I3/
     +        1X,'Total No. of D.O.Fs of constrained',
     +        1X,'system   =',I3/
     +        1X,'Order of finite time element',
     +        1X,'matrices        =',I3/
     +        1X,'Nodal number corresponding to applied',
     +        1X,'load  =',I3/)
 1114 FORMAT(16X,'BEAM SIMPLY SUPPORTED AT ITS ENDS'/
     +   '+',15X,'_________________________________'/)
 1115 FORMAT(1X,'COMPLEX TIMOSHENKO BEAM ELEMENT (TM544)
     +       '+','_______ __________ ____ _______'/)
 1116 FORMAT(1X,'SIMPLE TIMOSHENKO BEAM ELEMENT'/
     +       '+','______ __________ ____ _______'/)
 1117 FORMAT(1X,I6,3X,F15.8)
 1119 FORMAT(1X/)
 1122 FORMAT(1X,'Mass of the rotor               =',F19.5/
     +        1X,'Eccentricity of the mass    =',F19.5/
     +        1X,'Rotor/support mass ratio    =',F19.5/)
 1123 FORMAT(1X,'System 1st natural frequency=',F19.5/
     +        1X,'System 1st natural period   =',F19.5/
     +        1X,'System highest frequency    =',F19.5/
     +        1X,'System shortest period      =',F19.5/
     +        1X,'Time step/shortest period   =',F19.5/
     +       '0','Rotor operating speed       =',F19.5/
     +        1X,'Rotor acceleration time     =',F19.5)
 1125 FORMAT(1X,'Rotor initial speed         =',F19.5/)
 3300 FORMAT(5X,'SMN=',F10.3,3X,'STP=',F10.3,3X,'e/C=',F
     +        5X,'N  =',F8.1,5X,'W  =',F8.1,5X,'PAR=',F10
C
      RETURN
      END
C
CC
CCC   Subroutine FRAME (version for Model 2)
CC
C
      SUBROUTINE FRAME(NBE,NCE,NE,IE,IR,IT,NL,ISM,MWK,M,
     +            K,C,E,AA,BB,DD,WK,NG,Z,V,Q,WV0,WV1,WV2)
C
      REAL*8  M(IR,IR),K(IR,IR),C(IR,IR),BB(ISM),AA(ISM)
      REAL*8  DD(IR),E(IE,IE), Z(IT,IT),V(IT,IT),WK(MWK)
      REAL*8  WV0(IT),WV1(IT),WV2(IT),Q(IT)
C
      REAL*8  ALP,BET,GAM,DEL,EPS,ZET,PI,GKA,BML,CNL,TO
      REAL*8  C1,C2,C3,C4,C5,CK,D1,D2,D3,D4,D5,F1,F2,F3
```

University of Alberta

```
0007          REAL*8  EL,EMO,SMO,ARE,SMA,RHO,PRO,ECC,MR,OMO,OMN
0008          REAL*8  OMR,OMT,OMS,OMA,DT,TA,T,TX,FX,PREV,LAST,X
0009          REAL*8  Y,X0,Y0,PREVX,LASTX,PREVY,LASTY,HOM,TR,TN
0010          REAL*8  TG(4),HG(4),OMI,SHF
        C
        C
0011          INTEGER NG(NE,IE)
        C
        C     Gaussian quadrature internal points and  weighting
        C     factors
        C
0012          TG(1)=-0.861136311594053D+00
0013          TG(2)=-0.339981043584856D+00
0014          TG(3)=-TG(2)
0015          TG(4)=-TG(1)
0016          HG(1)=0.347854845137454D+00
0017          HG(2)=0.652145154862546D+00
0018          HG(3)=HG(2)
0019          HG(4)=HG(1)
0020          READ(5,1001)NDT,DT,ALP,BET,GAM,DEL
0021          IF(NDT .GT. 0) GO TO 449
0022          WRITE(6,1112)
0023          GO TO 450
0024      449 WRITE(6,1107)
0025      450 CONTINUE
0026          WRITE(6,1113)
0027          IF(IE .EQ. 6) GO TO 453
0028          WRITE(6,1115)
0029          GO TO 454
0030      453 WRITE(6,1116)
0031      454 CONTINUE
0032          WRITE(6,1100)NE,NBE,NCE
0033          WRITE(6,1111)IE,IR,IT,NL
0034          WRITE(6,1106)
0035          IF(IE .EQ. 10) GO TO 551
0036          READ(5,1000)((NG(I,J),J=1,IE),I=1,NE)
0037          WRITE(6,1101)((NG(I,J),J=1,IE),I=1,NE)
0038          GO TO 552
0039      551 READ(5,2000)((NG(I,J),J=1,IE),I=1,NE)
0040          WRITE(6,2101)((NG(I,J),J=1,IE),I=1,NE)
0041      552 CONTINUE
0042          WRITE(6,1105)
0043          READ(5,1002)PRO,EMO,RHO,SHF,ECC,EPS
0044          PI=3.141592654D+00
0045          SMO=0.5*EMO/(1.0+PRO)
0046          RHO=RHO/386.16
0047          READ(5,1002)BML,ARE,SMA
0048          EL=BML/NBE
0049          READ(5,1002)MR
0050          WRITE(6,1102)PRO,EMO,RHO,SHF,BML,ARE,SMA
0051          GKA=SMO*SHF*ARE
        C
```

University of Alberta

```
          C     Evaluate coefficients for static test
          C
0052                  C1=(BML**3)/(96.0*EMO*SMA)
0053                  C2=(9.0*BML**2)/32.0
0054                  C3=BML/(4.0*GKA)
0055                  C4=0.5/EMO
0056                  C5=(9.0*BML**3)/(64.0*EMO*ARE)
0057                  CK=SMA/BML
0058                  D1=1.0/(12.0*EMO)
0059                  D2=0.5
0060                  D3=1.0/(GKA*BML)
0061                  D4=2.0/(EMO*BML**2)
0062                  D5=BML/(4.0*EMO*ARE)
          C
          C     Evaluate beam element  mass and stiffness matrices
          C     and assemble them into system global matrices
          C
0063                  DO 10 I=1,IR
0064                     DO 10 J=1,IR
0065                        M(I,J)=0.0
0066               10       K(I,J)=0.0
0067                  IF(IE .EQ. 6) GO TO 661
0068                  CALL KCTMBM(EL,GKA,ARE,EMO,SMA,E)
0069                  GO TO 662
0070              661 CALL KSTMBM(EL,GKA,ARE,EMO,SMA,E)
0071              662 CONTINUE
          C
          CC
          C
0072                  DO 12 NK=1,NBE
0073               12    CALL ASSZW(E,NK,IE,NE,IR,K,NG)
0074                  IF(IE .EQ. 6) GO TO 663
0075                  CALL MCTMBM(EL,ARE,SMA,RHO,E)
0076                  GO TO 664
0077              663 CALL MSTMBM(EL,GKA,ARE,EMO,SMA,RHO,E)
0078              664 CONTINUE
0079                  DO 14 NK=1,NBE
0080               14    CALL ASSZW(E,NK,IE,NE,IR,M,NG)
          C
          C     Read in column geometry parameters
          C     CNL - length of column
          C     ARE - cross-secyional area
          C     SMA - second moment of cross-section area
          C
0081                  READ(5,1002)CNL,ARE,SMA
0082                  EL=CNL/NCE
0083                  MR=MR+EPS*2.0*CNL*ARE*RHO
0084                  GKA=SMO*SHF*ARE
          C
          C     Continue evaluation of coefficients for analytical
          C     determination of maximum  static  displacements at
          C     midspan of a frame beam.
```

University of Alberta

```
         C
0085            CK=CK*CNL/SMA
0086            C1=C1*(1.0+2.0*CK)/(2.0+CK)
0087            C2=C2/((CNL*GKA)*(2.0+CK)**2)
0088            C4=C4*CNL/ARE
0089            C5=C5/(CNL*(2.0+CK))**2
0090            D1=D1*(2.0+3.0*CK)*CNL**3/(SMA*(1.0+6.0*CK))
0091            D2=D2*CNL/GKA
0092            D3=D3*(3.0*CK*CNL/(1.0+6.0*CK))**2
0093            D4=D4*(CNL/ARE)*(3.0*CK*CNL/(1.0+6.0*CK))**2
0094            P=1000.0
0095            Y0=-P*(C1+C2+C3+C4+C5)
0096            X0=P*(D1+D2+D3+D4+D5)
         C
         C      Evaluate columns' elements matrices (stiffness and
         C      mass matrices and  assemble them into system ones.
         C
0097            IF(IE .EQ. 6) GO TO 666
0098            CALL KCTMCN(EL,GKA,ARE,EMO,SMA,E)
0099            GO TO 667
0100        666 CALL KSTMCN(EL,GKA,ARE,EMO,SMA,E)
0101        667 CONTINUE
         C
         CC
         C
0102            NS=NBE+1
0103            NF=NS+NCE-1
0104            DO   16   NK=NS,NF
0105         16 CALL ASSZW(E,NK,IE,NE,IR,K,NG)
0106            IF(IE .EQ. 6) GO TO 668
0107            DO 17 I=1,10
0108               E(1,I)=-E(1,I)
0109               E(6,I)=-E(6,I)
0110               E(I,1)=-E(I,1)
0111               E(I,6)=-E(I,6)
0112               E(2,I)=-E(2,I)
0113               E(7,I)=-E(7,I)
0114               E(I,2)=-E(I,2)
0115         17    E(I,7)=-E(I,7)
0116        668 CONTINUE
0117            NS=NF+1
0118            NF=NS+NCE-1
0119            DO 18 NK=NS,NF
0120         18 CALL ASSZW(E,NK,IE,NE,IR,K,NG)
0121            IF(IE .EQ. 6) GO TO 669
0122            CALL MCTMCN(EL,ARE,SMA,RHO,E)
0123            GO TO 670
0124        669 CALL MSTMCN(EL,GKA,ARE,EMO,SMA,RHO,E)
0125        670 CONTINUE
         C
         CC
         C
```

```
      NS=NBE+1
      NF=NS+NCE-1
      DO   20   NK=NS,NF
   20 CALL ASSZW(E,NK,IE,NE,IR,M,NG)
      IF(IE .EQ. 6) GO TO 671
      DO 21 I=1,10
         E(1,I)=-E(1,I)
         E(6,I)=-E(6,I)
         E(I,1)=-E(I,1)
         E(I,6)=-E(I,6)
         E(2,I)=-E(2,I)
         E(7,I)=-E(7,I)
         E(I,2)=-E(I,2)
   21    E(I,7)=-E(I,7)
  671 CONTINUE
      NS=NF+1
      NF=NS+NCE-1
      DO 22 NK=NS,NF
   22 CALL ASSZW(E,NK,IE,NE,IR,M,NG)
      IF(NDT .GT. 0) GO TO 772
      NX=NL-1
      M(NX,NX)=M(NX,NX)+MR
      WRITE(6,1103)CNL,ARE,SMA
  771 CONTINUE
      M(NL,NL)=M(NL,NL)+MR
      EPS=MR/(BML*ARE*RHO)
      WRITE(6,1122)MR,ECC,EPS
C
C     Determine system natural frequencies & eigenvector
C
      DO 37 I=1,IR
         JR=I
         DO 38 J=1,JR
            IS=I*(I-1)/2.0+0.5+J
            AA(IS)=K(I,J)
            BB(IS)=M(I,J)
   38    CONTINUE
   37 CONTINUE
      CALL EIGZS(AA,BB,IR,1,DD,C,IR,WK,IER)
      DO 39 I=1,IR
   39    DD(I)=DD(I)**0.5
      OMO=DD(1)
      HOM=DD(IR)
      TO=(PI*2.0D+00)/OMO
      TN=2.0*PI/HOM
      WRITE(6,1104)OMO,TO,HOM,TN
      WRITE(6,1120)
      DO 40 I=1,IR
   40    WRITE(6,1117)I,DD(I)
      DO 45 I=1,IR
         WRITE(6,1127)I,(C(I,J),J=1,5)
   45 CONTINUE
```

University of Alberta

University of Alberta

```
 1127 FORMAT(1X,I3,10(2X,E10.4))
C
C     Static test
C
      IDGT=0
      DO 69 I=1,IR
         DO 69 J=1,IR
   69       C(I,J)=K(I,J)
      DO 71 I=1,IR
   71       DD(I)=0.0
      DD(NL)=-P
      CALL LEQT2F(C,1,IR,IR,DD,IDGT,WK,IER)
      WRITE(6,1119)
      DO 73 I=1,IR
   73    WRITE(6,1117)I,DD(I)
      ERR=DABS(100.0*(DD(NL)-Y0)/Y0)
      WRITE(6,1118)Y0,ERR
      DO 74 I=1,IR
   74    DD(I)=0.0
      DD(NX)=1000.0
      IDGT=0
      DO 75 I=1,IR
         DO 75 J=1,IR
   75       C(I,J)=K(I,J)
      CALL LEQT2F(C,1,IR,IR,DD,IDGT,WK,IER)
      WRITE(6,1119)
      DO 78 I=1,IR
   78    WRITE(6,1117)I,DD(I)
      ERR=DABS(100.0*(DD(NX)-X0)/X0)
      WRITE(6,1121)X0,ERR
  772 CONTINUE
C
      READ(5,1001)I,OMN,OM0,HOM
      OMR=DEL*OMN
      Y0=(MR*ECC*OMR**2)*(C1+C2+C3+C4+C5)
      T0=2*PI/OM0
      TN=2*PI/HOM
      TA=GAM*T0
      ZET=DT/TN
      WRITE(6,1126)I
      WRITE(6,1108)DT,NDT,ALP,BET,GAM,DEL
      WRITE(6,1124)OM0,T0,HOM,TN,ZET,OMN,OMR,TA
C
C     Evaluate system global damping matrix
C
      DO 90 I=1,IR
         DO 90 J=1,IR
   90       C(I,J)=ALP*M(I,J)+BET*K(I,J)
C
C     Call subroutines to create submatrices of a finite
C     time formulation and modify them.
C
```

```
      CALL FTZ12(IR,IT,DT,M,C,K,Z)
      Z(NL,NL+IR)=Z(NL,NL+IR)+MR
      Z(NL+IR,NL)=Z(NL+IR,NL)-MR
      Z(NL+IR,NL+IR)=Z(NL+IR,NL+IR)+MR*DT
      Z(NL+2*IR,NL)=Z(NL+2*IR,NL)-MR*DT
      Z(NL+2*IR,NL+IR)=Z(NL+2*IR,NL+IR)+0.8*MR*DT**2
      Z(NL+2*IR,NL+2*IR)=Z(NL+2*IR,NL+2*IR)+MR*DT**3/60.
      Z(NX,NX+IR)=Z(NX,NX+IR)+MR
      Z(NX+IR,NX)=Z(NX+IR,NX)-MR
      Z(NX+IR,NX+IR)=Z(NX+IR,NX+IR)+MR*DT
      Z(NX+2*IR,NX)=Z(NX+2*IR,NX)-MR*DT
      Z(NX+2*IR,NX+IR)=Z(NX+2*IR,NX+IR)+0.8*MR*DT**2
      Z(NX+2*IR,NX+2*IR)=Z(NX+2*IR,NX+2*IR)+MR*DT**3/60.
      IDGT=0
C
C     Invert modified submatrix (Z12)
C
      CALL LINV2F(Z,IT,IT,V,IDGT,WK,IER)
      DO 95 I=1,IT
         DO 95 J=1,IT
   95       Z(I,J)=V(I,J)
      CALL FTZ11(IR,IT,DT,M,C,K,V)
      V(NL,NL+IR)=V(NL,NL+IR)-MR
      V(NL+IR,NL)=V(NL+IR,NL)+MR
      V(NL+2*IR,NL)=V(NL+2*IR,NL)+MR*DT
      V(NL+2*IR,NL+IR)=V(NL+2*IR,NL+IR)+0.2*MR*DT**2
      V(NL+2*IR,NL+2*IR)=V(NL+2*IR,NL+2*IR)+MR*DT**3/60.
      V(NX,NX+IR)=V(NX,NX+IR)-MR
      V(NX+IR,NX)=V(NX+IR,NX)+MR
      V(NX+2*IR,NX)=V(NX+2*IR,NX)+MR*DT
      V(NX+2*IR,NX+IR)=V(NX+2*IR,NX+IR)+0.2*MR*DT**2
      V(NX+2*IR,NX+2*IR)=V(NX+2*IR,NX+2*IR)+MR*DT**3/60.
C
C     Determine vector of nodal acceleration at time t=0
C
      DO 100 I=1,IT
         Q(I)=0.0
  100    WV0(I)=0.0
      DO 110 I=1,IR
  110    WV1(I)=0.0
      WV1(NL)=-MR*ECC*2.0*OMR/TA
      IDGT=0
      CALL LEQT2F(M,1,IR,IR,WV1,IDGT,WK,IER)
      DO 120 I=1,IR
  120    WV0(IT-IR+I)=WV1(I)
C
C     Direct integration of a system equations of motion
C
      NPTX=0
      PREVX=-0.1
      LASTX=0.0
      NPTY=0
```

University of Alberta

```
      PREVY=-0.1
      LASTY=0.0
      T=0.0
      WRITE(6,1109)
      DO 130 L=1,NDT
         CALL LOADY(T,DT,TA,MR,OMR,ECC,TG,HG,F1,F2,F3)
         Q(NL)=F1
         Q(NL+IR)=F2
         Q(NL+2*IR)=F3
         CALL LOADX(T,DT,TA,MR,OMR,ECC,TG,HG,F1,F2,F3)
         Q(NX)=F1
         Q(NX+IR)=F2
         Q(NX+2*IR)=F3
         CALL MMULT(V,WVO,IT,IT,1,WV1)
         DO 135 I=1,IT
  135       WV2(I)=Q(I)-WV1(I)
         CALL MMULT(Z,WV2,IT,IT,1,WVO)
         IF(LASTY .GT. PREVY  .AND.  LASTY .GT. WVO(NL))
     +                                         GO TO 1977
         GO TO 1966
 1977    NPTY=NPTY+1
         X=T/TO
         Y=LASTY/YO
         WRITE(6,1110)NPTY,T,LASTY,X,Y
 1966    IF(LASTX .GT. PREVX  .AND.  LASTX .GT. WVO(NX))
     +                                         GO TO 1988
         GO TO 1955
 1988    NPTX=NPTX+1
         X=T/TO
         Y=LASTX/YO
         WRITE(7,1110)NPTX,T,LASTX,X,Y
 1955    T=T+DT
         PREVX=LASTX
         LASTX=WVO(NX)
         PREVY=LASTY
         LASTY=WVO(NL)
  130 CONTINUE
      NPTX=999
      NPTY=999
      WRITE(7,1110)NPTX
      WRITE(6,1110)NPTY
C
 1000 FORMAT(6I5)
 2000 FORMAT(10I5)
 1001 FORMAT(I6,5D20.8)
 1002 FORMAT(9D20.8)
 1100 FORMAT(1X,'Total number of finite elements used',
     +       8X,'=',I3/
     +       1X,'Number of finite elements in beam   ',
     +       8X,'=',I3/
     +       1X,'Number of finite elements in column ',
     +       8X,'=',I3/)
```

University of Alberta

University of Alberta

```
 1101 FORMAT(1X,6I5)
 2101 FORMAT(1X,I3,9I5)
 1102 FORMAT(1X,'Poisson  ratio                  =',F19.5/
     +         1X,'Young  modulus                  =',F19.5/
     +         1X,'Density                         =',F19.5/
     +         1X,'Shape factor                    =',F19.5//
     +         1X,'Total beam length               =',F19.5/
     +         1X,'Beam cross-section area         =',F19.5/
     +         1X,'Beam second moment of area      =',F19.5/)
 1103 FORMAT(1X,'Column height                   =',F19.5/
     +         1X,'Column cross-section area       =',F19.5/
     +         1X,'Column second moment area       =',F19.5/)
 1104 FORMAT(1X,'System 1st natural frequency    =',F19.5/
     +         1X,'System 1st natural period       =',F19.5/
     +         1X,'System highest frequency        =',F19.5/
     +         1X,'System shortest period          =',F19.5)
 1105 FORMAT(1X/16X,'STRUCTURE AND MATERIAL PROPERTIES'/
     +         16X,'---------------------------------'/)
 1106 FORMAT(1X/1X,'Array NG(NE,IE):'/
     +  '+','________________'/)
 1107 FORMAT(1X/16X,'FORCED VIBR.  TRANSIENT SOLUTION'/
     +       '+',15X,'____________  __________________'/)
 1108 FORMAT(1X,'Time step                        = ',F19.5/
     +         1X,'No. of time steps                = ',I13/
     +         1X,'Alpha                            = ',F19.5/
     +         1X,'Beta                             = ',F19.5/
     +         1X,'Gamma                            = ',F19.5/
     +         1X,'Delta                            = ',F19.5/)
 1109 FORMAT(12X,'TIME',6X,'DEFLECTION',8X,'TIME/TO',
     +        9X,'DRFactor'/
     +        12X,'----',6X,'----------',8X,'-------',
     +        9X,'--------'//)
 1110 FORMAT(1X,I3,5X,F8.4,5X,E11.5,5X,F10.3,5X,F10.3)
 1111 FORMAT(1X,'Number of degree of freedom per',
     +        1X,'element     =',I3/
     +        1X,'Total No. of D.O.Fs of constrained',
     +        1X,'system   =',I3/
     +        1X,'Order of finite time element',
     +        1X,'matrices       =',I3/
     +        1X,'Nodal number corresponding to applied',
     +        1X,'load  =',I3/)
 1112 FORMAT(1X/16X,'NATURAL FREQUENCIES & STATIC TEST'/
     +      '+',15X,'_________________________________')
 1113 FORMAT(16X,'RIGID PORTAL FRAME WITH CLAMPED LEGS'/
     +   '+',15X,'____________________________________')
 1115 FORMAT(1X,'COMPLEX TIMOSHENKO BEAM ELEM. (TM544)'/
     +      '+','_______ __________ ____ _______'/)
 1116 FORMAT(1X,'SIMPLE TIMOSHENKO BEAM ELEMENT'/
     +      '+','______ __________ ____ _______'/)
 1117 FORMAT(1X,I6,3X,F15.8)
 1118 FORMAT('0','static test (y-deflec.   at midspan)'/
     +       '+','___________'/
```

University of Alberta

```
                +       1X,'exact solution  =',F15.8/
                +       1X,'percentage error=',F15.8/)
       0321   1119 FORMAT(1X/)
       0322   1120 FORMAT(1X/1X,'System natural frequencies:'/
                +       '+','___________________________')
       0323   1121 FORMAT('0','static test (x-deflec.   at midspan)'/
                +       '+','__________'/
                +       1X,'exact solution  =',F15.8/
                +       1X,'percentage error=',F15.8/)
       0324   1122 FORMAT(1X,'Mass of the rotor              = ',F19.5/
                +       1X,'Eccentricity of the mass       = ',F19.5/
                +       1X,'Rotor/support mass ratio       = ',F19.5/)
       0325   1124 FORMAT(1X,'System 1st natural frequency= ',F19.5/
                +       1X,'System 1st natural period     = ',F19.5/
                +       1X,'System highest frequency      = ',F19.5/
                +       1X,'System shortest period        = ',F19.5/
                +       1X,'Time step/shortest period     = ',F19.5/
                +      '0','Highest passed frequency      = ',F19.5/
                +       1X,'Rotor operating speed         = ',F19.5/
                +       1X,'Rotor acceleration time       = ',F19.5/)
       0326   1125 FORMAT(1X,'Rotor initial speed           = ',F19.5/)
       0327   1126 FORMAT(1X/1X,'ROTOR SPEED PASSING',I3,2X,'NATUR',
                +       'AL FREQUENCY')
              C
       0328        RETURN
       0329        END
              C
              CC
              CCC  Subroutine to multiply matrices
              CC
              C
       0001        SUBROUTINE MMULT(A,B,M,KK,N,C)
       0002        REAL*8 A(M,KK),B(KK,N),C(M,N)
       0003        DO 1 I=1,M
       0004           DO 1 J=1,N
       0005              C(I,J)=0.0
       0006              DO 1 L=1,KK
       0007        1        C(I,J)=C(I,J)+A(I,L)*B(L,J)
       0008        RETURN
       0009        END
              C
              CC
              CCC  Subroutine  to create  finite time  element matrix
              CCC  from  system mass, damping and stiffness  matrices
              CC   (for matrix Z12)
              C
       0001        SUBROUTINE FTZ12(IR,IT,DT,A,B,C,Z)
       0002        REAL*8 A(IR,IR),B(IR,IR),C(IR,IR),Z(IT,IT),DT
       0003        DO 1 I=1,IR
       0004           DO 1 J=1,IR
       0005              Z(I,J)=         B(I,J)+DT*C(I,J)/2.
       0006              Z(I,J+IR)=      A(I,J)-DT**2*C(I,J)/10.
```

```
            Z(I,J+2*IR)=      DT**3*C(I,J)/120.
            Z(I+IR,J)=        -A(I,J)+DT*(B(I,J)/2.0+DT*
     +                        C(I,J)*5./14.)
            Z(I+IR,J+IR)=     DT*(A(I,J)+DT*(B(I,J)/10.-
     +                        DT*C(I,J)*13./210.))
            Z(I+IR,J+2*IR)=   DT**3*(-B(I,J)/120.+DT*
     +                        C(I,J)/210.)
            Z(I+2*IR,J)=      DT*(-A(I,J)+DT*(B(I,J)*
     +                        2./7.+DT*C(I,J)*23./84.))
            Z(I+2*IR,J+IR)=   (A(I,J)*4./5.+DT*(B(I,J)*13
     +                        /105.-DT*C(I,J)/24.))*DT**2
            Z(I+2*IR,J+2*IR)=(A(I,J)/60.-DT*(B(I,J)/105.
     +                        -DT*C(I,J)/336.))*DT**3
    1 CONTINUE
      RETURN
      END
C
CC
CCC   Subroutine  to  create  finite time element matrix
CCC   from  system mass, damping and stiffness  matrices
CC    (for matrix Z11)
C
      SUBROUTINE FTZ11(IR,IT,DT,A,B,C,V)
      REAL*8 A(IR,IR),B(IR,IR),C(IR,IR),V(IT,IT),DT
      DO 1 I=1,IR
         DO 1 J=1,IR
            V(I,J)=           -B(I,J)+DT*C(I,J)/2.
            V(I,J+IR)=        -A(I,J)+DT**2*C(I,J)/10.
            V(I,J+2*IR)=       DT**3*C(I,J)/120.
            V(I+IR,J)=         A(I,J)+DT*(-B(I,J)/2.+DT*
     +                         C(I,J)/7.)
            V(I+IR,J+IR)=      DT**2*(-B(I,J)/10.+DT*
     +                         C(I,J)*4./105.)
            V(I+IR,J+2*IR)=    DT**3*(-B(I,J)/120.+DT*
     +                         C(I,J)/280.)
            V(I+2*IR,J)=       DT*(A(I,J)+DT*(-B(I,J)*
     +                         2./7.+DT*C(I,J)*5./84.))
            V(I+2*IR,J+IR)=    (A(I,J)/5.-DT*(B(I,J)*8./
     +                         105.-DT*C(I,J)/56.))*DT**2
            V(I+2*IR,J+2*IR)=(A(I,J)/60.-DT*(B(I,J)/140.
     +                         -DT*C(I,J)/560.))*DT**3
    1 CONTINUE
      RETURN
      END
C
CC
CCC   Subroutine to create  element stiffness matrix for
CCC   the simple Timoshenko beam element
CC
C
      SUBROUTINE KSTMBM(EL,GKA,ARE,EMO,SMA,EK)
      REAL*8 EK(6,6)
```

University of Alberta

```
      REAL*8 EL,GKA,ARE,SMA,EMO,FI,C
      FI=12.*EMO*SMA/(GKA*EL**2)
      C=(EMO*SMA/EL**3)/(1.0+FI)
      EK(1,1)=ARE*EMO/EL
      EK(2,1)=0.0
      EK(2,2)=12.*C
      EK(3,1)=0.0
      EK(3,2)=6.0*EL*C
      EK(3,3)=C*(4.+FI)*EL**2
      EK(4,1)=-EK(1,1)
      EK(4,2)=0.0
      EK(4,3)=0.0
      EK(4,4)=EK(1,1)
      EK(5,1)=0.0
      EK(5,2)=-EK(2,2)
      EK(5,3)=-EK(3,2)
      EK(5,4)=0.0
      EK(5,5)=EK(2,2)
      EK(6,1)=0.0
      EK(6,2)=EK(3,2)
      EK(6,3)=C*(2.0-FI)*EL**2
      EK(6,4)=0.0
      EK(6,5)=EK(5,3)
      EK(6,6)=EK(3,3)
      DO 10 I=1,5
         K=I+1
         DO 10 J=K,6
   10       EK(I,J)=EK(J,I)
      RETURN
      END
C
CC
CCC   Subroutine to create  element mass  matrix for the
CCC   simple Timoshenko beam element
CC
C
      SUBROUTINE MSTMBM(EL,GKA,ARE,EMO,SMA,RHO,EM)
      REAL*8 EM(6,6),EL,GKA,ARE,EMO,SMA,RHO,FI,C,D
      FI=12.*EMO*SMA/(GKA*EL**2)
      C=(RHO*ARE*EL)/(1.0+FI)**2
      D=(SMA/ARE)/EL**2
      EM(1,1)=RHO*ARE*EL/3.0
      EM(2,1)=0.0
      EM(2,2)=C*(13./35.+0.7*FI+FI**2/3.+1.2*D)
      EM(3,1)=0.0
      EM(3,2)=C*EL*(11./210.+11.*FI/120.+FI**2/24.+D*
     +        (0.1-FI/2.))
      EM(3,3)=C*EL**2*(1./105.+FI/60.+FI**2/120.+D*
     +        (2./15.+FI/6.+FI**2/3.0))
      EM(4,1)=EM(1,1)/2.
      EM(4,2)=0.0
      EM(4,3)=0.0
```

University of Alberta

```
      EM(4,4)=EM(1,1)
      EM(5,1)=0.0
      EM(5,2)=C*(9./70.+0.3*FI+FI**2/6.-1.2*D)
      EM(5,3)=C*EL*(13./420.+3.*FI/40.+FI**2/24.-D*(0.1
     +        -FI/2.))
      EM(5,4)=0.0
      EM(5,5)=EM(2,2)
      EM(6,1)=0.0
      EM(6,2)=-EM(5,3)
      EM(6,3)=C*EL**2*(D*(FI**2/6.-FI/6.-1./30.)-1./140.
     +        -FI/60.-FI**2/120.)
      EM(6,4)=0.0
      EM(6,5)=-EM(3,2)
      EM(6,6)=EM(3,3)
C
      DO 10 I=1,5
         K=I+1
         DO 10 J=K,6
   10       EM(I,J)=EM(J,I)
      RETURN
      END
C
CC
CCC   Subroutine to create element stiffness  matrix for
CCC   the simple Timoshenko beam element (for column)
CC
C
      SUBROUTINE KSTMCN(EL,GKA,ARE,EMO,SMA,EK)
      REAL*8 EK(6,6)
      REAL*8 EL,GKA,ARE,SMA,EMO,FI,C
      FI=12.*EMO*SMA/(GKA*EL**2)
      C=(EMO*SMA/EL**3)/(1.0+FI)
      EK(1,1)=12.*C
      EK(2,1)=0.0
      EK(2,2)=ARE*EMO/EL
      EK(3,1)=-6.0*EL*C
      EK(3,2)=0.0
      EK(3,3)=C*(4.+FI)*EL**2
      EK(4,1)=-EK(1,1)
      EK(4,2)=0.0
      EK(4,3)=-EK(3,1)
      EK(4,4)=EK(1,1)
      EK(5,1)=0.0
      EK(5,2)=-EK(2,2)
      EK(5,3)=0.0
      EK(5,4)=0.0
      EK(5,5)=EK(2,2)
      EK(6,1)=EK(3,1)
      EK(6,2)=0.0
      EK(6,3)=C*(2.0-FI)*EL**2
      EK(6,4)=-EK(3,1)
      EK(6,5)=0.0
```

University of Alberta

```
      EK(6,6)=EK(3,3)
      DO 10 I=1,5
         K=I+1
         DO 10 J=K,6
   10       EK(I,J)=EK(J,I)
      RETURN
      END
C
CC
CCC   Subroutine to create  element  mass matrix for the
CCC   simple Timoshenko beam element (for column)
CC
C
      SUBROUTINE MSTMCN(EL,GKA,ARE,EMO,SMA,RHO,EM)
      REAL*8 EM(6,6),EL,GKA,ARE,EMO,SMA,RHO,FI,C,D
      FI=12.*EMO*SMA/(GKA*EL**2)
      C=(RHO*ARE*EL)/(1.0+FI)**2
      D=(SMA/ARE)/EL**2
      EM(1,1)=C*(13./35.+0.7*FI+FI**2/3.+1.2*D)
      EM(2,1)=0.0
      EM(2,2)=RHO*ARE*EL/3.0
      EM(3,1)=-C*EL*(11./210.+11.*FI/120.+FI**2/24.+D*
     +          (0.1-FI/2.))
      EM(3,2)=0.0
      EM(3,3)=C*EL**2*(1./105.+FI/60.+FI**2/120.+D*
     +          (2./15.+FI/6.+
     +          FI**2/3.0))
      EM(4,1)=C*(9./70.+0.3*FI+FI**2/6.-1.2*D)
      EM(4,2)=0.0
      EM(4,3)=-C*EL*(13./420.+3.*FI/40.+FI**2/24.-D*
     +          (0.1-FI/2.))
      EM(4,4)=EM(1,1)
      EM(5,1)=0.0
      EM(5,2)=EM(2,2)/2.0
      EM(5,3)=0.0
      EM(5,4)=0.0
      EM(5,5)=EM(2,2)
      EM(6,1)=-EM(4,3)
      EM(6,2)=0.0
      EM(6,3)=C*EL**2*(D*(FI**2/6.-FI/6.-1./30.)-1./140.
     +          -FI/60.-FI**2/120.)
      EM(6,4)=-EM(3,1)
      EM(6,5)=0.0
      EM(6,6)=EM(3,3)
      DO 10 I=1,5
         K=I+1
         DO 10 J=K,6
   10       EM(I,J)=EM(J,I)
      RETURN
      END
C
CC
```

University of Alberta

```
CCC   Subroutine to calculate components  (in X-direc.)
CCC   of load vector. Subroutine uses 4-point  Gaussian
CCC   quadrature to evaluate integrals.
CC
C
      SUBROUTINE LOADX(T,DT,T1,MR,OMR,ECC,TG,HG,
     +               F1,F2,F3)
      REAL*8 T,DT,T1,MR,OMR,ECC,F1,F2,F3,TG(4),HG(4),TX
      REAL*8 OMT,OMS,OMA,FX
      F1=0.0
      F2=0.0
      F3=0.0
      DO 10 I=1,4
         TX=DT*(TG(I)+1.0)/2.0
         IF(T .GT. T1) GO TO 1
         OMT=OMR*T1*((T+TX)/T1)**2*(3.0-(T+TX)/T1)/3.0
         OMS=OMR*(T+TX)*(2.0-(T+TX)/T1)/T1
         OMA=OMR*2.0*(1.0-(T+TX)/T1)/T1
         GO TO 2
    1    OMT=OMR*((T+TX)-T1/3.0)
         OMS=OMR
         OMA=0.0
    2    CONTINUE
         FX=MR*ECC*(OMS**2*DCOS(OMT)+OMA*DSIN(OMT))
         F1=F1+HG(I)*FX
         F2=F2+HG(I)*TX*FX
   10    F3=F3+HG(I)*TX**2*FX
      F1=F1*DT/2.0
      F2=F2*DT/2.0
      F3=F3*DT/2.0
      RETURN
      END
C
CC
CCC   Subroutine to calculate components (in Y-direc.)
CCC   of load vector. Subroutine uses 4-point Gaussian
CCC   quadrature to evaluate integrals
CC
C
      SUBROUTINE LOADY(T,DT,T1,MR,OMR,ECC,TG,HG,F1,F2
     +               ,F3)
C
      REAL*8 T,DT,T1,MR,OMR,ECC,F1,F2,F3,TG(4),HG(4),TX
      REAL*8 OMT,OMS,OMA,FX
C
      F1=0.0
      F2=0.0
      F3=0.0
      DO 10 I=1,4
         TX=DT*(TG(I)+1.0)/2.0
         IF(T .GT. T1) GO TO 1
         OMT=OMR*T1*((T+TX)/T1)**2*(3.0-(T+TX)/T1)/3.0
```

University of Alberta

```
         OMS=OMR*(T+TX)*(2.0-(T+TX)/T1)/T1
         OMA=OMR*2.0*(1.0-(T+TX)/T1)/T1
         GO TO 2
    1    OMT=OMR*((T+TX)-T1/3.0)
         OMS=OMR
         OMA=0.0
    2    CONTINUE
         FX=MR*ECC*(OMS**2*DSIN(OMT)-OMA*DCOS(OMT))
         F1=F1+HG(I)*FX
         F2=F2+HG(I)*TX*FX
   10    F3=F3+HG(I)*TX**2*FX
      F1=F1*DT/2.0
      F2=F2*DT/2.0
      F3=F3*DT/2.0
      RETURN
      END
C
CC
CCC   Subroutine to create Timoshenko  beam (beam-truss)
CCC   element (TM544) stiffness  matrix (for beam)
CC
C
      SUBROUTINE KCTMBM(EL,GKA,ARE,EMO,SMA,K)
      REAL*8 K(10,10),EL,GKA,ARE,SMA,EMO
      K(1,1)=ARE*EMO/EL
      K(1,2)=0.0
      K(1,3)=0.0
      K(1,4)=0.0
      K(1,5)=0.0
      K(1,6)=-K(1,1)
      K(1,7)=0.0
      K(1,8)=0.0
      K(1,9)=0.0
      K(1,10)=0.0
      K(2,2)=6.*GKA/(5.0*EL)
      K(2,3)=K(2,2)*EL/2.0
      K(2,4)=-K(2,3)/(6.0*ARE)
      K(2,5)=-K(2,4)*ARE*EL/SMA
      K(2,6)=0.0
      K(2,7)=-K(2,2)
      K(2,8)=K(2,3)
      K(2,9)=K(2,4)
      K(2,10)=-K(2,5)
      K(3,3)=K(2,3)*EL/2.0+6.0*EMO*SMA/(5.0*EL)
      K(3,4)=K(2,4)*EL/2.0
      K(3,5)=K(2,5)*EL/2.0+EMO/10.0
      K(3,6)=0.0
      K(3,7)=-K(2,3)
      K(3,8)=K(2,3)*EL/2.0-6.0*EMO*SMA/(5.0*EL)
      K(3,9)=K(3,4)
      K(3,10)=-K(2,5)*EL/2.0+EMO/10.0
      K(4,4)=-4.0*K(3,4)*2.0/(3.0*ARE)
```

University of Alberta

```
      K(4,5)=K(3,4)*EL/(6.0*SMA)
      K(4,6)=0.0
      K(4,7)=-K(2,4)
      K(4,8)=K(3,4)
      K(4,9)=-K(4,4)/4.0
      K(4,10)=-K(4,5)
      K(5,5)=K(2,5)*EL**2/(12.0*SMA)+2.*EMO*EL/(15.*SMA)
      K(5,6)=0.0
      K(5,7)=-K(2,5)
      K(5,8)=-K(3,10)
      K(5,9)=K(4,5)
      K(5,10)=-K(2,5)*EL**2/(12.0*SMA)-EMO*EL/(30.0*SMA)
      K(6,6)=K(1,1)
      K(6,7)=0.0
      K(6,8)=0.0
      K(6,9)=0.0
      K(6,10)=0.0
      K(7,7)=K(2,2)
      K(7,8)=-K(2,3)
      K(7,9)=K(4,7)
      K(7,10)=K(2,5)
      K(8,8)=K(3,3)
      K(8,9)=K(3,4)
      K(8,10)=-K(3,5)
      K(9,9)=K(4,4)
      K(9,10)=K(4,10)
      K(10,10)=K(5,5)
      DO 10 I=2,10
         N=I-1
         DO 10 J=1,N
   10       K(I,J)=K(J,I)
      RETURN
      END
C
CC
CCC   Subroutine to create Timoshenko beam  (beam-truss)
CCC   element (TM544) stiffness  matrix (for column)
CC
C
      SUBROUTINE KCTMCN(EL,GKA,ARE,EMO,SMA,K)
      REAL*8 K(10,10),EL,GKA,ARE,SMA,EMO
      K(1,1)=1.2*GKA/EL
      K(1,2)=0.0
      K(1,3)=-0.6*GKA
      K(1,4)=0.1*GKA/ARE
      K(1,5)=-0.1*GKA*EL/SMA
      K(1,6)=-K(1,1)
      K(1,7)=0.0
      K(1,8)=K(1,3)
      K(1,9)=K(1,4)
      K(1,10)=-K(1,5)
      K(2,2)=ARE*EMO/EL
```

University of Alberta

University of Alberta

```
      K(2,3)=0.0
      K(2,4)=0.0
      K(2,5)=0.0
      K(2,6)=0.0
      K(2,7)=-K(2,2)
      K(2,8)=0.0
      K(2,9)=0.0
      K(2,10)=0.0
      K(3,3)=-K(1,3)*EL/2.0+6.0*EMO*SMA/(5.0*EL)
      K(3,4)=-K(1,4)*EL/2.0
      K(3,5)=-K(1,5)*EL/2.0+EMO/10.0
      K(3,6)=-K(1,3)
      K(3,7)=0.0
      K(3,8)=K(3,6)*EL/2.0-6.0*EMO*SMA/(5.0*EL)
      K(3,9)=K(3,4)
      K(3,10)=K(1,5)*EL/2.0+EMO/10.0
      K(4,4)=-4.0*K(3,4)*2.0/(3.0*ARE)
      K(4,5)=K(3,4)*EL/(6.0*SMA)
      K(4,6)=-K(1,4)
      K(4,7)=0.0
      K(4,8)=K(3,4)
      K(4,9)=-K(4,4)/4.0
      K(4,10)=-K(4,5)
      K(5,5)=-K(1,5)*EL**2/(12.0*SMA)+.4*EMO*EL/(3.*SMA)
      K(5,6)=-K(1,5)
      K(5,7)=0.0
      K(5,8)=-K(3,10)
      K(5,9)=K(4,5)
      K(5,10)=K(1,5)*EL**2/(12.0*SMA)-EMO*EL/(30.0*SMA)
      K(6,6)=K(1,1)
      K(6,7)=0.0
      K(6,8)=-K(1,3)
      K(6,9)=-K(1,4)
      K(6,10)=K(1,5)
      K(7,7)=K(2,2)
      K(7,8)=0.0
      K(7,9)=0.0
      K(7,10)=0.0
      K(8,8)=K(3,3)
      K(8,9)=K(3,4)
      K(8,10)=-K(3,5)
      K(9,9)=K(4,4)
      K(9,10)=K(4,10)
      K(10,10)=K(5,5)
      DO 10 I=2,10
         N=I-1
         DO 10 J=1,N
   10       K(I,J)=K(J,I)
      RETURN
      END
C
CC
```

```
CCC   Subroutine to create Timoshenko beam element
CCC   (TM544) consistent mass matrix (for beam)
CC
C
      SUBROUTINE MCTMBM(EL,ARE,SMA,RHO,M)
      REAL*8 M(10,10),EL,ARE,SMA,RHO
      M(1,1)=RHO*ARE*EL/3.0
      M(1,2)=0.0
      M(1,3)=0.0
      M(1,4)=0.0
      M(1,5)=0.0
      M(1,6)=M(1,1)/2.0
      M(1,7)=0.0
      M(1,8)=0.0
      M(1,9)=0.0
      M(1,10)=0.0
      M(2,2)=RHO*ARE*EL*13/35.0
      M(2,3)=RHO*ARE*EL**2*17/280.0
      M(2,4)=-M(2,3)*44/(51*ARE)
      M(2,5)=M(2,3)*EL*7/(102*SMA)
      M(2,6)=0.0
      M(2,7)=M(2,2)*9/26.0
      M(2,8)=-M(2,3)*11/17.0
      M(2,9)=-M(2,4)*13/22.0
      M(2,10)=M(2,5)
      M(3,3)=M(2,3)*EL/4.5+13*RHO*SMA*EL/35.
      M(3,4)=M(2,4)*19*EL/88.0
      M(3,5)=M(2,5)*EL*11/42.+11*RHO*EL**2/210.
      M(3,6)=0.0
      M(3,7)=-M(2,8)
      M(3,8)=-M(2,3)*EL*28/153.+9*RHO*SMA*EL/70.
      M(3,9)=-M(3,4)*45/57.0
      M(3,10)=M(2,5)*EL*11/42.-13*RHO*EL**2/420.
      M(4,4)=-M(3,4)*16/(19*ARE)
      M(4,5)=-M(2,5)*9*EL/(42*ARE)
      M(4,6)=0.0
      M(4,7)=M(2,4)*13/22.0
      M(4,8)=M(3,9)
      M(4,9)=-M(4,4)*3/4.0
      M(4,10)=M(4,5)
      M(5,5)=-M(4,5)*(EL*ARE/(9*SMA)+32/(3*EL))
      M(5,6)=0.0
      M(5,7)=M(2,5)
      M(5,8)=-M(3,10)
      M(5,9)=-M(4,10)
      M(5,10)=M(5,9)*(EL*ARE/(9*SMA)-8/EL)
      M(6,6)=M(1,1)
      M(6,7)=0.0
      M(6,8)=0.0
      M(6,9)=0.0
      M(6,10)=0.0
      M(7,7)=M(2,2)
```

University of Alberta

University of Alberta

```
      M(7,8)=-M(2,3)
      M(7,9)=-M(2,4)
      M(7,10)=M(2,5)
      M(8,8)=M(3,3)
      M(8,9)=M(3,4)
      M(8,10)=-M(3,5)
      M(9,9)=M(4,4)
      M(9,10)=M(5,9)
      M(10,10)=M(5,5)
      DO 10 I=2,10
         N=I-1
         DO 10 J=1,N
   10       M(I,J)=M(J,I)
      RETURN
      END
C
CC
CCC   Subroutine to create Timoshenko beam element
CCC   (TM544) consistent mass matrix (for column)
CC
C
      SUBROUTINE MCTMCN(EL,ARE,SMA,RHO,M)
      REAL*8 M(10,10),EL,ARE,SMA,RHO
      M(1,1)=RHO*ARE*EL*13/35.0
      M(1,2)=0.0
      M(1,3)=-RHO*ARE*EL**2*17/280.0
      M(1,4)=-M(1,3)*44/(51*ARE)
      M(1,5)=M(1,3)*EL*7/(102*SMA)
      M(1,6)=M(1,1)*9/26.0
      M(1,7)=0.0
      M(1,8)=-M(1,3)*11/17.0
      M(1,9)=-M(1,4)*13/22.0
      M(1,10)=M(1,5)
      M(2,2)=RHO*ARE*EL/3.0
      M(2,3)=0.0
      M(2,4)=0.0
      M(2,5)=0.0
      M(2,6)=0.0
      M(2,7)=M(2,2)/2.0
      M(2,8)=0.0
      M(2,9)=0.0
      M(2,10)=0.0
      M(3,3)=-M(1,3)*EL/4.5+13*RHO*SMA*EL/35.
      M(3,4)=-M(1,4)*19*EL/88.0
      M(3,5)=-M(1,5)*EL*11/42.+11*RHO*EL**2/210.
      M(3,6)=-M(1,8)
      M(3,7)=0.0
      M(3,8)=M(1,3)*EL*28/153.+9*RHO*SMA*EL/70.
      M(3,9)=-M(3,4)*45/57.0
      M(3,10)=-M(1,5)*EL*11/42.-13*RHO*EL**2/420.
      M(4,4)=-M(3,4)*16/(19*ARE)
      M(4,5)=M(1,5)*9*EL/(42*ARE)
      M(4,6)=M(1,4)*13/22.0
      M(4,7)=0.0
      M(4,8)=M(3,9)
      M(4,9)=-M(4,4)*3/4.0
      M(4,10)=M(4,5)
      M(5,5)=-M(4,5)*(EL*ARE/(9*SMA)+32/(3*EL))
      M(5,6)=M(1,5)
      M(5,7)=0.0
      M(5,8)=-M(3,10)
      M(5,9)=-M(4,10)
      M(5,10)=M(5,9)*(EL*ARE/(9*SMA)-8/EL)
      M(6,6)=M(1,1)
      M(6,7)=0.0
      M(6,8)=-M(1,3)
      M(6,9)=-M(1,4)
      M(6,10)=M(1,5)
      M(7,7)=M(2,2)
      M(7,8)=0.0
      M(7,9)=0.0
      M(7,10)=0.0
      M(8,8)=M(3,3)
      M(8,9)=M(3,4)
      M(8,10)=-M(3,5)
      M(9,9)=M(4,4)
      M(9,10)=M(5,9)
      M(10,10)=M(5,5)
      DO 10 I=2,10
        N=I-1
        DO 10 J=1,N
   10     M(I,J)=M(J,I)
      RETURN
      END
C
CC
CCC   Subroutine to assemble element matrices into
CCC   global ones
CC
C
      SUBROUTINE ASSZW(EMAT,NK,IE,NE,IR,GMAT,NSORT)
      REAL*8 EMAT(IE,IE),GMAT(IR,IR)
      INTEGER NSORT(NE,IE)
      DO 10 I=1,IE
        DO 15 J=1,IE
          N1=NSORT(NK,I)
          N2=NSORT(NK,J)
          IF((N1 .GT. IR) .OR. (N2 .GT. IR)) GO TO 20
          GMAT(N1,N2)=GMAT(N1,N2)+EMAT(I,J)
   20     CONTINUE
   15     CONTINUE
   10     CONTINUE
      RETURN
      END
```

University of Alberta

```
C
CC
CCC   Subroutine FORCE to calculate components (in X and
CCC   and Y  directions)  of  dynamic oil-film forces in
CCC   in journal bearing. S/r uses 4th order Runge-Kutta
CCC   method to solve equations of journal centre motion
CC
C
      SUBROUTINE FORCE(T,DX,IP,TA,EPS,PSI,VEP,VPS,OMR,
     &        OMI,MAR,WT,MC,ME,PAR,TX,PX,PY,OMT,OMS,OMA)
C
      REAL*8 T,DX,TA,EPS,PSI,VEP,VPS,OMR,OMI,OMT,OMS,OMA
      REAL*8 TX(IP),PX(IP),PY(IP),WT,MC,ME,P1,P2
      REAL*8 AK,AL,AM,AN,GK,GL,GM,GN,S1,S2,S3,S4
C
      CALL ROTTSA(MAR,T,OMI,OMR,TA,OMT,OMS,OMA)
      IPM1=IP-1
      DO 10 J=1,IPM1
         CALL BF(PAR,EPS,VEP,VPS,OMS,P1,P2)
         TX(J)=T
         PX(J)=-(P1*DSIN(PSI)+P2*DCOS(PSI))
         PY(J)=P1*DCOS(PSI)-P2*DSIN(PSI)+WT
         S1=EPS
         S2=PSI
         S3=VEP
         S4=VPS
         CALL RKA(DX,P1,P2,WT,ME,MC,EPS,PSI,VEP,VPS,OMT,
     &            OMS,OMA,AK,AL,AM,AN)
         GK=AK
         GL=AL
         GM=AM
         GN=AN
         EPS=S1+AM/2.0D+00
         PSI=S2+AN/2.0D+00
         VEP=S3+AK/2.0D+00
         VPS=S4+AL/2.0D+00
         T=T+DX/2.0D+00
         CALL ROTTSA(MAR,T,OMI,OMR,TA,OMT,OMS,OMA)
         CALL BF(PAR,EPS,VEP,VPS,OMS,P1,P2)
         CALL RKA(DX,P1,P2,WT,ME,MC,EPS,PSI,VEP,VPS,OMT,
     &            OMS,OMA,AK,AL,AM,AN)
         GK=GK+AK*2.0D+00
         GL=GL+AL*2.0D+00
         GM=GM+AM*2.0D+00
         GN=GN+AN*2.0D+00
         EPS=S1+AM/2.0D+00
         PSI=S2+AN/2.0D+00
         VEP=S3+AK/2.0D+00
         VPS=S4+AL/2.0D+00
         CALL BF(PAR,EPS,VEP,VPS,OMS,P1,P2)
         CALL RKA(DX,P1,P2,WT,ME,MC,EPS,PSI,VEP,VPS,OMT,
     &            OMS,OMA,AK,AL,AM,AN)
```

University of Alberta

```
         GK=GK+AK*2.0D+00
         GL=GL+AL*2.0D+00
         GM=GM+AM*2.0D+00
         GN=GN+AN*2.0D+00
         EPS=S1+AM
         PSI=S2+AN
         VEP=S3+AK
         VPS=S4+AL
         T=T+DX/2.0D+00
         CALL ROTTSA(MAR,T,OMI,OMR,TA,OMT,OMS,OMA)
         CALL BF(PAR,EPS,VEP,VPS,OMS,P1,P2)
         CALL RKA(DX,P1,P2,WT,ME,MC,EPS,PSI,VEP,VPS,OMT,
     &            OMS,OMA,AK,AL,AM,AN)
         EPS=S1+(GM+AM)/6.0D+00
         PSI=S2+(GN+AN)/6.0D+00
         VEP=S3+(GK+AK)/6.0D+00
         VPS=S4+(GL+AL)/6.0D+00
   10 CONTINUE
      CALL BF(PAR,EPS,VEP,VPS,OMS,P1,P2)
      J=IP
      TX(J)=T
      PX(J)=-(P1*DSIN(PSI)+P2*DCOS(PSI))
      PY(J)=P1*DCOS(PSI)-P2*DSIN(PSI)+WT
      RETURN
      END
C
CC
CCC   Subroutine RKA (Runge-Kutta 4th order) to calcula-
CCC   te increments in  displacements and  velocities at
CC    each time step
CC
C
      SUBROUTINE RKA(DX,P1,P2,WT,ME,MC,EPS,PSI,VEP,VPS,
     &              OMT,OMS,OMA,AK,AL,AM,AN)
C
      REAL*8 DX,P1,P2,WT,ME,MC,EPS,PSI,VEP,VPS,OMT,OMS
      REAL*8 OMA,A,SP,CP,SA,CA,TW,AK,AL,AM,AN
C
      A=OMT-PSI
      SP=DSIN(PSI)
      CP=DCOS(PSI)
      SA=DSIN(A)
      CA=DCOS(A)
      TW=2.0D+00
      AK=DX*((P1+WT*CP+ME*OMS**2*CA+ME*OMA*SA)/MC+EPS*
     +   VPS**2)
      AL=DX*((P2-WT*SP+ME*OMS**2*SA-ME*OMA*CA)/MC-VEP*
     +   VPS*TW)/EPS
      AM=DX*VEP
      AN=DX*VPS
      RETURN
      END
```

University of Alberta

```
C
CC
CCC   Subroutine BF to calculate bearing dynamic forces
CCC   (in polar coordinates) at each time subinterval
CC
C
      SUBROUTINE BF(PAR,EPS,VEP,VPS,OMS,P1,P2)
      REAL*8 PAR,EPS,VEP,VPS,OMS,P1,P2
      REAL*8 E2,EB,OB,EB2,EBS,PI,TW,A
C
      PI=3.141592654D+00
      TW=2.0D+00
      E2=EPS*EPS
      EB=1.0D+00-E2
      OB=OMS-VPS*TW
      EB2=EB*EB
      A=PAR/EB2
      EBS=EB**0.5
      P1=-A*(PI*(1.0D+00+E2*TW)*VEP/EBS+OB*E2*TW)
      P2=A*(EPS*VEP*TW*TW+OB*PI*EPS*EBS/TW)
      RETURN
      END
C
CC
CCC   Subroutine ROTTSA to calculate rotor angular
CCC   travel, speed and acceleration
CC
C
      SUBROUTINE ROTTSA(MAR,T,OMI,OMR,TA,OMT,OMS,OMA)
      REAL*8 T,OMI,OMR,TA,OMT,OMS,OMA,A,TX
      IF(MAR .EQ. 2) GO TO 2
      IF(MAR .EQ. 3) GO TO 3
    2 A=(OMR-OMI)/TA
      TX=T/TA
      OMA=A*(1.0D+00-TX)*2.0D+00
      OMS=A*T*(2.0D+00-TX)+OMI
      OMT=A*T**2*(1.0D+00-TX/3.0D+00)+OMI*T
      RETURN
    3 OMA=0.0D+00
      OMS=OMR
      OMT=OMR*T-(OMR-OMI)*TA/3.0D+00
      RETURN
      END
C
CC
CCC   Subroutine SPLINT to integrate discrete functions,
CCC   using cubic spline method
CC
C
      SUBROUTINE SPLINT(N,DX,X,Y,B,C,F1,F2,F3)
      REAL*8 DX,X(N),Y(N),B(N),C(N),F1,F2,F3,SUM1,SUM2,T
      NM1=N-1
```

University of Alberta

```
      K=1
      X(1)=0.0D+00
      DO 1 I=2,N
    1    X(I)=X(I-1)+DX
    5 C(2)=(Y(2)-Y(1))/DX
      DO 10 I=2,NM1
         B(I)=DX*4.0D+00
         C(I+1)=(Y(I+1)-Y(I))/DX
   10    C(I)=C(I+1)-C(I)
      B(1)=-DX
      B(N)=-DX
      C(1)=0.0D+00
      C(N)=0.0D+00
      IF(N .EQ. 3) GO TO 15
      C(1)=(C(3)-C(2))/(DX*2.0D+00)
      C(N)=(C(N-1)-C(N-2))/(DX*2.0D+00)
      C(1)=C(1)*DX/3.0D+00
      C(N)=-C(N)*DX/3.0D+00
   15 DO 20 I=2,N
         T=DX/B(I-1)
         B(I)=B(I)-T*DX
   20    C(I)=C(I)-T*C(I-1)
      C(N)=C(N)/B(N)
      DO 30 IB=1,NM1
         I=N-IB
   30    C(I)=(C(I)-DX*C(I+1))/B(I)
      SUM1=0.0D+00
      SUM2=0.0D+00
      DO 40 I=1,NM1
         SUM1=SUM1+Y(I)+Y(I+1)
   40    SUM2=SUM2+C(I)+C(I+1)
      T=(SUM1-SUM2*DX**2/2.0D+00)*DX/2.0D+00
      IF(K .EQ. 1) F1=T
      IF(K .EQ. 2) F2=T
      IF(K .EQ. 3) F3=T
      DO 50 I=1,N
   50    Y(I)=Y(I)*X(I)
      K=K+1
      IF(K .EQ. 4) GO TO 6
      GO TO 5
    6 RETURN
      END
C
CC
CCC   Subroutine to calculate components of load vector.
CCC   Subroutine  uses  4-point  Gaussian  quadrature  to
CCC   evaluate integrals.
CC
C
      SUBROUTINE LOADYB(MAR,T,DT,TA,MR,OMR,OMI,ECC,TG,HG
     +                      ,F1,F2,F3)
C
```

```
      REAL*8 T,DT,TA,MR,OMR,OMI,ECC,TG(4),HG(4),F1,F2,F3
      REAL*8 TX,OMT,OMS,OMA,FX,A,X,XT
C
      F1=0.0D+00
      F2=0.0D+00
      F3=0.0D+00
      IF(MAR .EQ. 2) GO TO 2
      IF(MAR .EQ. 3) GO TO 3
    2 A=(OMR-OMI)/TA
      DO 10 I=1,4
         TX=DT*(TG(I)+1.0D+00)/2.0D+00
         X=T+TX
         XT=X/TA
         OMT=A*X**2*(1.0D+00-XT/3.0D+00)+OMI*X
         OMS=A*X*(2.0D+00-XT)+OMI
         OMA=A*(1.0D+00-XT)*2.0D+00
         FX=-MR*ECC*(OMS**2*DCOS(OMT)+OMA*DSIN(OMT))
         F1=F1+HG(I)*FX
         F2=F2+HG(I)*TX*FX
   10    F3=F3+HG(I)*TX**2*FX
      GO TO 4
    3 A=(OMR-OMI)*TA/3.0D+00
      DO 20 I=1,4
         TX=DT*(TG(I)+1.0D+00)/2.0D+00
         X=T+TX
         OMT=OMR*X-A
         FX=-MR*ECC*OMR**2*DCOS(OMT)
         F1=F1+HG(I)*FX
         F2=F2+HG(I)*TX*FX
   20    F3=F3+HG(I)*TX**2*FX
    4 CONTINUE
      A=DT/2.0D+00
      F1=F1*A
      F2=F2*A
      F3=F3*A
      RETURN
      END
```

University of Alberta